INTERNATIONAL ATOMIC ENERGY AGENCY
UNITED NATIONS EDUCATIONAL, SCIENTIFIC AND CULTURAL ORGANIZATION
INTERNATIONAL CENTRE FOR THEORETICAL PHYSICS
I.C.T.P., P.O. BOX 586, 34100 TRIESTE, ITALY. CABLE CENTRATOM TRIESTE

H4.SMR/845-19

Second Winter College on Optics

20 February - 10 March 1995

Laser Molecular Spectroscopy

M. Inguscio

European Laboratory for
Nonlinear Spectroscopy
University of Florence
Florence, Italy

MAIN BUILDING STRADA COSTIERA, 11 TEL. 2240111 TELEFAX 224163 TELEX 460392 ADRIATICO GUEST HOUSE VIA GRIGNANO, 9 TEL.224241 TELEFAX 224531 TELEX 460449
MICROPROCESSOR LAB. VIA BEIRUT, 31 TEL. 224471 TELEFAX 224600 TELEX 460392 GALILEO GUEST HOUSE VIA BEIRUT, 7 TEL. 22401 TELEFAX 2240310 TELEX 460392

HIGH RESOLUTION FAR INFRARED SPECTROSCOPY

L.R. Zink, M. Prevedelli, K.M. Evenson *
and M. Inguscio

European Laboratory for
Nonlinear Spectroscopy (LENS)
Florence, Italy

*National Institute of
Standards and Technology (NIST)
Boulder, Colorado, USA

INTRODUCTION

The far infrared (FIR) spectral region (which we will define as 0.3 - 10 THz [1mm to 30 μm]) plays an important role in molecular and atomic spectroscopy. The pure rotational transitions of light molecules, for example diatomic hydrides, occur in this region; FIR measurements provide the only accurate means of determining their rotational structure and associated characteristics such as line strengths, pressure broadening parameters, and permanent electric dipole moments. Heavier molecules can also be observed in the FIR. Their rotational transitions in this region involve high quantum numbers and therefore small but important centrifugal distortion effects can be measured. In atoms, transitions between fine structure levels as well as metastable levels occur at FIR frequencies.

Laboratory spectroscopic measurements in the far infrared are increasingly important for other branches of science. Radio astronomers are now making measurements in the FIR and rely heavily on the laboratory measured transition frequencies. The FIR molecular and atomic transitions are important in the characterization of interstellar molecular clouds; FIR measurements are useful for identifying species, measuring concentrations, and determining temperature profiles.[1] FIR spectroscopy is also important in the monitoring and modeling of the earth's atmosphere. For instance the concentration of the hydroxyl radical (an important molecule in the ozone production cycle) is monitored in balloon flights by observing its FIR spectrum.[2,3] Accurate determination of the concentration requires laboratory measurements of the pressure broadening coefficient at the appropriate frequency.

Applied Laser Spectroscopy, Edited by W. Demtröder and M. Inguscio, Plenum Press, New York, 1990

FIR SPECTROMETERS

Classical spectrometers in the FIR use interferometric techniques coupled with blackbody sources and high sensitivity bolometric detectors. At present, the best available Fourier transform spectrometers provide complete coverage of the FIR region with 20 MHz spectral resolution and accuracy approaching 1 MHz.[4,5] They also have the advantage of performing wide spectral scans in fairly short periods and have a frequency range extending into the visible.

FIR laser spectroscopy is limited by the fact that no broadly tunable, narrow-band lasers exist in this region. However, over 1000 optically pumped, fixed frequency FIR laser lines do exist, with about 1 kHz linewidth;[6] the only problem is lack of tunability between lines. To overcome this problem laser magnetic resonance (LMR) was developed.[7] LMR uses a magnetic field to Zeeman tune a molecule or atom into resonance with the fixed frequency laser. Intracavity FIR LMR is one of the most sensitive spectroscopic techniques (it exhibits a minimum detectability of 5×10^{-10} cm^{-1}) and has wide applications in spectroscopy and chemical kinetics. For detailed LMR reviews, the reader is referred to references 8 and 9, reference 10 provides a good overview of the use of LMR in atomic spectroscopy.

As powerful and useful as FTS and LMR are in the far infrared, there are limitations to both techniques. LMR is only applicable to species with open electronic shells, has an accuracy limited to about 1 MHz, and requires the unravelling of the Zeeman splittings . With FTS, the resolution is often insufficient to observe hyperfine structure and the maximum accuracy of several MHz is only available on a few of the best spectrometers. For these reasons, other coherent sources have been developed. These all take advantage of nonlinear mixing to generate tunable, narrow-band far infrared radiation.

Harmonic multiplication of microwave oscillators was developed in the 1960's and at present provides microwave resolution and accuracy at frequencies up to 1 THz.[11] Frequencies above one THz have been synthesized in several different ways: 1) CO_2 laser difference frequency generation in GaAs[12] and other crystals[13]; 2) Generation of microwave sidebands on FIR laser radiation[14-17]; and 3) CO_2 laser difference frequency generation in metal-insulator-metal (MIM) diodes.[18] The first technique has never been employed for spectroscopy and will not be discussed further.

The generation of tunable FIR laser sidebands in a Schottky diode is used for spectroscopy in several laboratories and has produced fine results; however there are several serious drawbacks to this method. Although over 1000 FIR laser lines exist, sideband generation requires the most powerful FIR laser lines. This limits the spectral range to frequencies below 3 THz and also limits the coverage below 3 THz. The molecular transitions which can be measured are limited to those in the vicinity of a strong FIR laser line. The typical absolute

accuracy obtainable is ± 2 X 10^{-7},[19] (± 200 kHz at 1 Thz) determined by the re-settability of the FIR laser. This value is for a system designed for high frequency reproducibility; the frequency uncertainty can increase for a system designed to yield high FIR power. This limitation can in principle be overcome by measuring the FIR laser frequency simultaneously with the FIR spectra. The separation of the sideband radiation from the carrier is a less serious problem . Although these systems generate tens of μw sideband power, the sensitivity is limited by the presence of the stronger carrier. Even after interferometric separation of the sidebands, the power at the carrier frequency still limits the sensitivity to about 2 X 10^{-6} cm^{-1}.

Generation of tunable FIR (TuFIR) radiation by the difference frequency between two CO_2 lasers in a MIM diode was first accomplished in 1984.[18] Later in the same laboratory microwave sidebands were generated on the difference frequency.[20] This method is superior in both frequency coverage and accuracy to the FIR laser sideband system and has comparable sensitivity. The frequency range extends from 0.3 to 6 THz, with greater than 95% coverage. The accuracy is limited by the accuracy of the CO_2 lasers, which are frequency stabilized to 25 kHz, yielding an FIR accuracy of 35 kHz. And although the FIR power generated is less than that using the FIR laser sideband method, the sensitivity is roughly the same because there is no strong carrier laser causing excess noise on the detector. The third order technique of CO_2 laser difference frequency plus microwave sidebands has been employed in a new spectrometer at LENS and will be described below.

THIRD ORDER SPECTROMETER AT LENS

Figure 1 is a schematic of the third order TuFIR spectrometer. The radiation from lasers I and II are combined on a beamsplitter and coupled onto the diode by a 25 mm focal length lens. The microwave radiation is coupled onto the diode by a bias tee connected to the diode junction. The generated FIR is radiated from the diode's whisker in a long wire antenna pattern.[21] This FIR is then collected and collimated by a 30 mm focal length off-axis section of a parabolic mirror. After passing through an absorption cell the FIR is detected on a liquid He cooled Si bolometer. The FIR radiation is frequency modulated (via frequency modulation of the CO_2 lasers) and phase sensitive detected in a lock-in amplifier. The microwave frequency is swept by a personal computer, which also collects the data from the lock-in. Thus we are able to average scans for increased sensitivity. This is essentially the same experimental arrangement as described in ref. 20 only without the acousto-optic modulators isolating the lasers from the diode.

Both CO_2 lasers are frequency stabilized to the 4.3 μm saturated fluorescence signal from low pressure CO_2 cells[22] (not shown in figure 1). These frequencies have been measured to an absolute frequency of better than 5 kHz,[23,24] but without the special locking techniques used in refs. 23 and 24 our measured stability is 25 kHz for each laser. The overall uncertainty of

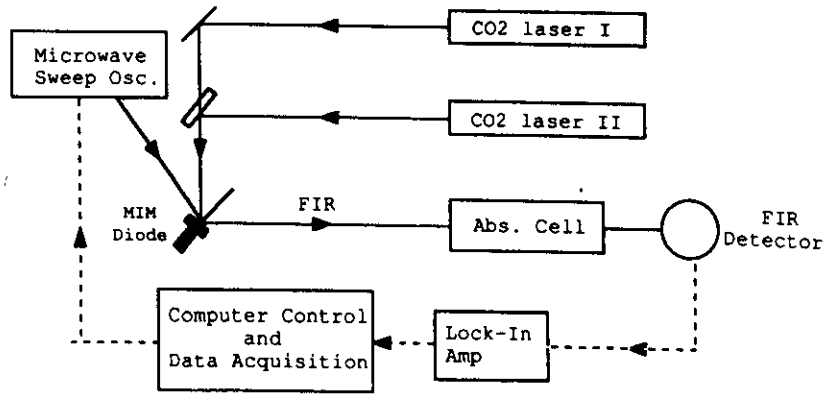

Fig. 1. Block diagram of the third order tunable FIR spectrometer. $\nu_{FIR}=\nu_I-\nu_{II} \pm \nu_{\mu w}$.

our FIR is thus 2 X 25 kHz or 35 kHz. For further information on frequency stabilization of CO_2 lasers, the reader is referred to the article by L. Zink in this publication.

The frequency range of the spectrometer is from 0.3 to 6 THz. The lower limit is set by our bolometer and the upper limit by the largest difference frequency between $^{12}C^{16}O_2$ lasers. Over 100 lines oscillate on each CO_2 laser plus ± 20 GHz tunability of the microwave sweeper yield a 95% coverage of this region, the only gaps occur above 4.5 THz. The range could possibly be extended to 9.28 THz by substituting an ammonia laser for one of the CO_2 lasers.

The spectrometer sensitivity is limited by the FIR power and the sensitivity of the bolometer. 150 mW from each laser and 6-10 dBm of microwave power are applied to the MIM diode, generating about 10^{-7} W of FIR radiation. Although there are two orders of magnitude less power than with the FIR laser sideband technique, the noise sources are also less. Our typical minimum detectable absorption is 10^{-4} in a 1 s time constant, which for a meter long cell corresponds to 10^{-6} cm^{-1}. This is of comparable sensitivity to the laser sideband technique.

MIM Diodes

The heart of the spectrometer is the metal-insulator-metal diode. Used as a rectifier for many years, its possible use for rectification of very high frequencies was noted as early as 1948.[25] The MIM diode has been used for laser frequency measurements since 1969[26,27] and used to measure frequencies up to 200 THz[28] and difference frequencies of visible light.[29] The measurement at 200 THz enabled the most accurate determination of the speed of light[30] and led to the re-definition of the meter.[31]

(2)

The diode consists of an electrochemically sharpened tungsten whisker (25 μm in diameter and typically 3 to 7 mm long) contacting a metal base. The metal base has a naturally occurring thin oxide insulating layer. In the generation of the difference frequency between two CO_2 lasers (second order) nickel is the best material for the base. In third order operation (difference frequency plus sidebands) cobalt appears to be superior. Good second order diodes generate very little third order FIR and vice versa. We also find that sharper tungsten whiskers produce more third order radiation. In general, third order diodes produce about 1/3 as much tunable FIR radiation as second order diodes and are more difficult to make, yet have the advantage of increased tunability. The physical properties of an ideal base material are not yet understood, hopefully in the future different materials or processing techniques will yield even greater TuFIR power.

Applications in Spectroscopy

The spectrometer at LENS has just been completed and the first results will be described below. However, a second order TuFIR spectrometer at the National Institute of Standards and Technology (NIST), in Boulder, Colorado has been in operation for several years and demonstrates the usefulness of this technique for high resolution spectroscopy. Spectra have been obtained for abundant, stable molecules such as CO,[20] providing accurate standards for Fourier transform spectrometers. Free radicals and transient species have been observed,[32] including the molecular ions H_2D^+ and H_3O^+. In addition to absorption spectroscopy the tunable FIR has been employed in an IR-FIR double resonance experiment;[33] for FIR Stark spectroscopy;[34] and in O_2 pressure broadening measurements.[35]

The first molecule observed with the third order system at LENS (during the first week of this school) was ^{13}CO. Traces of the J= 6 - 5 and the J= 26 - 25 lines are shown in figure 2. In all, seven transitions were measured, extending up to the J= 30 - 29 transition at 3.3 THz. New molecular parameters were determined with a 50 kHz (1σ) standard deviation of the fit.

Because of the high frequency accuracy of this technique, small pressure induced shifts of the transition frequency can be measured. Pressure broadening and shift measurements of the CH_3CN molecule have been performed on transitions ranging from J=31 - 30 at 570 GHz to the J= 81 - 80 transition at 1.5 Thz. Although this data is still being analyzed, it does serve to compare our instrument with one of the FIR laser sideband spectrometers. Figure 3 illustrates different K components of the J= 57 - 56 transition measured by the two techniques; eight components were observed with video detection with a FIR laser sideband technique[36] and 12 components were measured with phase sensitive detection using the LENS third order spectrometer (four of which are shown in figure 3). The FIR laser sideband experiment using phase sensitive detection yielded a signal to noise of 50,[17] slightly less than our S/N of 90. Not only were more k components measured with our system, but the accuracy of these measurements is about one order of magnitude higher. The

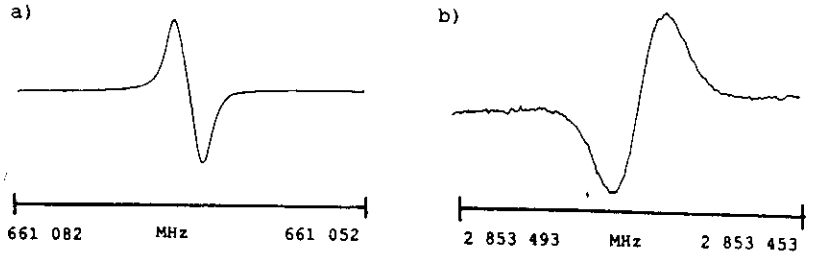

Figure 2. FIR rotational transitions of ^{13}CO observed with the TuFIR spectrometer at LENS. a) J=6-5 b) J=26-25.

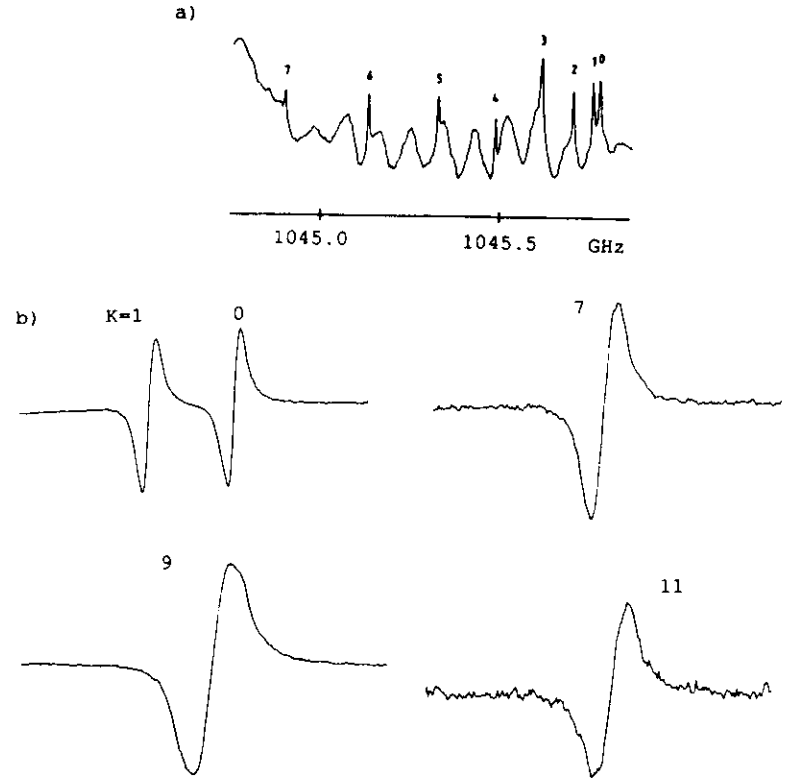

Figure 3. Observed transitions of the CH_3CN molecule; J=57-56, ΔK=0. a) 8 K components seen in video detection with a FIR laser sideband spectrometer (from ref. 36). b) 4 of the 12 components observed in phase sensitive detection with the third order spectrometer at LENS.

accuracy in ref. 36 is 300 - 700 kHz (determined by the resettability of the FIR laser) compared to our accuracy of 55 - 100 kHz. Our uncertainty was limited by the S/N and the transition linewidth.

SUMMARY

The new third order TuFIR spectrometer at the European Laboratory for Nonlinear Spectroscopy has been described and the first results presented. This spectrometer provides nearly complete coverage from 0.3 to 6 THz, with 35 kHz accuracy and a minimum detectable absorption of 0.01% in a 1 second time constant. Plans for this system include the study of astrophysically important molecules, the study of molecular ions, and, taking advantage of the accuracy, measurements on trapped atomic ions (see the article by G. Werth in this publication).

REFERENCES

1. D.M. Watson, R. Genzel, C.H. Townes, and J.W.V. Storey, Astrophys. J. 298, 316 (1985).
2a. B. Carli, F. Mencaraglia, A. Bonetti, M. Carlotti, and I. Nolt, Int. J. IR and MM waves 6, 149 (1985).
b. W.A. Traub and K.V. Chance, Geophys. Res. Lett. 8, 1075 (1981).
3. W.S. Heaps and T.J. McGee, J. Geophys. Res. 90, 7913 (1985).
4. J.W.C. Johns, J. Opt. Soc. Am. B 2, 1340 (1985).
5. P. DeNatale, L.R. Zink, F. Pavone, M. Inguscio, and K.M. Evenson, "Far Infrared Spectrum of 13CO", to be published in J. Mol. Spectrosc.
6. M. Inguscio, G. Moruzzi, K.M. Evenson, and D.A. Jennings, J. Appl. Phys. 60, R161 (1986).
7. K.M. Evenson, H.P. Broida, J.S. Wells, R.J. Mahler, and M. Mizushima, Phys. Rev. Lett. 21, 1083 (1968).
8. K.M. Evenson, R.J. Saykally, D.A. Jennings, R.F. Curl Jr., and J.M. Brown, in Chemical and Biochemical Applications of Lasers: Vol. V edited by C.B. Moore (Academic Press, London, 1980), pp 95-138.
9. K.M. Evenson, Farad. Disc. Roy. Soc. no. 71, (1981).
10. M. Inguscio, Physica Scripta 37, 699 (1988).
11. P. Helminger, J.K. Messer, and F.C. DeLucia, Appl. Phys. Lett. 42, 309 (1983).
12. R.L. Aggerwal, B. Lax, H.R. Fetterman, P.E. Tannenwald, and B.J. Clifton, J. Appl. Phys. 45, 3972 (1974).
13. R.L. Aggerwal and B. Lax, in Nonlinear Infrared Generation edited by Y.R. Shen (Springer-Verlag, Berlin, 1977), pp 19-80.
14. D.D. Bicanic, B.F.J. Zuidberg, and A. Dymanus, Appl. Phys. Lett. 32, 367 (1978).
15. W.A.M. Blumberg, D.D. Peck, and H.R. Fetterman, Appl. Phys. Lett. 39, 857 (1981).
16. J. Farhoomand, G.A. Blake, M.A. Frerking, and H.M. Pickett, J. Appl. Phys. 57, 1763 (1985).
17. G. Piau, F.X. Brown, D. Dangoisse, and P. Glorieux, IEEE J. Quant. Electron. QE-23, 1388 (1987).
18. K.M. Evenson, D.A. Jennings, and F.R. Petersen, Appl. Phys. Lett. 44, 576 (1984).

19. M. Inguscio, L.R. Zink, K.M. Evenson, and D.A. Jennings, "Accurate Frequency of the 119 μm Methanol Laser from Tunable Far Infrared Absorption Spectroscopy", submitted to IEEE J. Quant. Electron.
20. I.G. Nolt, J.V. Radostitz, G. DiLonardo, K.M. Evenson, D.A. Jennings, K.R. Leopold, M.D. Vanek, L.R. Zink, A. Hinz, and K.V. Chance, J. Mol. Spectrosc. 125, 274 (1987).
21. K.M. Evenson, M. Inguscio, and D.A. Jennings, J. Appl. Phys. 57, 956 (1985).
22. C. Freed and A. Javan, Appl. Phys. Lett. 17, 53 (1970).
23. F.R. Petersen, E.C. Beatty, and C.R. Pollock, J. Mol. Spectrosc. 102, 112 (1983).
24. L.C. Bradley, K.L. Soohoo, and C. Freed, IEEE J. Quant. Electron. QE-22, 234 (1986).
25. H.C. Torrey and C.A. Whitmer, Crystal Rectifiers (McGraw-Hill, New York, 1948), p. 7.
26. V. Daneu, D. Sokoloff, A. Sanchez, and A. Javan, Appl. Phys. Lett. 15, 398 (1969).
27. An excellent review of frequency measurements using MIM diodes as well as other devices is provided by: D.A. Jennings, K.M. Evenson, and D.J.E. Knight, Proc. IEEE 74, 168 (1986).
28. K.M. Evenson, D.A. Jennings, F.R. Petersen, and J.S. Wells, in Laser Spectroscopy III, edited by J.L. Hall and J.L. Carlsten (Springer-Verlag, Berlin, 1977), pp 56-58.
29. R.E. Drullinger, K.M. Evenson, D.A. Jennings, F.R. Petersen, J.C. Berquist, and L. Berkins, Appl. Phys. Lett. 42, 137 (1983).
30. D.A. Jennings, C.R. Pollock, F.R. Petersen, R.E. Drullinger, K.M. Evenson, J.S. Wells, J.L. Hall, and H.P. Layer, Opt. Lett. 8, 136 (1983).
31. Comptes Rendus des Seances de la 17e CGPM, BIPM, Sevres, France (1983).
32. For a more complete listing and references see: K.M. Evenson, D.A.Jennings, and M.D. Vanek, in Frontiers of Laser Spectroscopy of Gases (NATO ASI Series C; Vol. 234), edited by A.C.P. Alves, J.M. Brown, and J.M. Hollas (Kluwer Academic Publishers, Dordrecht, 1988).
33. M. Inguscio, L.R. Zink, K.M. Evenson, and D.A. Jennings, Opt. Lett. 12, 867 (1987).
34. L.R. Zink, D.A. Jennings, K.M. Evenson, A. Sasso, and M. Inguscio, J. Opt. Soc. Am. B 4, 1173 (1987).
35. D.A. Jennings, K.M. Evenson, M.D. Vanek, I.G. Nolt, J.V. Radostitz, and K.V. Chance, Geophys. Res. Lett. 14, 722 (1987).
36. F.X. Brown, D. Dangoisse, and J. Demaison, J. Mol. Spectrosc. 129, 483 (1988).

High-Resolution and High-Sensitivity Spectroscopy Using Semiconductor Diode Lasers.

M. INGUSCIO

Dipartimento di Fisica and European Laboratory for Nonlinear Spectroscopy (LENS)
Università degli Studi di Firenze - largo E. Fermi 2, I - 50125 Firenze, Italia

1. – Introduction.

As clearly discussed by Prof. SCHAWLOW in his introductory lecture[1], we spectroscopists still have the problem of finding tunable lasers and, once the laser is tunable, we want it to be more and more monochromatic. Indeed, due to the central role played by the radiation source in coherent spectroscopy, the scientific achievements strictly followed the technical development of lasers.

Semiconductor diode lasers (SDL) are certainly lasers with a wide wavelength tuning range. Although they were invented more than thirty years ago, they were not used much in atomic spectroscopy until recently[2]. In the early times, diode lasers had to be operated at low temperatures, they emitted over several cavity modes and were unreliable. Recently, semiconductor diode lasers have been rapidly improving in power, spectral purity and wavelength coverage: they can now operate c.w. at room temperature and produce tens of milliwatt on a single mode. Nowadays these lasers are showing some specific properties which make them suitable sources of radiation for very-high-resolution and/or extremely-high-sensitivity experiments. In general, an extreme simplification of sophisticated experimental schemes can be obtained. As an example let us refer to the resolution of Lamb shift of H_α transition in hydrogen. This measurement constitutes one of the cornerstones of atomic spectroscopy and the historical recording, obtained in 1972 at Stanford University by a dye-laser spectrometer, is reported both in Schawlow and Hänsch lectures[1,3]. The same recording is reported in fig. 1, as obtained in Munich[4] nearly twenty years later by using an InGaAlP free-running laser diode.

In this lecture, we show some of the possibilities offered by semiconductor

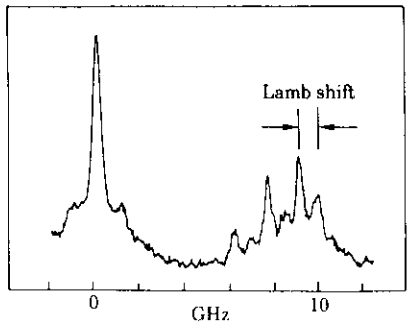

Fig. 1. – Doppler-free saturation spectrum of the red Balmer-α line of atomic hydrogen with resolved fine-structure components as recorded in Munich (ref. [4]) using a free-running InGaAlP laser diode.

diode lasers in atomic and molecular spectroscopy by describing experiments recently performed in the visible ((650 ÷ 690) nm) and near infrared ((750 ÷ 850) nm).

2. – Overview on diode laser characteristics and operation.

The diode laser basically works as a p-n junction biased in the forward direction. The recombination of electrons and holes takes place at the junction and leads to the emission of radiation at a frequency depending on the energy gap between the conduction and the valence bands. The reflectivity of the cleaved facets of the diode is sufficient to have dominance of stimulated emission.

In order to have continuous-wave operation of the laser, it is necessary to confine the carriers and the photons in a well-defined region in order to have enough gain. This is commonly obtained using double heterostructures, where the active region is sandwiched between two layers of semiconductors with a larger band gap. This prevents the carriers from escaping the active region, but also light is confined in the same active region because a higher band gap corresponds to a smaller index of refraction. In the first lasers, confinement was achieved only in the direction in which the current was injected (gain-guided lasers), while now also «index-guided» lasers are available, in which the active region is limited in all directions by a higher-band-gap material. It is evident that real devices have complex structures and require important technological advances [5]. More recently, also quantum-well and multiple-quantum-well lasers became available, with lower threshold currents and higher output powers compared with normal double heterostructures.

Important characteristics which are relevant for the use of SDL sources in atomic and molecular spectroscopy are spectral coverage, tunability, spectral linewidth and amplitude stability.

The emission wavelength depends on the band gap and in principle it should be possible to construct lasers at all wavelengths by choosing the proper stoichiometric abundance for the dopant element, provided that direct interband transitions can occur. For instance, one could obtain emission from 1100 to 1650 nm using InGaAsP, or cover the (700 ÷ 890) nm and (630 ÷ 690) nm intervals by means of GaAlAs and AlGaInP, respectively. Of course, the material must have good optical and electrical characteristics in order to minimize losses. For this reason, for instance, room temperature operation in the blu-green region was only recently demonstrated. In practice, laser diodes are commercially available only at sparsely distributed emission wavelengths and the experimentalist soon faces the problem of tuning the laser to the precise atomic or molecular absorption. At a first attempt, one can change the emitted wavelength by changing the diode temperature. Indeed, the semiconductor gap depends on the temperature and overall spans of the order of some 20 nm can easily be obtained, considering that operation at low temperatures is even more efficient and that operation down to liquid-helium temperature has been demonstrated. Tuning by temperature, however, is discontinuous, and this is a significant limitation. Changes in temperature lead to a change of the cavity length and hence of the cavity modes. Typical tuning with this effect is of the order of 0.06 nm/°C (– 30 GHz/°C). At the same time, the gain curve shifts by about 0.25 nm/°C. Since the two temperature dependences are different, we have a continuous tuning (– 30 GHz/°C) until the longitudinal-mode hopping caused by the gain curve shift: the general aspect is that of a staircase with sloping steps, essentially causing wavelength changes in a rather unpredictable way. From the above considerations we also learn that an extremely good thermal stability (better than 1 mK) is required in view of narrow-linewidth operation. Thermal tuning is also obtained via Joule effect by changing the current of operation. This tuning, at a rate of about 3 GHz/mA, is rather slow while a faster control, of about 300 MHz/mA, can be obtained thanks to the change in the medium refractive index caused by the change in the current density. Also in this case we deduce that an injection current stability of at least 1 μA is required to reduce effects on the linewidth.

Let us now in fact discuss the problem of spectral linewidth. An exhaustive treatment of the different factors determining the linewidth can be found in ref. [6]. However, these lasers are so small, 100 to 500 μm long, 0.1 to 2 μm thick and 2 to 20 μm wide, that the predominant broadening is caused by the quantum fluctuations of the phase as early described by SCHAWLOW and TOWNES [7], who showed the limit linewidth to be inversely proportional to the output power and to the square of the optical-mode volume. Here we report, from ref. [8], the modified formula which, by the introduction of a factor α, takes into account the

dependence of the refractive index on the carrier density:

$$(1) \qquad \Delta\nu_{\mathrm{FWHM}} = \frac{h\nu}{8\pi P_0}\left(\frac{c}{nL}\right)^2\left[aL + \ln\left(\frac{1}{R}\right)\right]\ln\left(\frac{1}{R}\right)n_{\mathrm{sp}}(1+\alpha^2),$$

where P_0 is the output power, L is the cavity length, R is the facet reflectivity, a gives the distributed losses in the cavity, c/n the group velocity, and n_{sp} the spontaneous-emission factor which is of the order of unity. In the case of a typical diode laser ($P_0 = 10\,\mathrm{mW}$, $L = 300\,\mu\mathrm{m}$, $R = 0.3$, $\alpha \sim 4 \div 5$), a linewidth of several MHz can be estimated. An increase of the cavity length or, more generally, of the cavity quality factor Q is hence needed to reduce the linewidth. As we shall see, this is at the base of the development of external optical cavities for line-narrowing purposes.

As for amplitude stability, the intrinsic stability of the structure of the semiconductor laser reduces the sources of noise. The properties of the active medium give rise to a peculiar AM and FM noise spectrum, which has been accurately investigated by HOLLBERG at NIST[9]. However, in the low-frequency range (frequencies lower than 10 MHz), typical for simple absorption spectroscopy experiments, an amplitude noise only $(10 \div 20)\,\mathrm{dB}$ above the shot noise level has been measured[10], while the corresponding one for dye lasers can be even two orders of magnitude larger. At 800 nm and 5 mW power, we can compute a shot noise level of the order of 10^{-8}, hence a factor 10 dB worse yields for the SDL a relative amplitude stability of the order of $10^{-6} \div 10^{-7}$, at 1 Hz bandwidth. This impressive stability is at the base of the development of high-sensitivity absorption spectroscopy, for instance applied to molecular forbidden transitions, as we shall discuss in the last section of this contribution.

3. – Line narrowing and tuning with grating feedback.

We have seen that the linewidth of commercial SDLs is too large for applications in high-resolution spectroscopy, however it can be easily reduced by means of electronic or optical feedbacks[10].

In electronic-feedback schemes, the injection current is changed and very fast electronics is needed since the FM noise extends to high frequencies. The change in the injection current produces changes not only in the emitted frequency but also in the emitted power and this introduces an additional amplitude noise. Of course, the electronic stabilization method does not provide any control of the emission wavelength.

More popular are certainly optical-feedback methods. They are based on the simple idea of increasing the Q factor by coupling the diode to another cavity. Weak-feedback and strong-feedback regimes are both successful. The first is, for instance, ensured by the coupling with a high-Q Fabry-Perot interferometer, while in the second the laser is operated in an external cavity. If the feedback is selective in wavelength, it is possible consequently to control the emission. In this lecture we concentrate on the scheme using the strong feedback, which has been the most used in our laboratory after learning the art from HOLLBERG during his visit to LENS[11]. Our design, as the many others nowadays used all over the world, is a sort of compromise between easy construction, reliability, good spectral characteristics for high-resolution and high-sensitivity spectroscopy. Typically we can obtain a reduction by about two orders of magnitude of the emission linewidth and achieve a continuous wavelength tuning within a range of several nanometers at fixed temperature. In general one should use antireflection coating on the diode facet in order to increase the amount of feedback light coupled in. However, many of the best diode lasers available on the market are already provided with a high-reflectance coating on the back facet and a reduced-reflectance coating on the output facet. This allows one to operate the diode lasers in a pseudo-external-cavity configuration, as schematically shown in fig. 2. The first-order diffracted beam from a grating, mounted in the Littrow configuration, is fed back into the laser diode. An intracavity beam splitter ((20 ÷ 30)% reflectance) provides an additional output to the zeroth-order one and somewhat controls the feedback amount. Indeed a higher feedback reduces the out-coupled power, but also increases the wavelength tuning range. Further details concerning collimating lens and in general the actual construction can be found elsewhere[12], as well as the description of how the diode temperature and injection current stability stringent requirements can be fulfilled.

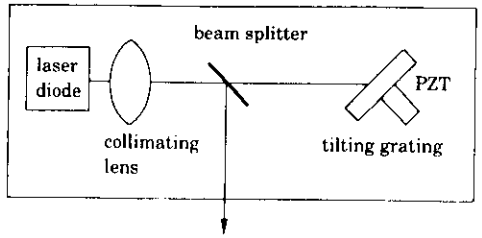

Fig. 2. – Scheme of the «pseudo-external-cavity» configuration adopted for the frequency narrowing and tuning of commercial semiconductor diode lasers.

The simple rotation of the grating allows the coarse tuning of the extended-cavity lasers over a range of $\sim 10\,\mathrm{nm}$. In particular, because of the finite reflectivity of the chip facets, the longitudinal modes of the solitary laser diode do not change, while the feedback from the grating allows one to select one of these modes and to drastically suppress other side modes. Fine tuning to the frequency of interest can then be achieved by slightly changing the temperature and the injection current of the diode. Continuous frequency scans of the order

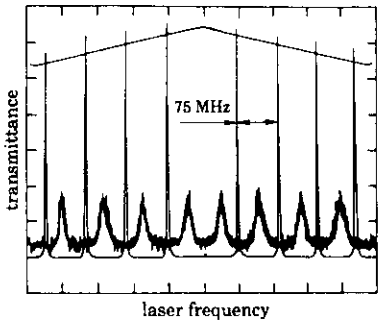

Fig. 3. – Superimposed transmission spectra from a 75 MHz free-spectral-range Fabry-Perot interferometer as the frequency of the diode laser is scanned up and down without optical feedback (broad peaks) and in the presence of optical feedback from a grating (narrow peaks). In the first case, the laser frequency was scanned up and down by sending a ramp (shown in the top of the figure) to the injection current supply. In the second case, the ramp was also sent to the PZT on the grating in order to simultaneously change the length of the external cavity.

of ~ 10 GHz are accomplished by synchronously sweeping the length of the cavity, by means of a piezoelectric transducer on the grating, and the injection current. The effect of the increased Q factor in the cavity and consequent line narrowing can be evidenced by recording the transmission peaks of a Fabry-Perot interferometer as the laser frequency is scanned. A typical situation is illustrated in fig. 3. Broad peaks are recorded by blocking the return beam from the grating (*i.e.* with the laser as is commercially available), while much narrower peaks (the figure is essentially a recording of the Fabry-Perot finesse) are obtained in the presence of the optical feedback. Figure 3 has been taken using an InGaP laser at 690 nm [13], but the results are rather general as we have experienced with AlGaAs lasers operating at 780, 820 and 850 nm, both using double heterostructures and multiple quantum wells. A more accurate analysis of the spectral properties of extended-cavity semiconductor diode lasers can be performed by observing the beat note from two of them superimposed in a nonlinear detector. This is illustrated in fig. 4 for the mixing in a fast photodiode of two extended-cavity multiple-quantum-well lasers at 850 nm. In the millisecond time scale the laser linewidth is of the order of 50 kHz, corresponding to $\Delta\nu/\nu \simeq 10^{-11}$, while acoustic noise is responsible for the increase to about 400 kHz over longer time scale. Heterodyne measurements require particular care in the optical isolation between the lasers, to avoid injection locking which can be caused by even a slight feedback.

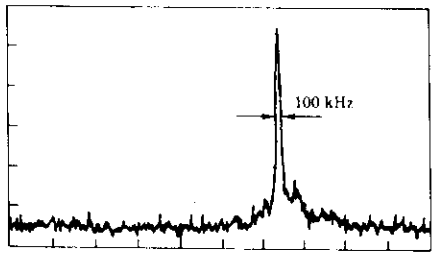

Fig. 4. – Beat note from the heterodyne between two free-running AlGaAs multiple-quantum-well lasers mounted in extended-cavity configuration. Wavelength is grating-tuned at $\lambda = 850$ nm and the two emissions are about 2.2 GHz apart. From the recording, a value of about 50 kHz can be estimated for the laser linewidth in the millisecond time scale.

4. – High-resolution spectroscopy of atoms.

The impressive characteristics of the conductor diode laser configurations so far described have already allowed a large number of interesting applications in atomic spectroscopy. Here we shall concentrate on very few of them particularly interesting to show the potentialities of these compact laser sources.

Let us start with the investigation of forbidden transitions. This is in general an important task for atomic spectroscopy mostly related to the possibility of developing laser-based frequency markers in the visible. We chose to detect the $5s\ ^1S^0$-$5p\ ^3P_1$ intercombination transition of strontium at 689.488 nm. This wavelength is accessible to the newly available InGaP lasers and the sub-Doppler recording can provide a significant test, as the atomic line has a radiative width of only 8 kHz [13]. Strontium atoms were produced in a hollow-cathode discharge designed to allow access to the counterpropagating beams necessary for the Doppler-free recording [14]. Indeed, in spite of the weakness of the transition, a 1% absorption signal could be directly detected with a small saturation dip (~ 5%) on top, thanks to the low-amplitude noise of the diode laser. The Doppler-free contribution to the signal could be consequently enhanced using a polarization spectroscopy scheme [15]. A typical recording is reported in fig. 5. Except for the radiation source, which in that case was a more conventional dye laser, a description of the experimental details can be found in [16]. The recorded linewidth was mostly determined by collisional effects due to the discharge environment and the laser jitter contribution could be estimated to be less than 1 MHz. More recently, the same intercombination transition has been observed and investigated in a Sr atomic beam [17] for a more careful analysis of the laser linewidth.

Let us now further illustrate the potentialities of grating-tuned semiconductor diode lasers showing and discussing some applications to the spectrum of atomic oxygen. Elusive to continuous-wave excitation from the ground state, this atom can conveniently be studied by means of laser spectroscopy of transi-

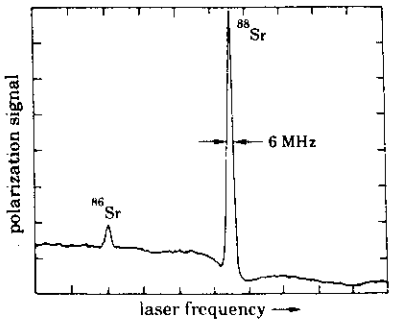

Fig. 5. – Doppler-free polarization spectroscopy of the $5s\,^1S_0$-$5p\,^3P_1$ intercombination transition of strontium at 689.488 nm as recorded with an InGaP semiconductor laser in extended-cavity configuration.

tions starting from excited levels produced in the same Ar or He discharge used for the dissociation of O_2 added in traces[18]. As evidenced in the scheme of fig. 6, transitions starting from the lowest triplet and quintet states are well suited for the investigation by means of AlGaAs lasers. The transition at 777 nm has immediately been recognized as interesting[11] because its lower level is metastable and possibly involved in a novel scheme for radiative cooling of

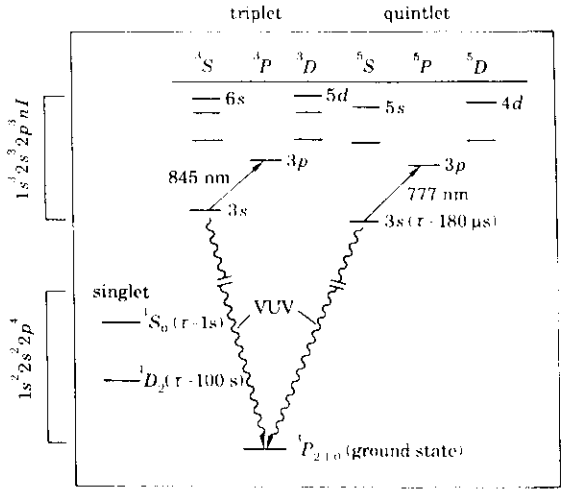

Fig. 6. – Simplified energy level scheme of atomic oxygen. Transitions studied with high resolution by means of AlGaAs diode lasers are evidenced.

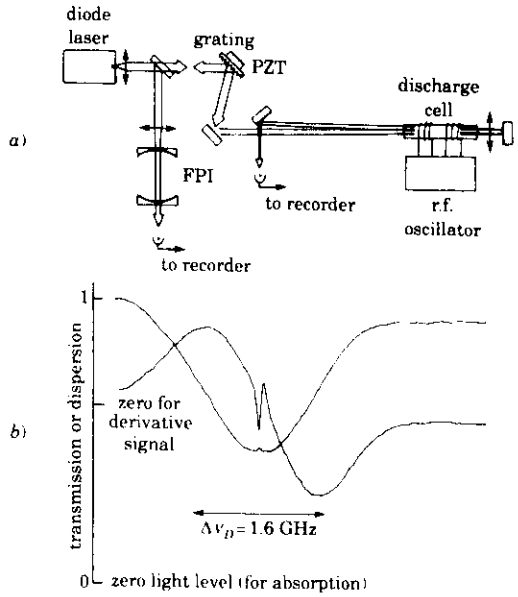

Fig. 7. – Oxygen absorption on the $^3S_2$-$^3P_3$ transition at 777 nm as detected with a grating-tuned AlGaAs semiconductor diode laser. Two counterpropagating beams are present in the cell and a saturation dip can be recorded at the line centre. This is evident in the derivative signal (*b*)) where phase-sensitive detection is applied.

oxygen. Also, the metastable level can be efficiently populated in a weak radiofrequency discharge and fig. 7*a*) reports the absorption signal as recorded on the transmitted light after passing twice through the cell: the laser beam was retroreflected by a mirror to allow saturation spectroscopy. It is worth noting the low noise level which reflects the extreme reduction in the laser amplitude fluctuations. By adding a modulation in the scanning piezo voltage, frequency modulation of the laser output can be easily achieved. This, in combination with phase-sensitive detection, allows the recording of a derivative signal and the enhancement of the saturation dip at the line centre, as displayed in fig. 7*b*). Let us now use this same atomic transition to illustrate more in general the versatility of the semiconductor laser as combined with different nonlinear spectroscopy techniques. The scheme of a general apparatus[19] is shown in fig. 8. A key role is played by the electro-optic modulator (EOM) which, in combination with the proper choice of the *A* and *B* optical devices, can act as a simple amplitude modulator, an alternate σ^+-σ^- polarizer, a π polarizer and so on. For instance, when *A* is not used and the EOM is placed between two parallel linear

(10)

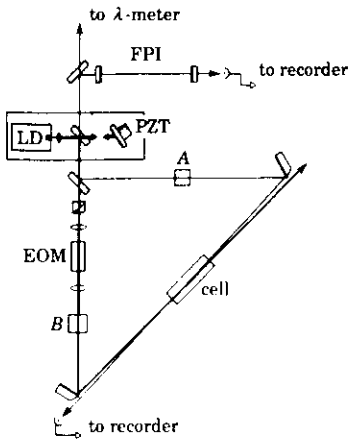

Fig. 8. – A general experimental apparatus used to combine a semiconductor diode laser with various Doppler-free spectroscopic schemes. *A* and *B* indicate different optical devices depending on the detection technique. A high-finesse Fabry-Perot interferometer (FPI) is used for the frequency scan calibration, while laser wavelength is determined by a λ-meter.

polarizers, the system is equivalent to a mechanical chopper and the scheme is essentially a Hänsch-type one. Consequently, a typical recording is shown in fig. 9*a*). As expected, only the sub-Doppler signal is recorded, while a broader pedestal is caused by the velocity-changing collisional effects [20]. The lineshape can be fitted to the sum of a Lorentzian and a Gaussian and the two contributions are separately shown in the lower part of fig. 9*b*). As is well known, the velocity-changing collision contribution to the signal can be reduced by changing the physical observable under investigation in the technique. In this respect an important example is provided by polarization spectroscopy, where the vapour birefringence, instead of the absorption, is recorded. For instance, the recording previously reported in fig. 5 for strontium showed no evidence for velocity-changing collisional pedestal, which on the contrary would have been rather important in a simple saturation spectroscopy scheme, the observed transition being originated from an atomic ground state. Coming back to the scheme of fig. 8, the pump beam can be manipulated in order to create an atomic orientation $\sum_J^{+J} n_{m_j} m_j \neq 0$ or an atomic alignment $\sum_J^{+J} n_{m_j} m_j^2 - (1/3)J(J+1) \neq 0$ with n_j and m_j, respectively, the relative population and the eigenvalue of the Zeeman sublevel J_z. Differently from the level population, observable involved in simple saturation spectroscopy, both the orientation and the alignment are significantly affected by collisions and the atoms emerging from a collision do no

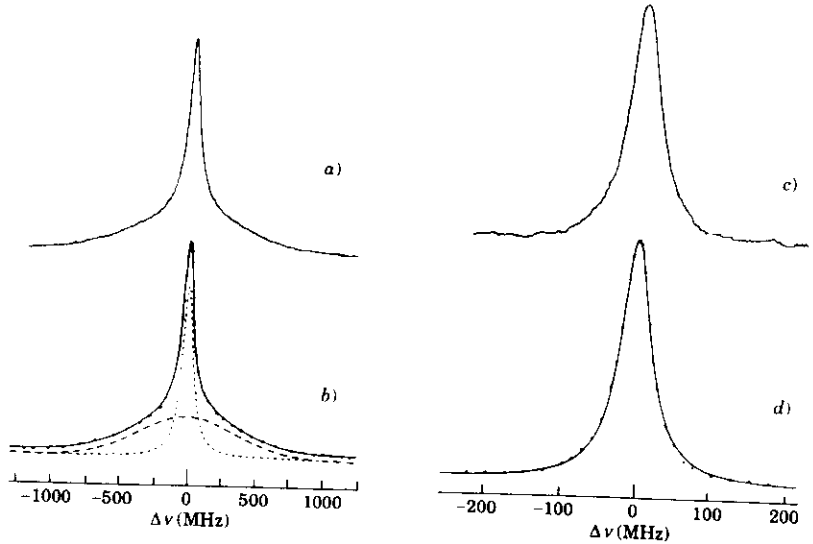

Fig. 9. – Examples of different sub-Doppler lineshapes obtained using the apparatus illustrated in fig. 8. In *a*), the saturation spectroscopy signal (Hänsch-type configuration) is the superposition of a Lorentzian and a Gaussian pedestal caused by the velocity-changing collisions, as evidenced by the fit in *b*). In *c*) the «alignment» spectroscopy configuration allows the elimination of the Gaussian contribution to the lineshape which in *d*) is fitted to a pure Lorentzian.

longer contribute to the recorded signal in the probe beam. This is clearly evident in fig. 9*c*), where the same transition of fig. 9*a*) and 7 is recorded using a configuration of «alignment» spectroscopy. The lineshape can be fitted using only a Lorentzian as shown in fig. 9*d*). The width of the Lorentzian is affected by some collisional broadening, since the experiment is performed in a cell. However, the sensitivity of the technique allowed the operation with low pressures (~ 100 mTorr of Ar buffer gas) and the extrapolation to zero pressure led to a determination of the radiative lifetime of the upper level of the transition ($^5P_3$, $\tau = 7$ ns). This lifetime is an important parameter for the real feasibility of the oxygen radiative cooling scheme proposed in [11] and analysed with a Monte Carlo simulation in [21].

The simplicity of the semiconductor lasers makes easy, and accessible to most laboratories, the operation of many of them in the same experiment. This is, for instance, useful when the experiments consist in the precise measurement of isotope shifts or atomic structures. Direct frequency measurements can indeed be obtained by heterodyning two independent lasers frequency-locked

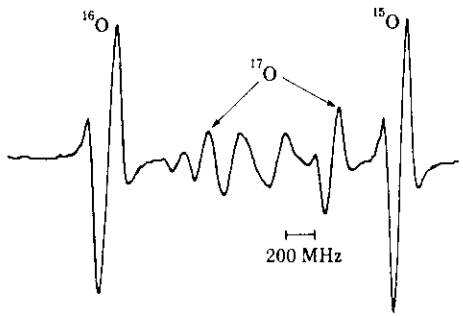

Fig. 10. – Sub-Doppler spectrum of the three stable isotopes of atomic oxygen as observed in an enriched sample ($^5S_2$-$^5P_3$ transition at 777 nm). The third-derivative signal is shown.

on two different atomic signals. For atomic oxygen this was the case for the $^{16,17,18}O$ isotope shift and for the hyperfine structure of ^{17}O. In fig. 10 the 777 nm transition using an enriched atomic sample[22] is recorded. A 3*f* detection scheme was used to eliminate the background slope, which instead is present in the first-derivative signal. The sample absorption was ~ 5% and the Lamb dip signal was ~ 5% of the absorption. The recording reported in the figure was obtained with a lock-in time constant of 1 ms. A servo loop (bandwidth ~ 10 Hz) was then used for frequency-locking each laser on the selected isotope signal. The scheme typically consisted of a lock-in, an integrator and a high-voltage amplifier; the output of the integrator was fed back to the high-voltage amplifier, which controlled the grating position by means of the piezoelectric transducer. The intrinsic frequency stability of such a laser system is determined by the increased Q of the optical cavity, which reduces the fast frequency fluctuations; only a relatively slow electronics is then required to correct long-term drifts. The beat note between two lasers can be observed using a spectrum analyser, as already shown in fig. 4. However, in the actual measurements with the lasers locked on the atomic third-derivative signals, a broadening of the beat note arises from the frequency modulation of the lasers and can be minimized by in-phase modulation. The accuracy of the heterodyne measurement is determined by the signal-to-noise ratio and width of the locking signal. From signals like those shown in fig. 10, isotope shifts and hyperfine structures could be measured with an accuracy of the order of 100 kHz. It is evident that heterodyne of semiconductor diode lasers can be a powerful and straightforward method for precise laser spectroscopy, in particular in combination with mixing schemes based on fast photodiodes or, even better, on GaAs Shottky diodes[9,23,24].

5. – High-sensitivity spectroscopy of forbidden molecular transitions.

As anticipated, the extremely good amplitude stability of semiconductor diode lasers opens the possibility of performing high-sensitivity absorption measurements directly on the light transmitted by the sample.

A first example is given by the detection and investigation of molecular oxygen at 760 nm. Transitions of O_2 in the visible-near infrared belong to the $\chi^3\Sigma_g^-$-$b^1\Sigma_g^+$ band first observed by BABCOCK and HERZBERG[27] in the atmospheric absorption from Mount Wilson. These are magnetic-dipole transitions with an absorption coefficient as low as $\alpha \sim 10^{-6}$ cm^{-1}. In the laboratory, they could be detected only by means of intracavity techniques involving dye lasers[28,29]. The powerfulness of stable diode lasers for the detection of these forbidden transitions was early suggested to us by the recording of an absorption from the room atmosphere after a path length of only 20 cm[30]. This opened the possibility of performing more systematic investigations using an extended-cavity semiconductor diode laser spectrometer. The scheme of the spectrometer, which, as we shall discuss, is also used more in general for overtone molecular spectroscopy, is shown in fig. 11. The laser frequency is controlled by changing PZT voltage and injection current as done for atomic spectroscopy. A dither (fast modulation) is added when phase-sensitive detection is used. The radiation transmitted by the sample is detected by means of a photodiode, while a second photodiode is used to obtain a reference for the laser amplitude and to eliminate the baseline (due to the amplitude modulation) by means of differential detection. The absorption cell is 150 cm long. Typical measurements for oxygen are illustrated in fig. 12. An absorption recorded

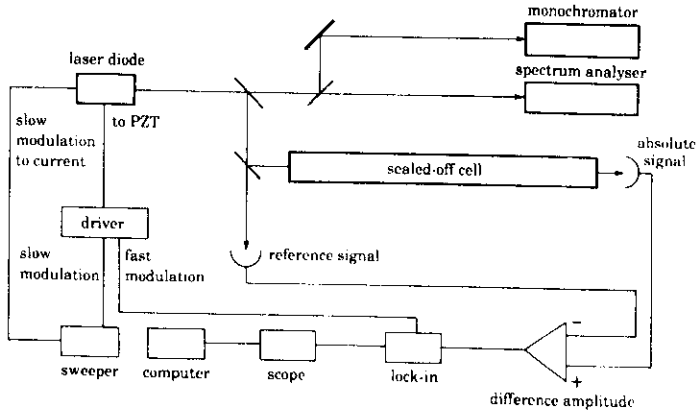

Fig. 11. – Scheme of the diode laser spectrometer used for the investigation of weak molecular absorptions.

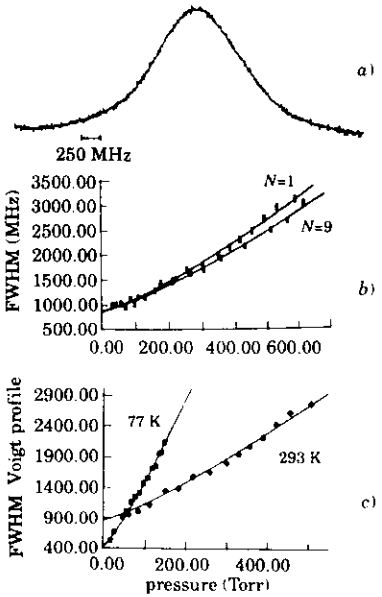

Fig. 12. – Absorption of molecular oxygen on the $^rP(K'' = 9)$, $v = 0$-0 component of the forbidden $\chi^3\Sigma_g^- - b^1\Sigma_g^+$ band (a)). In b) the dependence (on two different components) of the homogeneous contribution to the linewidth on the pressure is reported. In c) the behaviour of the collisional broadening on the same component at two different temperatures is shown.

with a gas pressure of 120 Torr is shown in fig. 12a). The lineshape is fitted to the convolution of a Gaussian and a Lorentzian. The latter contribution is due to collisional broadening and can be investigated at different pressures [31]. The results of different measurements in the (0 ÷ 1000) Torr range (on two different components) are plotted in fig. 12b), while in fig. 12c) the behaviour of the collisional broadening at two different temperatures is shown. This demonstrates how important parameters for atmospheric physics can be extracted from a relatively simple spectrometer. Wider applications can certainly be found in overtone molecular spectroscopy. Fundamental vibrations of molecules produce spectra in the medium infrared. The anharmonic contribution to the potential makes possible the excitation of overtone frequencies which can occur in the visible-near infrared, where more convenient tunable laser sources and room temperature sensitive detectors are available. Specially for polyatomic molecules, where also combination vibrations are present, overtone spectra are rich and interesting to be investigated also for a better modelling of the molecular structure. However, it is also well known that the intensity of successive

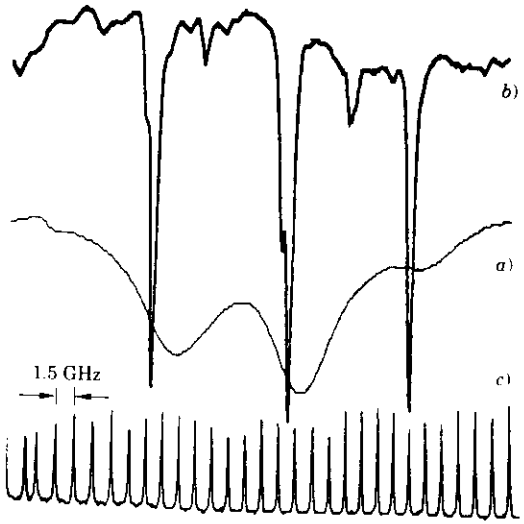

Fig. 13. – Recording of the absorption of CH_4, methane, around 886 nm by means of AlGaAs laser. Temperature and pressure are, respectively, 293 K and 100 Torr in a) and 77 K and 1 Torr in b). The total frequency scan is 42 GHz, as determined by the transmission of a reference Fabry-Perot (c)).

overtones and combination transitions decreases very rapidly with the increase of the number of vibrational modes and/or quanta involved. As a consequence, overtone molecular absorption in the visible is very weak ($\alpha \sim 10^{-6}$ cm^{-1} can be again a typical absorption coefficient) and constitutes an interesting challenge for the spectrometer based on our semiconductor diode lasers. A comprehensive list of the most interesting molecules and of the wavelengths at which they are accessible can be found elsewhere [32]. Let us illustrate the powerfulness of the technique using the detection of CH_4, methane, at 886 nm, where a number of combination bands are superimposed ($3\nu_1 + \nu_3$, $2\nu_1 + 2\nu_3$, $\nu_1 + 3\nu_3$, $4\nu_3$). This produces an almost continuous absorption [33] as, for instance, shown in fig. 13a). The spectrum is part of a systematic investigation performed at different temperatures to study the behaviour of the various components and possibly facilitate the line assignment. Indeed the room temperature recording, taken with CH_4, pressure of 100 Torr, is simplified when the temperature is lowered to 77 K, as shown in fig. 13b). In this case also the pressure could be reduced to 1 Torr and the linewidths are narrower because of the reduced Doppler and collisional broadenings. It is obvious that the signal-to-noise ratios observed for the detection of these overtone transitions, as well as of the oxygen forbidden

transitions, can constitute a good base for the development of high-sensitivity absorption measurements. Indeed, the transitions in methane provide a system to test and compare all the existing techniques mainly based on the modulation of the laser radiation [34]. Semiconductor lasers offer the advantage of achieving an easy and fast frequency modulation of the laser output itself by acting on the injection current. For this reason the diode lasers constitute optimal candidates for detection techniques as wavelength and frequency modulation.

In the wavelength modulation technique an a.c. component is added to the injection current of the diode laser; the frequency of modulation must be smaller than the linewidth of interest, so that the absorption is probed simultaneously by a number of sidebands. If the modulation frequency is increased to exceed the linewidth, only one sideband will be absorbed at a time, giving rise to a characteristic heterodyne beat signal at the modulation frequency. If the modulation index is chosen so that only one higher sideband and one lower sideband have appreciable amplitude, we are in the case of frequency modulation spectroscopy (one-tone FM).

A variation on the theme of the FM spectroscopy with respect to the one-tone technique, previously described, is represented by the two-tone spectroscopy: in this case the laser emission is simultaneously modulated at two distinct but closely spaced angular frequencies. Also here a heterodyne signal is obtained, but it occurs at the difference frequency between the two sidebands eliminating the need of high-speed detectors and making large-linewidth detections possible.

The trick of the modulation techniques is to observe the absorbed signal with an associated noise typical of the modulation-demodulation frequency and the electronic bandwidth chosen. Because of the $1/f$ behaviour of the amplitude noise in the power spectrum of semiconductor diode laser emission, the possibility of obtaining more sensitive detections is bound to the choice of higher demodulation frequencies.

In fig. 14*a*) the direct absorbed signal of one CH_4 component without any demodulation at 100 Torr is shown (corresponding to a relative absorption of 3.6%): the associated S/N is more than 20 and the bandwidth equal to 100 Hz. In fig. 14*b*) the demodulated signal (third derivative) is shown at 1 kHz, 100 Hz of bandwidth and a pressure of 100 mTorr, corresponding to a S/N of about 10.

Finally, in fig. 14*c*) the demodulated signal with the two-tone technique at frequencies around 500 MHz and 1 Hz of bandwidth is shown (pressure of 500 mTorr) corresponding to a S/N ratio of a few thousands.

A minimum detectable absorption has been demonstrated [34] (corresponding to a S/N ratio equal to 1) for the low-wavelength modulation (1 kHz), high-wavelength modulation (100 MHz) and two-tone frequency modulation ((390 ± 5) MHz) techniques, respectively, of $4.5(1) \cdot 10^{-7}$, $9.7(3) \cdot 10^{-8}$ and $6.4(2) \cdot 10^{-8}$.

Considering the absorption limit derived by the calculated shot noise, the minimum detectable absorptions measured in the high-frequency detection techniques are about 6 dB over this value.

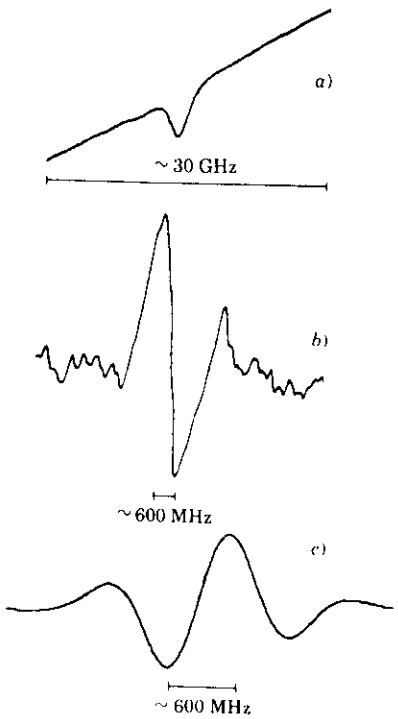

Fig. 14. – *a*) represents the direct absorbed signal of one CH_4 component without any demodulation at 100 Torr (corresponding to a relative absorption of 3.6%): the associated S/N is more than 20 and the bandwidth equal to 100 Hz. *b*) represents the demodulated signal (third derivative) at 1 kHz, 100 Hz of bandwidth and a pressure of 100 mTorr, corresponding to a S/N of about 10. *c*) represents the demodulated signal with the two-tone technique at frequencies around 500 MHz and 1 Hz of bandwidth (pressure of 500 mTorr) corresponding to a S/N ratio of a few thousands.

6. – Conclusions.

This overview should have convinced that semiconductor diode lasers are important coherent sources for atomic and molecular spectroscopy. They can potentially cover the visible and the near infrared, with gaps which can be reduced with optical feedback techniques and with the development of new ma-

terials. Coverage can be extended to blue and near ultraviolet by frequency doubling. Optical feedback techniques can drastically reduce the linewidths to the level which allows also very narrow transitions to be investigated. Available powers start to be comparable with that of dye lasers and, however, the extremely reduced amplitude fluctuations are making high-sensitivity measurements possible even with low power. Further important possibilities are opened by the possibility of fast frequency control of the laser emission. Complex experimental schemes can be simplified by the use of semiconductor diode lasers and experiments which could not even be conceived before can now be performed.

Progresses in the fascinating world of laser spectroscopy have always depended on the development of new sources of radiation and we are sure that the availability of these new laser devices will allow new important chapters to be written.

* * *

Many motivated researchers of Firenze (LENS and Department of Physics), Napoli (Department of Physics) and Pisa (Scuola Normale Superiore) have contributed to this work (M. BARSANTI, M. DE ANGELIS, P. DE NATALE, C. FORT, L. GIANFRANI, G. GIUSFREDI, F. MARIN, F. PAVONE, M. PREVEDELLI, A. SASSO) as well as many guest workers (G. DI LONARDO, K. ERNST, L. HOLLBERG, L. JULIEN, K. LEHMANN, M. ULBRICHT, L. ZINK). We owe special gratitude to F. BIRABEN, W. CHEBOTAEV, J. L. HALL, T. W. HÄNSCH, V. VELICHANSKY, C. ZIMMERMANN and S. SVANBERG, for stimulating discussions. Special thanks to F. PAVONE for a critical reading of this manuscript.

REFERENCES

[1] A. L. SCHAWLOW: this volume, p. 1.
[2] J. C. CAMPARO: *Contemp. Phys.*, **26**, 443 (1985).
[3] T. W. HÄNSCH: this volume, p. 297.
[4] Private communication (T. W. HÄNSCH and B. SCHEUMANN).
[5] C. HANKE: *High power diode lasers*, in *Solid State Lasers: Recent Developments and Applications*, edited by M. INGUSCIO and R. WALLENSTEIN (Plenum Press, New York, N.Y., 1993), p. 139.
[6] M. OHTSU and T. TAKO: *Coherence in semiconductor lasers*, in *Progress in Optics XXV*, edited by E. WOLF (Elsevier, Amsterdam, 1988), p. 191.
[7] A. L. SCHAWLOW and C. H. TOWNES: *Phys. Rev.*, **112**, 1940 (1958).
[8] D. WELFORD and A. MOORADIAN: *Appl. Phys. Lett.*, **40**, 865 (1982).
[9] See, for instance, R. FOX, G. TURK, N. MACKIE, T. ZIBROVA, S. WALTMAN, M. P. SASSI, J. MARQUARDT, A. S. ZIBROV, C. WEIMER and L. HOLLBERG: *Diode lasers and metrology*, in *Solid State Lasers: Recent Developments and Applications*, edited by M. INGUSCIO and R. WALLENSTEIN (Plenum Press, New York, N.Y., 1993), p. 279, and references therein.
[10] C. E. WIEMAN and L. HOLLBERG: *Rev. Sci. Instrum.*, **62**, 1 (1991).
[11] G. M. TINO, L. HOLLBERG, A. SASSO, M. INGUSCIO and M. BARSANTI: *Phys. Rev. Lett.*, **64**, 2999 (1990).
[12] G. M. TINO, M. DE ANGELIS, F. MARIN and M. INGUSCIO: *Semiconductor diode lasers in atomic spectroscopy*, in *Solid State Lasers: Recent Developments and Applications*, edited by M. INGUSCIO and R. WALLENSTEIN (Plenum Press, New York, N.Y., 1993), p. 287.
[13] G. M. TINO, M. DE ANGELIS, L. GIANFRANI, M. BARSANTI and M. INGUSCIO: *Appl. Phys. B*, **55**, 397 (1992).
[14] M. INGUSCIO: *J. Phys. (Paris)*, C7, 217 (1983).
[15] C. WIEMAN and T. W. HÄNSCH: *Phys. Rev. Lett.*, **36**, 1970 (1976).
[16] M. BARSANTI, L. GIANFRANI, F. PAVONE, A. SASSO, C. SILVESTRINI and G. M. TINO: *Z. Phys. D*, **23**, 145 (1992).
[17] F. S. PAVONE, G. GIUSFREDI, A. CAPANNI, M. INGUSCIO, G. TINO and M. DE ANGELIS: *Narrow linewidth visible diode laser at 690 nm: spectroscopy of the* SrI *intecombination line*, in *Frequency Stabilized Lasers and their Applications*, edited by Y. C. CHUNG, *SPIE*, Vol. **1837**, 366 (1992).
[18] M. INGUSCIO, P. MINUTOLO, A. SASSO and G. M. TINO: *Phys. Rev. A*, **37**, 4056 (1988).
[19] M. DE ANGELIS, M. INGUSCIO, L. JULIEN, F. MARIN, A. SASSO and G. M. TINO: *Phys. Rev. A*, **44**, 5811 (1991).
[20] P. W. SMITH and T. HÄNSCH: *Phys. Rev. Lett.*, **26**, 740 (1971).
[21] G. M. TINO: *Comments At. Mol. Phys.*, **29**, 5 (1993).
[22] F. MARIN, P. DE NATALE, M. INGUSCIO, M. PREVEDELLI, L. R. ZINK and G. M. TINO: *Opt. Lett.*, **17**, 148 (1992).
[23] H. U. DANIEL, B. MAURER and M. STEINER: *Appl. Phys. B*, **30**, 189 (1983).
[24] Marco PREVEDELLI at the Max Planck Institut for Quantum Optics (Garching) has recently observed beat notes up to several hundred gigahertz from diode lasers mixed in Shottky-barrier diodes in the frame of perfecting a new method for bisecting optical frequency intervals to develop phase-coherent measurements of atomic hydrogen [25, 26].
[25] H. R. TELLE, D. MESCHEDE and T. W. HÄNSCH: *Opt. Lett.*, **15**, 532 (1990).
[26] R. WYNANDS, T. MUKAI and T. W. HÄNSCH: *Opt. Lett.*, **17**, 1749 (1992).
[27] H. D. BABCOCK and L. HERZBERG: *Astrophys. J.*, **108**, 167 (1948).
[28] W. T. HILL III, R. A. ABREU and A. L. A. SCHAWLOW: *Opt. Comm.*, **32**, 96 (1980).
[29] S. J. HARRIS: *Appl. Opt.*, **23**, 1311 (1984).
[30] M. DE ANGELIS and G. M. TINO: private communication.
[31] M. DE ANGELIS, F. MARIN, F. S. PAVONE, G. M. TINO and M. INGUSCIO: *Pure absorption spectroscopy of molecular oxygen using a* cw AlGaAs *laser*, in *Monitoring of Gaseous Pollutants by Tunable Diode Lasers*, edited by R. GRISAR, H. BÖTTNER, M. TACKE and G. RESTELLI (Kluwer Academic Publisher, Amsterdam, 1991), p. 257.
[32] K. ERNST and F. PAVONE: *Overtone molecular spectroscopy with diode lasers*, in *Solid State Lasers: Recent Developments and Applications*, edited by M. INGUSCIO and R. WALLENSTEIN (Plenum Press, New York, N.Y., 1993), p. 303.
[33] K. LEHMAN, F. PAVONE and M. INGUSCIO: unpublished.
[34] F. S. PAVONE and M. INGUSCIO: *Appl. Phys. B*, **56**, 118 (1993).

OVERTONE MOLECULAR SPECTROSCOPY WITH DIODE LASERS

Krzysztof Ernst[1] and Francesco Pavone[2]

[1]Institute of Experimental Physics, Warsaw University
Hoza 69, 00681 Warsaw, Poland
[2]European Laboratory for Non-linear Spectroscopy
(LENS) Lgo E.Fermi 2, 50125 Florence, Italy

INTRODUCTION

All fundamental vibrational transitions of molecules are in the infrared region. At the same time only few molecules have electronic absorption bands in the visible. Such situation is not favourable for performing molecular spectroscopy measurements in the visible range which is very convenient for several reasons (tunable laser sources, sensitive detectors). On the other hand, due to transparency of molecular gases for visible radiation, the Sun light can easily penetrate through the atmosphere what is of the primary importance for all kind of life on the Earth.

The vibrational motion of a molecule besides of the fundamental frequencies, corresponding to different normal vibrational modes ν_i, contains also overtone frequencies $2\nu_i, 3\nu_i \ldots$ Actually overtone frequencies are not exactly two or three times the frequency of the fundamental. They are slightly less. For convenience, however, it is conventionally written $2\nu_i, 3\nu_i$. In addition, in polyatomic molecules combination vibrations as $\nu_i + \nu_k, \nu_i + 2\nu_k$ are also present.

Absorption lines corresponding to overtone and combination transitions are weak enough from the point of view of the atmosphere transparency, but at the same time they may be sufficiently strong for spectroscopic applications. However, such measurements require suitable laser sources and sensitive detection.

It has to be emphasized that the intensity of successive overtone and combination transitions decreases very rapidly with increasing number of vibrational modes and/or quanta involved. For instance, in the case of HCl molecule the intensity of the fourth overtone is more than four orders of magnitude weaker than that of the fundamental transition.

Recent progresses in semiconductor diode lasers[1]and in particular their output power, reliability, low cost, room temperature operation, and large spectral coverage have been of great importance for a continously increasing use both in pure and applied spectroscopy. In particular, the extension of operation from the infrared to the visible, have really made accessible the wide and important field of absorption measurements concerning the overtone molecular transitions. Various applications are possible with this sources in the field of the high resolution spectroscopy and high sensitivity detection. One of them is real time, non contact polution measurement.

As it was already mentioned, moving from the infrared fundamental vibrational transitions to the overtones in the visible, absorption coefficients decrease several orders of magnitude. On the other hand, in comparison with laser sources operating in the infrared including lead salt diodes, semiconductor diode lasers in the visible (and in the near IR) offer the advantage of much simpler operation and much better amplitude stability. Moreover, remote sensing of atmospheric species could be more useful in the visible than in the infrared because of the reduced opacity of the atmosphere.

Solid State Lasers: New Developments and Applications
Edited by M. Inguscio and R. Wallenstein, Plenum Press, New York, 1993

TECHNIQUES DEVELOPED TO DETECT VERY WEAK ABSORPTIONS

In order to reach a satisfactory sensitivity in absorption spectroscopy several detection methods have been proposed and successfully applied. The simplest possible technique is the direct absorption measurement which consists on sweeping the frequency and detecting the signal against the constant background. The sensitivity of such a method is obviously very low. We can improve it by modulating the amplitude of the light source, but we are still limited by background contribution.

In order to understand the motivation for developing specialized techniques for direct absorption spectroscopy (i.e., the direct measurement of the optical attenuation of a light beam through an absorbing sample) let us consider some general requirements concerning the signal-to-noise ratio (SNR).

The signal is usually a detector photocurrent and may be written as $S = kI$, where k represents the net attenuation of the laser intensity I incident upon the absorption sample. Noise contributions may be separated into three terms: N_e- originating from the detection electronics, and then independent of I, N_o–detector shot noise proportional to $\sqrt{I}$ and $N_s I$ - contribution of amplitude - fluctuation background proportional to I. The SNR may then be written[2]

$$SNR = \frac{kI}{[N_e^2 + (\beta\sqrt{I})^2 + (N_s I)^2]^{1/2}}$$

As the intensity I increases, the SNR increases proportionally to I until the I-dependent terms in the denominator exceed N_e. The SNR will then saturate at some value of I that depends on the relative values of β and N_s. As we can see the laser light amplitude modulation can not solve our problem, as this imparts a time dependence to I, which is common to both numerator and the denominator in the equation for SNR. However, by using frequency modulation, one may effectively modulate the signal kI without modulating the noise terms. In view of high sensitivity measurements this method has been developed in three different ways.

I. Wavelength Modulation (WM) Spectroscopy[3,4,5]

The single frequency laser is modulated at a relatively low frequency ($10^3 Hz$), small compared to the width of the spectroscopic feature of interest, so that the absorption is probed simultaneously by a number of sidebands. WM is a sensitive form of derivative spectroscopy. Unlike direct absorption methods where signal is detected as a change against a constant background, in WM spectroscopy the signal arises from the differ-

ence in the absorptions of different sidebands. Therefore, the sensitivity and spectral resolution are greatly enhanced, provided that the laser shows no or very little variation of intensity with wavelength and responsivity of the detector is independent of λ. Consider the current C from the detector, C =IGT, where I is the laser light intensity, T is the transmissivity of the sample, and G is responsivity of the detector. We can then write for the detector signal

$$\frac{1}{C}\frac{dC}{d\lambda}\Delta\lambda = \frac{1}{I}\frac{dI}{d\lambda}\Delta\lambda + \frac{1}{G}\frac{dG}{d\lambda}\Delta\lambda + \frac{1}{T}\frac{dT}{d\lambda}\Delta\lambda$$

where $\Delta\lambda$ is the wavelength modulation depth. Only the last term in the above expression should give a contribution to the signal. Unfortunately $dI/d\lambda$ is not negligible in the case of diode lasers and gives an unwanted contribution to the noise level.

II. Frequency Modulation (FM) Spectroscopy[6,7]

FM spectroscopy is a kind of extension of WM spectroscopy to much higher frequencies ($\approx 10^8 Hz$). Frequency modulation produces sidebands which are widely spaced in frequency so that the spectral feature of interest can be probed by only one sideband at a time. Viewed in frequency space, the spectral distribution of the modulated laser field consists of the strong carrier at ω_c and two sidebands of the same amplitude but 180^0 out of phase, displaced by the angular modulation frequency ω_m from the carrier. When there is no absorption present, the beat signal at ω_m between the carrier and the upper sideband exactly cancels with the beat signal between the carrier and the lower sideband. If, however, the laser frequency is tuned over an absorption, so that one of the sidebands is absorbed, the imperfect cancellation of two beats produces a *FM* signal.

If the modulation frequency does not exceed the absorption linewidth, the technique is usually called High Wavelength Modulation (HWM).

III. Two-Tone Frequency Modulation (TTFM)[8,9]

If we wish to investigate broad spectral features, such as absorption lines broadened by atmospheric pressure to 2 – 3 GHz, we must have correspondingly high modulation frequencies. The TTFM technique was applied in order to reduce the detection bandwidth requirement since detectors with bandwidth in GHz range are not easily available.

In the TTFM, the laser is modulated simultaneously at two distinct but closely spaced angular frequencies $\omega_1 = \omega_m + \Omega/2$ and $\omega_2 = \omega_m - \Omega/2$ ($\Omega/\omega_m < 10^{-3}$). The TTFM absorption signal arises from the difference between the absorption of the carrier and the sum of the absorptions of the sidebands. It is thus approximately analogous to a second derivative signal whereas single-tone FM is analogous to a first derivative signal. In both cases, however, there is no background signal if there is no absorption. The most attractive feature of TTFM resides in the fact that the signal is detected at Ω instead of ω_m.

Unfortunately pure frequency modulation is rarely achieved. There is always some residual amplitude modulation (RAM) present, especially in diode lasers where any change in the injection current changes not only the frequency of the laser but also its output power. It is evident that RAM is undesirable feature in all kinds of frequency

modulation spectroscopy. It gives rise to a background signal with accompanying noise, even when there is no absorption present, and thus limits the detection sensitivity.

It is worthwhile to mention here that a wide variety of laser techniques allowing high sensitivity and high resolution have been proposed and successively applied. Let us give few examples as laser-induced fluorescence (LIF)[10], optoacoustic spectroscopy(OA)[11], optogalvanic spectroscopy (OG)[11], resonance ionisation spectroscopy (RIS)[12], and laser-intracavity absorption[13]. With the exception of direct absorption methods described above, all these techniques monitor some indirect effects of the optical absorption.

Any qualitative comparison of each of these methods would be extremely difficult since their applicability depends essentially on specific aims and experimental conditions of the desired measurements. However, two important advantages of the extracavity direct absorption should be emphasized: simple callibration procedure and remote-sensing possibilities. All of them are very important from the point of view of environmental studies.

OVERTONE SPECTROSCOPY

Several overtone transitions of various molecules have been already studied using various light sources and different detection techniques. Table 1 contains selected information concerning molecules with overtone or combination absorption lines in two spectral ranges (630 – 690 and 750 – 900nm) covered by diode lasers. As one can see only in a few recent works diode lasers have been applied. Other data were obtained with dye lasers or even with methods of pre-laser spectroscopy. Some overtone transitions in the selected ranges refer to reported numerical values and can be considered as potential candidates for future experimental research.

Table 1. Overtone and combination transitions in spectral ranges covered by diode lasers.

Molecule	absorp. line (nm)	transition	laser and det.tech.	sensitivity other inf.	reference
H_2O	818	$2\nu_1 + \nu_2 + \nu_3$	Diode	min.det.abs.	14
			WM	$3.1x10^{-4}$	
			FM	$2.8x10^{-4}$	
			TTFM	$2.4x10^{-6}$	
	789	$\nu_2 + 3\nu_3$	Diode		15
			FM	$3x10^{-4}$	
	818-831	$2\nu_1 + \nu_2 + \nu_3$	Diode FM		15
HI	820	$v = 6 \Leftarrow 0$	Diode		16

Table 1. (cont'd)

C_2H_2	789	$\nu_1 + 3\nu_3$	Diode WM	min.det.conc. 0.2ppm per km	17
	640	$5\nu_3$	Dye	intra-cav.	18
	670	$\nu_1 + \nu_2 + \nu_3$	OA		
	848	$2\nu_1 + \nu_2 + \nu_3$			19
CH_4	886	$3\nu_1 + \nu_3$	Diode LWM HWM TTMF	min.det.abs. $4.5x10^{-7}$ $9.7x10^{-8}$ $6.4x10^{-8}$	20
	860	$2\nu_1 + 2\nu_3$	Diode	$3x10^{-5}$	21
	682	$2\nu_1 + 3\nu_3$		White cell	22
	782	$2\nu_1 + \nu_2 + 2\nu_3$			23
C_2H_6	741	$5 \Leftarrow 0$ CH str.	OA		24
NH_3	790	$4\nu_1$ $2\nu_1 + 2\nu_3$	Diode FM	min.det.abs. $3x10^{-4}$	21
	792	$4\nu_1$	Diode		25
	647	$5\nu_1$ $4\nu_1 + \nu_3$	Dye	intra-cav	26
	647	$4\nu_1 + \nu_3$	photoplate		27
C_6H_6	865- 877	$4 \Leftarrow 0$ CH str.	opto-thermal		28
H_2O_2	793	$5\nu_{OH} + \nu_{OO}$	Dye		29
HCl	640	$v = 6 \Leftarrow 0$	Dye	intra-cav	30
	750	$v = 5 \Leftarrow 0$	OA		
CO_2	869	$5\nu_3$			31
	789	$2\nu_2 + 5\nu_3$			
	783	$\nu_1 + 5\nu_3$			
C_3H_4	787	$4\nu_1$	OA		24
	737	$5 \Leftarrow 0$			
HCN	790	$4\nu_3$			32
CO	804	$v = 6 \Leftarrow 0$			33
NO	800	$v = 7 \Leftarrow 0$			33
HF	877	$v = 3 \Leftarrow 0$			33
	675	$v = 4 \Leftarrow 0$			33

Results obtained for H_2O and CH_4 were used for comparing the sensitivity of different frequency modulation techniques. In the first experimental work[14] dedicated to H_2O the authors found that the difference in sensitivity between FM and TTFM was about two orders of magnitude. In other work[20] the minimum detectable absorption was measured using methane - the gas of obvious interest because of environmental applications. A component of a combination band at $886nm$ has been chosen as a test transition, mainly because of its strength. Two recordings are shown in Figure 1:a) pure absorption signal at pressure of 100 Torr corresponding

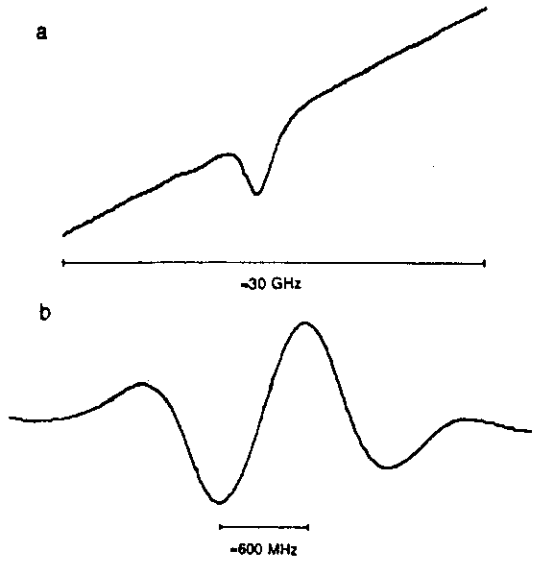

Figure 1. *a*) Pure absorption signal on the third overtone of methane at 100 Torr in $1.5m$ pathway. *b*) Derivative lineshape of a two-tone recording at 500 mTorr.

to an absorption of $3.6x10^{-2}$($1.5m$ pathway, $100Hz$ detection bandwidth, S/N ratio of about 20); *b*) derivative lineshape of a two-tone signal at pressure of 500 mTorr corresponding to an absorption of $1.8x10^{-4}$($1.5m$ pathway, $1Hz$ detection bandwidth) with a measured S/N ratio of a few thousands.

Minimum detectable absorption for the HWM and TTFM techniques turned out to be of the same order of magnitude, while for the value referred to LW modulation it is about one order of magnitude less, as indicated in Table 1. In the last case the detection limit value is determined by the laser amplitude $1/f$ excess noise, while in the first two cases this noise contribution is negligible with respect to other ones as detector induce shot noise, thermal and RAM noises. The detection limits well agree with the calculated "quantum limited" values based on measured laser power, modulation index, noise of the electronic components, and other parameters of the apparatus.

In most of the measurements with diode lasers the frequency modulation was produced by modulating the injection current. In the case of C_2H_2 the diode laser was

used in an extended cavity configuration. Low frequency modulation could be then produced by both changing the injection laser current and/or varying the external cavity length (by means of a PZT). With the extended cavity configuration we have measured a reduction of the linewidth (to less than 1 MHz) and better short term stability (100 ms). Another advantage of such a configuration is that wavelength modulation by varying the cavity length leads to the lower level RAM noise than direct injection current modulation.

The experimental apparatus used for C_2H_2 overtone absorption measurements[17] is schematically shown in Figure 2. The extended cavity configuration is outlined in Figure 3. The first order beam diffracted from a grating was fed-back into the laser diode. The tilting of the grating allows to select one of the longitudinal modes within tuning range of about $20nm$.

Molecular transitions could be observed either in pure absorption or in a phase sensitive detection scheme. In the latter case, the lock-in derivative signals were

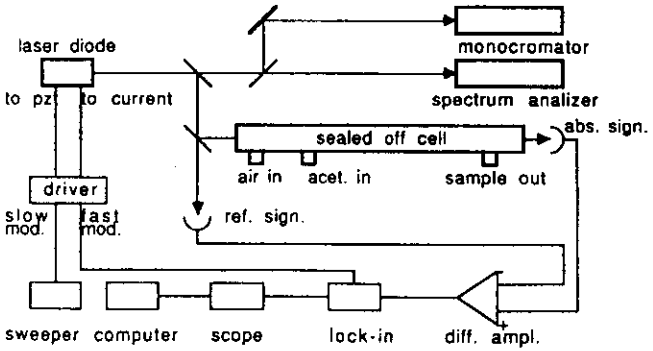

Figure 2. Schematic of the experimental apparatus for measuring the overtone absorption in acetylene.

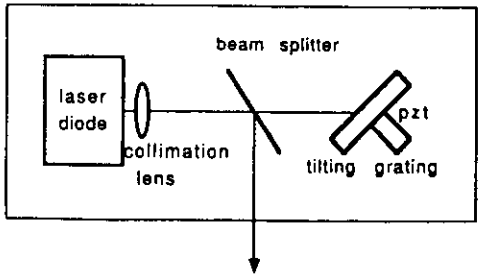

Figure 3. Schematic of the extended cavity diode laser configuration using a grating for wavelength control.

recorded by introducing a kHz modulation on the cavity length. The derivative signal for the $P(11)$ component of the $12646.966cm^{-1}$ transition is shown in Figure 4 at two different gas pressures. We measured $\alpha S/N$ value of a few thousands and an absorption of about 6% at 30 Torr (trace a), and S/N = 6 at 36 mTorr (b). The latter measurement gives a minimum relative absorption of 10^{-4} which is comparable with that obtained by means of TTMF[14]. This result is also consistent with the recent report[34] where WM and TTFM techniques have been compared for lead salt diodes.

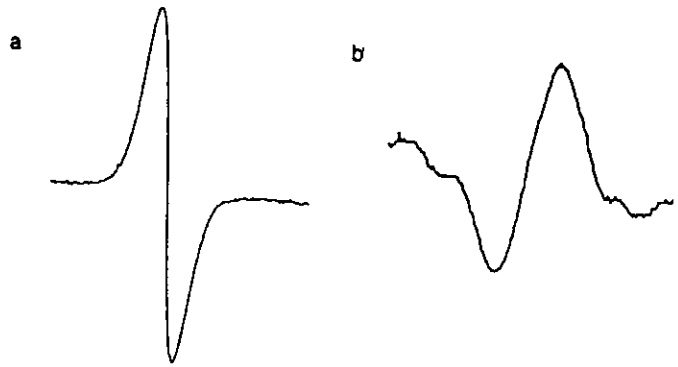

Figure 4. Derivative signal for the $P(11)$ component at 10 Torr (a) and 36 mTorr (b).

Regarding possible environmental trace gases detection we have also extracted the minimum acetylene pressure in presence of air at atmospheric pressure still keeping a signal with a S/N ratio of a few units. We are able to detect 0.1 ppm per km of acetylene in air.

The narrow linewidth emission obtained with the extended cavity configuration has also permitted to perform the lineshape analysis measuring self and air pressure broadening parameter for two different components of the combination band. The Pade method [35] has been used to extract the collisional Lorentzian contribution from the Voigt profile and thus the pressure broadening parameter. Air broadening measurements have been performed on the P(11) and R(5) components. Our results are reported in Table 2 together with earlier measurements of other components of C_2H_2 as well as recent measurements of pressure broadening for H_2O, CH_4 and NH_3 using diode lasers. As one can see the air broadening coefficients for overtone transitions are very close to that for the fundamental transition.

For many practical applications it is requested to monitor gas traces in open-path configuration in the atmosphere. For this reason the knowledge of air broadening parameters can be useful. However, some problems arise for such experiments at atmospheric pressures. Widths of absorption lines due to pressure broadening are of the order of GHz what leads to the substantial decrease of the detection sensitivity. Moreover, the overlapping of different lines may also occur and it has to be taken into consideration.

Table 2. Pressure broadening parameters.

Molecule	Transition	γ (MHz/Torr) air	self	Refer.
C_2H_2	$789(\nu_1+3\nu_3)$			20
	P(11)	8.0	11.0	
	R(5)	9.0		
	$862(\nu_2+3\nu_3)$			36
	R(7)		12.3	
	$849(2\nu_1+\nu_2+\nu_3)$			36
	R(7)		9.9	
	ν_5			
	R(5)	7.0		37
	P(11)	6.2		
H_2O	$822(2\nu_1+\nu_2+\nu_3)$	5.9		15
CH_4	$860(2\nu_1+2\nu_3)$	3.2	3.7	21
NH_3	$790(2\nu_1+2\nu_3)$		21.7	21
	$792(4\nu_1)$		27.2	21

As for the sensitivity of diode laser systems destinated to monitoring the atmosphere one should think about its improvement. The stabilization of the diode lasers operating at wavelength below $1\mu m$ could also be important for use in conjunction with efficient pulsed solid state laser (such as Titan Saphire) operating in the same region. This can be interesting in the frame of LIDAR[38,39] measurements, where amplification or injection seeding control could make possible to perform detection at larger distances with an improved sensitivity and an easier spectral control.

References

1. C.Wieman and L.Hollberg, Rev.Sci.Instr., 62:1(1991).
2. M.Gehrtz, G.Bjorklund and E.Whitaker, JOSA, B2:1510(1985).
3. J.Telle and C.Tang, Appl.Phys.Lett., 24:85(1974).
4. E.Moses and C.Tang, Opt.Lett., 1:115(1977).
5. P.Pokrowsky, W.Zapka, F.Chu and G.Bjorklund, Opt.Commun., 44:175(1983).
6. G.Bjorklund, Opt.Lett., 5:15(1980).
7. G.Bjorklund, M.Levenson, W.Lenth and C.Ortiz, Appl.Phys., B32:145(1983).
8. G.Janik, C.Carlisle and T.Gallagher, JOSA, B3:1070(1986).
9. D.Cooper and R.Warren, JOSA, B4:470(1987).
10. W.Demtroder, Laser Spectroscopy, Springer Verlag, 1981, p.416.
11. K.Ernst and M.Inguscio, Rivista del Nuovo Cimento, 11: no.2 (1988).
12. G.Hurst, M.Payne, S.Kramer and J.Young, Rev.Mod.Phys., 51:767 1979).
13. L.Pakhomycheva, E.Sviridenkov, A.Suchkov, L.Titova and S.Churilov, JETP Lett., 12:43(1970).
14. L.Wang, H.Riris, C.Carlisle and T.Gallagher, Appl.Opt., 27:2071(1988).

15. A.Lucchesini, L.Dell'Amico, I.Longo, C.Gabbanini, S.Gozzini and L.Moi, Il Nuovo Cimento, 13D:677(1991).
16. F.Matsushima, S.Kakihata and K.Tagaki, J.Chem.Phys., 94:2408 1991).
17. F.Pavone, F.Marin, M.Inguscio, K.Ernst and G.di Lonardo, Appl.Opt., in print.
18. G.Scherer, K.Lehmann and W.Klemperer, J.Chem.Phys., 78:2817 (1983).
19. G.Funke and E.Lindholm, Z.Physik, 106:518(1937).
20. F.Pavone and M.Inguscio, submitted to Appl.Phys.B.
21. A.Lucchesini, I.Longo, C.Gabbanini, S.Gozzini and L.Moi, Proc. of SPIE Conf. "High Performance Optical Spectrometry", Warsaw, June 1992.
22. L.Giver, J.Quant.Spectrosc.Rad.Transfer, 19:311(1978).
23. H.Vedder and R.Mecke, Z.Physik, 86:137(1933).
24. M.Crofton, C.Stevens, D.Klenerman, J.Gutow and R.Zare, J.Chem.Phys., 89:7100(1988).
25. K.Nakagawa and T.Shimizu, Jap.Journ.Appl.Phys., 26:L1697(1987).
26. E.Antonov, E.Berik and V.Koloshnikov, J.Quant.Spectrosc.Rad. Transfer, 22:45(1979).
27. Siu-Hung Chao, Phys.Rev., 150:27(1936).
28. M.Scotoni, C.Leonardi and D.Bassi, preprint.
29. X.Luo, P.Fleming, T.Seckel and T.Rizzo, J.Chem.Phys., 93:9194 (1990).
30. K.Reddy, J.Mol.Spectr., 82:127(1980).
31. A.Adel and D.Dennison, Phys.Rev., 43:716(1933).
32. R.Badger and J.Binder, Phys.Rev., 37:800(1931).
33. D.Proch, J.Wanner, Report IPP IV/17 of Max Planck Institut fur Plasmaphysik, Garching, 1971.
34. D.Bomse, A.Stanton and J.Silver, Appl.Opt., 31:718(1992).
35. P.Minguzzi and A.di Lieto, J.Mol.Spectr., 109:388(1985).
36. Y.Ohsugi and N.Ohashi, J.Mol.Spectr., 131:215(1988).
37. D.Lambot and G.Blanquet, J.Mol.Spectr., 136:86(1989).
38. S.Svanberg, NATO-ASI Applied Laser Spectroscopy, San Miniato Italy, September 1989, and references therein.
39. P.Rairoux, These, EPFL, Lausanne, 1991.

(20)

The electromagnetic spectrum

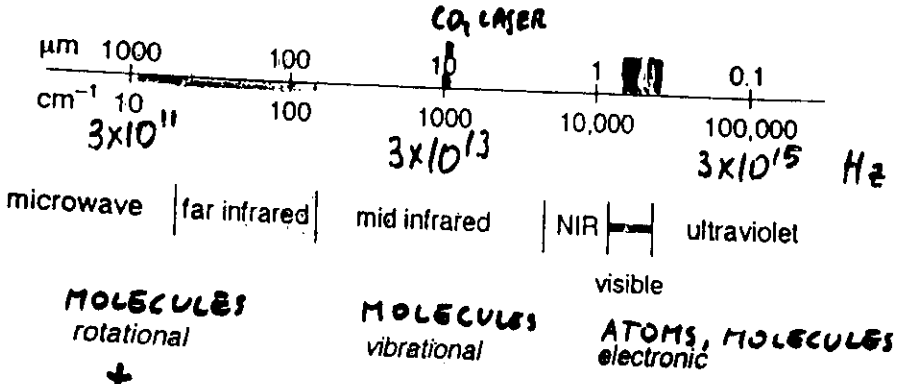

frequency measurements

wavelength measurements

$c = \lambda \nu$

$p \sim \frac{\hbar}{a}$

$E_e \sim \frac{p^2}{2m} \sim \frac{\hbar^2}{m a^2}$ a few eV visible, 1 Å UV

$\omega_e = \sqrt{\frac{k}{m}}$

$\omega_N = \sqrt{\frac{k}{M}}$

$\frac{\hbar\omega_e}{\hbar\omega_N} \simeq \sqrt{\frac{m}{M}}$

$E_N \simeq \sqrt{\frac{m}{M}}\, E_e$ $\sqrt{10^{-2}}$ 0.5 ↓ 50 μm

$I = \frac{M a^2}{2}$ $\frac{\hbar^2}{2I}\ell(\ell+1)$

$E_R \simeq \frac{\hbar^2}{M a^2} \simeq \frac{m}{M} E_e$ $10^{-3} \sim 10^{-5}$

$B\ J(J+1)$

$\uparrow$

$J \rightarrow J \pm 1$

$2\ B\ J$

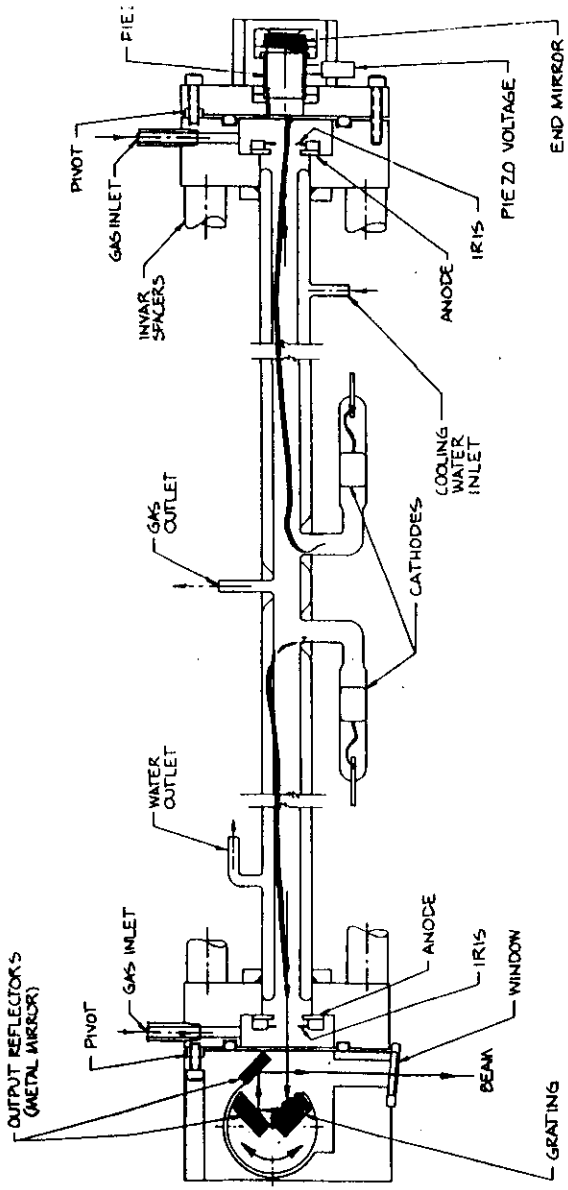

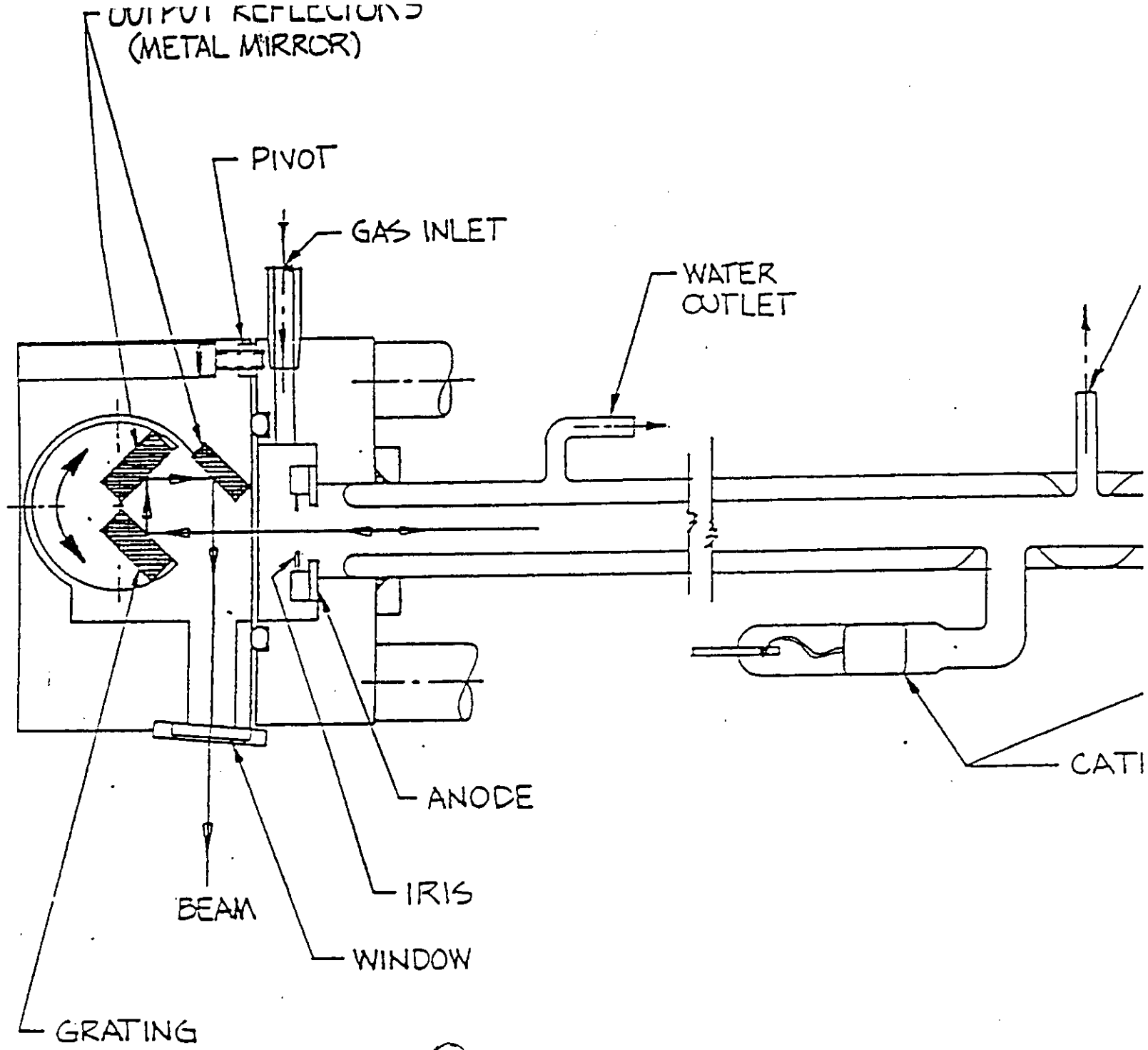
OUTPUT REFLECTORS
(METAL MIRROR)
PIVOT
GAS INLET
WATER
OUTLET
ANODE
CATI
IRIS
BEAM
WINDOW
GRATING

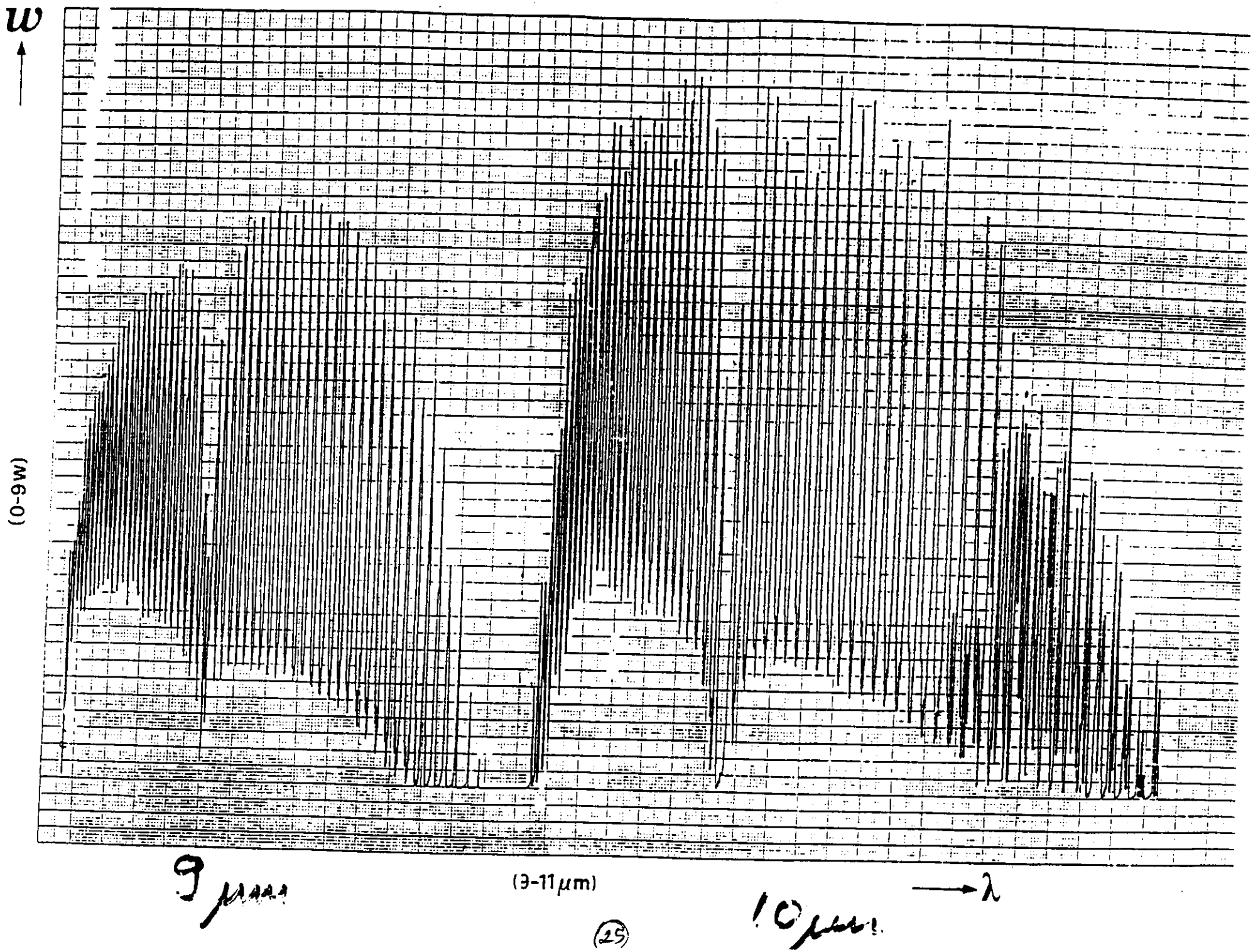
w
(0-9w)
(3-11μm)
λ
9 μm
10 μm

ALLARGAMENTO DOPPLER DI RIGHE SPETTRALI (1° ordine)

DOPPLER BROAD. (1st ORDER)

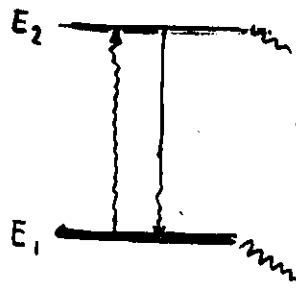

$$\hbar\omega_0 = E_2 - E_1$$

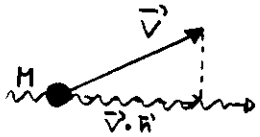

$$\nu = \nu_0 \left(1 + \frac{\vec{v}\cdot\vec{n}}{c}\right)$$

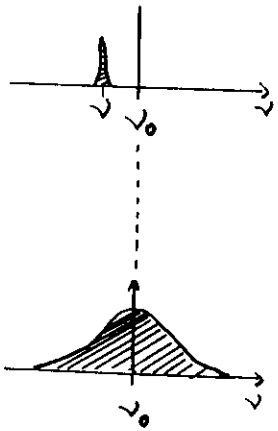

NOTE! $\Delta\nu_D$ independent from $\vec{\nu}$

AT room temp $\frac{\Delta\nu}{\nu} \sim 2\cdot10^{-6}$

$$I = I_0 \exp\left[-\frac{Mc^2}{2KT}\left(\frac{\nu-\nu_0}{\nu_0}\right)^2\right]$$

$$\boxed{\Delta\nu_D = 7.163\times10^{-7}\nu_0\sqrt{\frac{T}{A}}}$$

$10^8 - 10^{10}$ Hz

$\Delta\nu_D \gtrsim 10^2 \Delta\nu_{NAT}$ in the VIS

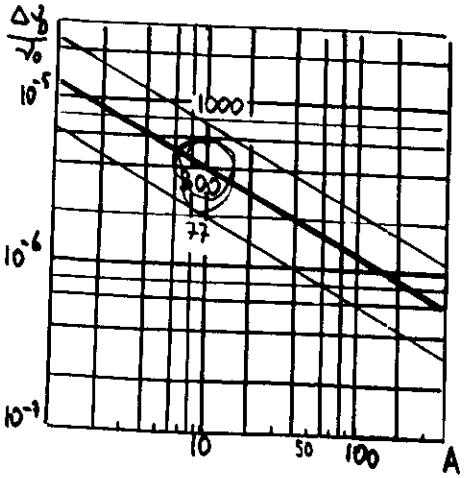

TRANSIZIONI TRA STATI ECCITATI

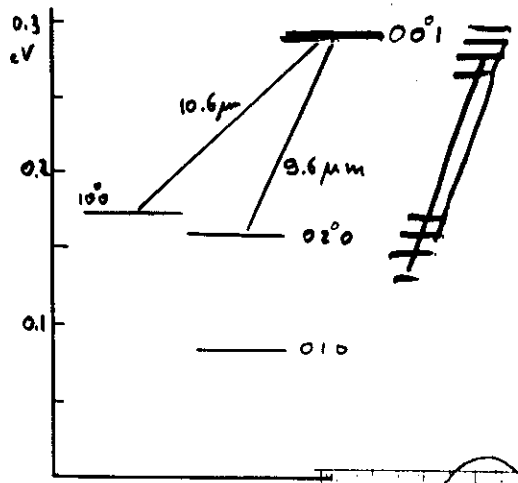

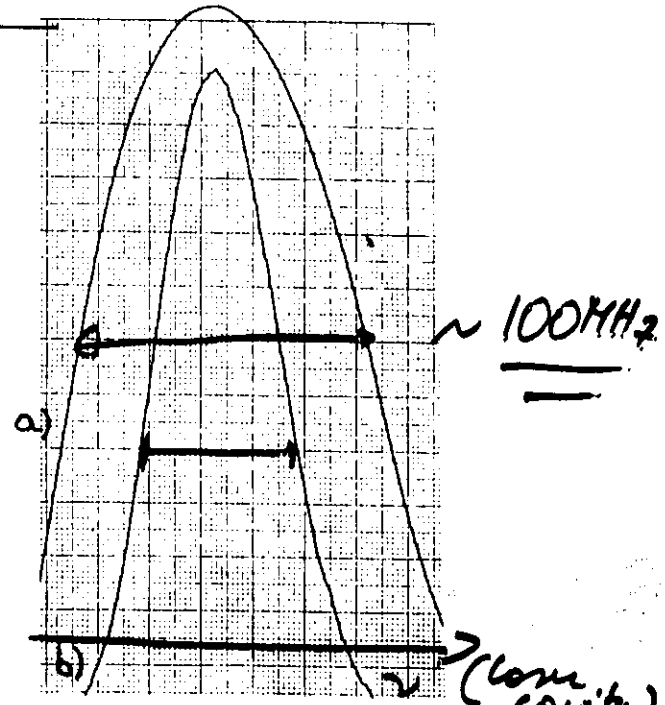

a) CO_2 LASER 9-P(16) ~ 1 WATT

b) SEGNALE OA da CO_2 (~ 1/2 Torr)

SUBDOPPLER SPECTROSCOPY

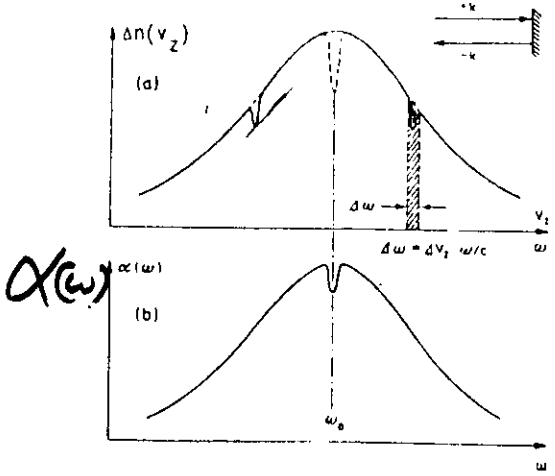

$\alpha(\omega)$

2.1

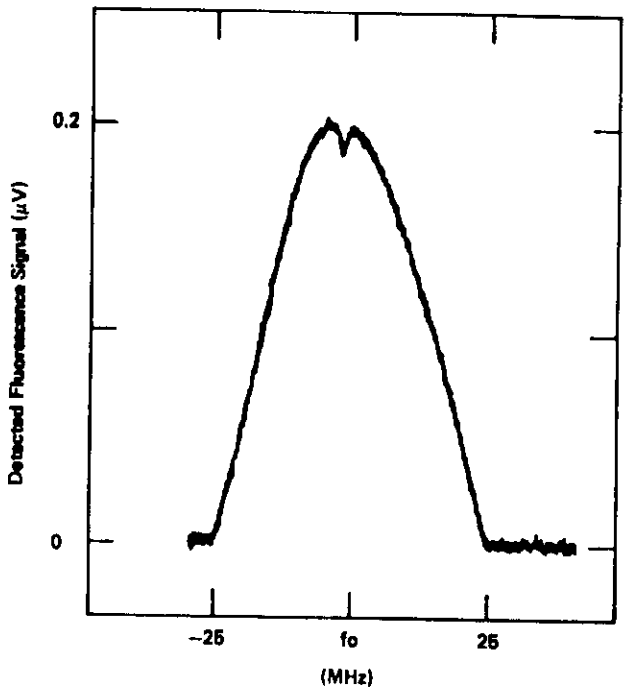

FLUOR.

OPTOGAL.

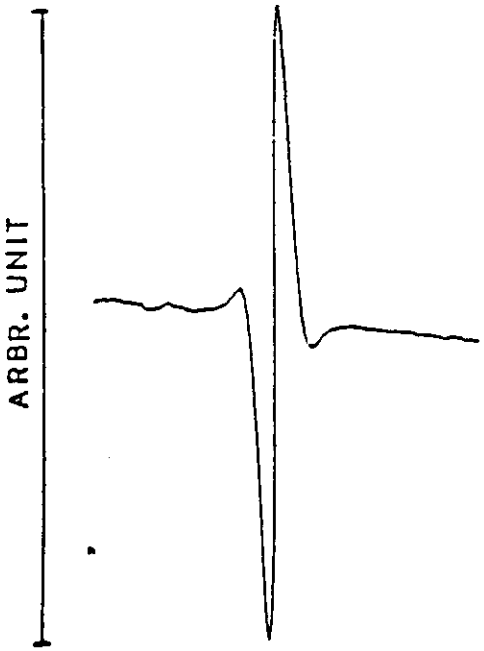

a)

1 1

1 MHz

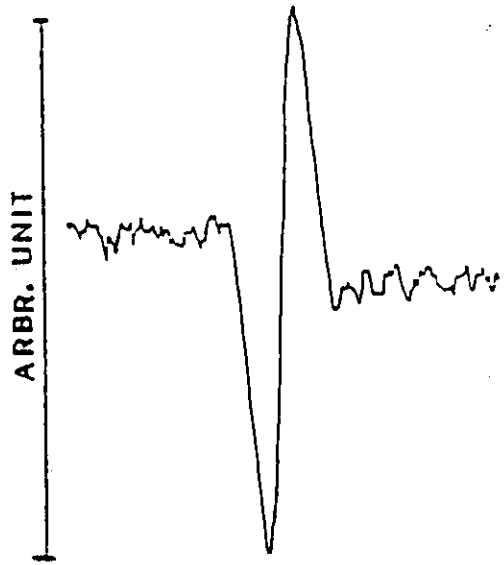

b)

1 1

3 MHz

~ 3rd Der.

NORMAL CO_2 LASERS

10 μm

P(60)	2707	7607.5077	903.2117	6484
P(58)	2714	6404.4578	905.5065	8408
P(56)	2721	4396.1809	907.7745	4384
P(54)	2728	1588.8741	910.0158	5084
P(52)	2734	7988.4259	912.2307	0148
P(50)	2741	3600.4235	914.4192	8214
P(48)	2747	8430.1601	916.5817	6938
P(46)	2754	2482.6413	918.7183	3017
P(44)	2760	5762.5914	920.8291	2210
P(42)	2766	8274.4599	922.9142	9359
P(40)	2773	0022.4271	924.9739	8407
P(38)	2779	1010.4094	927.0083	2419
P(36)	2785	1242.0651	929.0174	3596
P(34)	2791	0720.7986	931.0014	3295
P(32)	2796	9449.7656	932.9604	2043
P(30)	2802	7431.8776	934.8944	9550
P(28)	2808	4669.8055	936.8037	4726
P(26)	2814	1165.9839	938.6882	5692
P(24)	2819	6922.6147	940.5480	9793
P(22)	2825	1941.6703	942.3833	3608
P(20)	2830	6224.8967	944.1940	2961
P(18)	2835	9773.8165	945.9802	2931
P(16)	2841	2589.7314	947.7419	7060
P(14)	2846	4673.7246	949.4793	1361
P(12)	2851	6026.6628	951.1922	6324
P(10)	2856	6649.1983	952.8808	4927
P(8)	2861	6541.7701	954.5450	8632
P(6)	2866	5704.6061	956.1849	8202
P(4)	2871	4137.7235	957.8005	3691
P(2)	2876	1840.9300	959.3917	4460
V(0)	2880	8813.8246	960.9585	9171
R(0)	2883	2026.2225	961.7328	7396
R(2)	2887	7902.4412	963.2631	3990
R(4)	2892	3046.4336	964.7689	8140
R(6)	2896	7457.0695	966.2503	6076
R(8)	2901	1133.0097	967.7072	3331
R(10)	2905	4072.7058	969.1395	4739
R(12)	2909	6274.3988	970.5472	4435
R(14)	2913	7736.1185	971.9302	5845
R(16)	2917	8455.6817	973.2885	1688
R(18)	2921	8430.6909	974.6219	3965
R(20)	2925	7658.5324	975.9304	3960
R(22)	2929	6136.3740	977.2139	2224
R(24)	2933	3861.1629	978.4722	8575
R(26)	2937	0829.6231	979.7054	2084
R(28)	2940	7038.2525	980.9132	1071
R(30)	2944	2483.3197	982.0955	3089
R(32)	2947	7160.8609	983.2522	4916
R(34)	2951	1066.6762	984.3832	2542
R(36)	2954	4196.3256	985.4883	1157
R(38)	2957	6545.1250	986.5673	5137
R(40)	2960	8108.1417	987.6201	8028
R(42)	2963	8880.1900	988.6466	2533
R(44)	2966	8855.8259	989.6465	0491
R(46)	2969	8029.3420	990.6196	2866
R(48)	2972	6394.7621	991.5657	9723
R(50)	2975	3945.8353	992.4848	0211
R(52)	2978	0676.0297	993.3764	2542
R(54)	2980	6578.5263	994.2404	3971
R(56)	2983	1646.2123	995.0766	0771
R(58)	2985	5871.6737	995.8846	8212

±3KH₂

9 μm

P(60)	3014	3456.0742	1005.4774	6515
P(58)	3021	2223.6949	1007.7713	0607
P(56)	3028	0322.1201	1010.0428	2503
P(54)	3034	7743.7465	1012.2917	6841
P(52)	3041	4481.1364	1014.5178	8812
P(50)	3048	0527.0251	1016.7209	4183
P(48)	3054	5874.3277	1018.9006	9322
P(46)	3061	0516.1462	1021.0569	1219
P(44)	3067	4445.7759	1023.1893	7509
P(42)	3073	7656.7119	1025.2978	6496
P(40)	3080	0142.6555	1027.3821	7169
P(38)	3086	1897.5199	1029.4420	9223
P(36)	3092	2915.4360	1031.4774	3083
P(34)	3098	3190.7583	1033.4879	9917
P(32)	3104	2718.0700	1035.4736	1655
P(30)	3110	1492.1877	1037.4341	1009
P(28)	3115	9508.1671	1039.3693	1486
P(26)	3121	6761.3064	1041.2790	7402
P(24)	3127	3247.1518	1043.1632	3901
P(22)	3132	8961.5006	1045.0216	6964
P(20)	3138	3900.4054	1046.8542	3425
P(18)	3143	8060.1774	1048.6608	0978
P(16)	3149	1437.3897	1050.4413	8194
P(14)	3154	4028.8804	1052.1955	4524
P(12)	3159	5831.7547	1053.9235	0313
P(10)	3164	6843.3878	1055.6250	6805
P(8)	3169	7061.4264	1057.3001	6151
P(6)	3174	6483.7910	1058.9487	1415
P(4)	3179	5108.6771	1060.5706	6576
P(2)	3184	2934.5560	1062.1659	6536
V(0)	3188	9960.1764	1063.7345	7121
R(0)	3191	3172.5743	1064.5088	5347
R(2)	3195	8996.0672	1066.0373	6066
R(4)	3200	4017.3872	1067.5391	1025
R(6)	3204	8236.2544	1069.0140	9289
R(8)	3209	1652.6660	1070.4623	0849
R(10)	3213	4266.8953	1071.8837	6618
R(12)	3217	6079.4907	1073.2784	8423
R(14)	3221	7091.2743	1074.6464	9008
R(16)	3225	7303.3400	1075.9878	2021
R(18)	3229	6717.0518	1077.3025	2013
R(20)	3233	5334.0411	1078.5906	4423
R(22)	3237	3156.2043	1079.8522	5580
R(24)	3241	0185.7000	1081.0874	2682
R(26)	3244	6424.9456	1082.2962	3794
R(28)	3248	1876.6140	1083.4787	7831
R(30)	3251	6543.6298	1084.6351	4549
R(32)	3255	0429.1653	1085.7654	4528
R(34)	3258	3536.6360	1086.8697	9163
R(36)	3261	5869.6965	1087.9483	0644
R(38)	3264	7432.2354	1089.0011	1941
R(40)	3267	8228.3702	1090.0283	6790
R(42)	3270	8262.4421	1091.0301	9670
R(44)	3273	7539.0104	1092.0067	5790
R(46)	3276	6062.8469	1092.9582	1067
R(48)	3279	3838.9297	1093.8847	2107
R(50)	3282	0872.4368	1094.7864	6180
R(52)	3284	7168.7402	1095.6636	1206
R(54)	3287	2733.3987	1096.5163	5728
R(56)	3289	7572.1515	1097.3448	8889
R(58)	3292	1690.9198	1098.1493	0411

FREE RUNNING

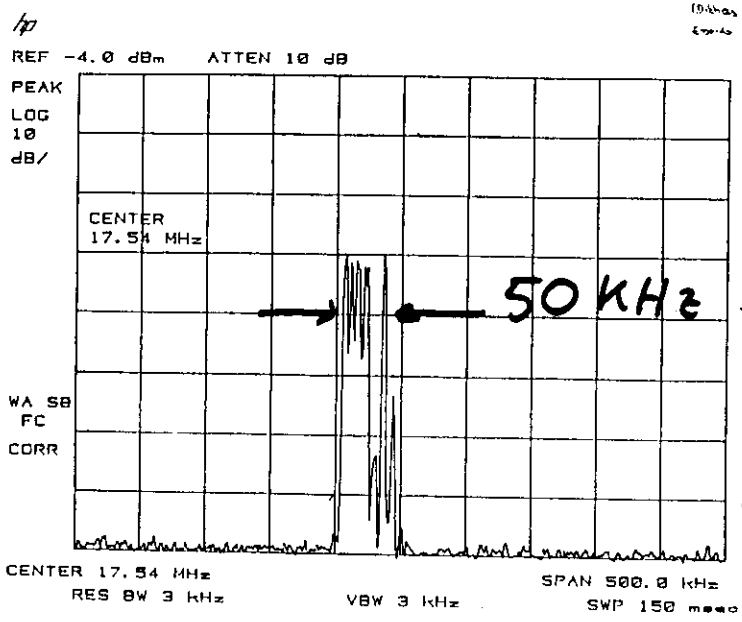

50 KHz

FAST LINEWIDTH $< 10^{-8}$

150 msec

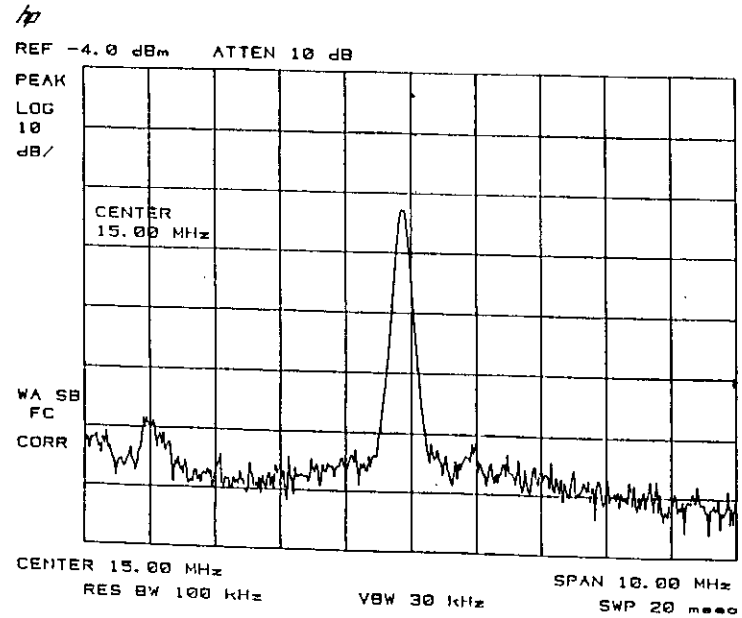

20msec

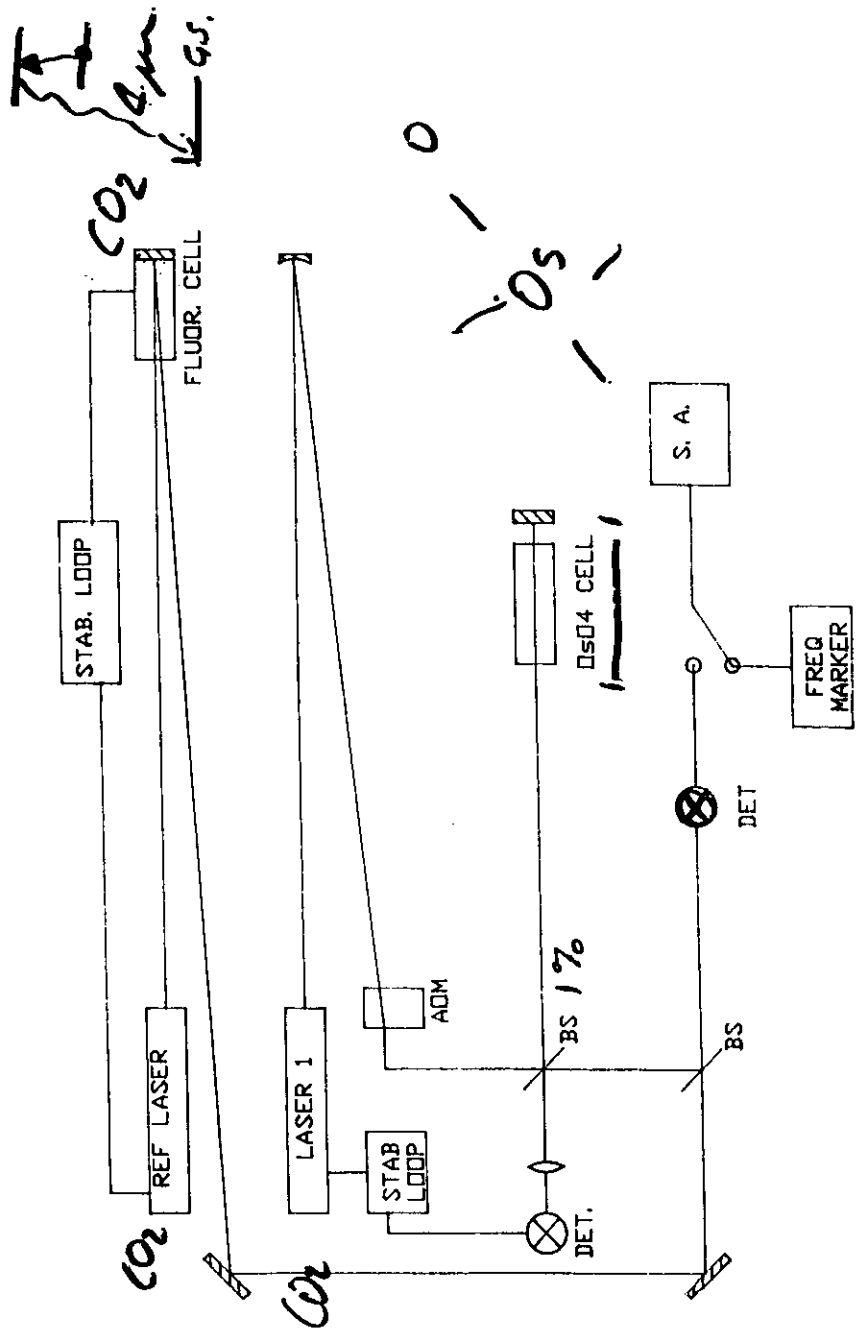

OsO_4

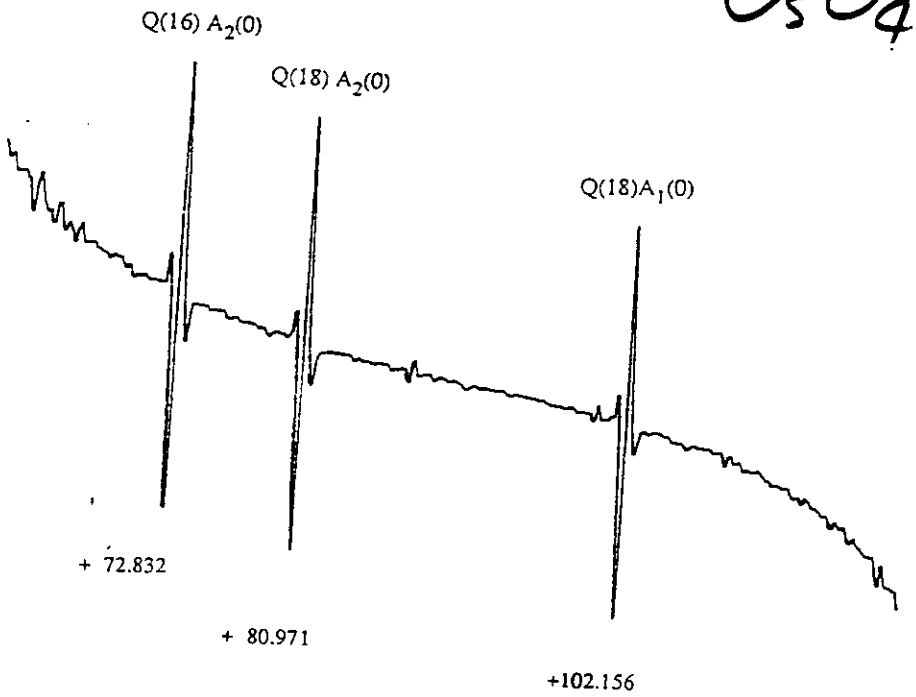

(9)

OsO_4 Ricci et al J. Chem. Phys. 1990

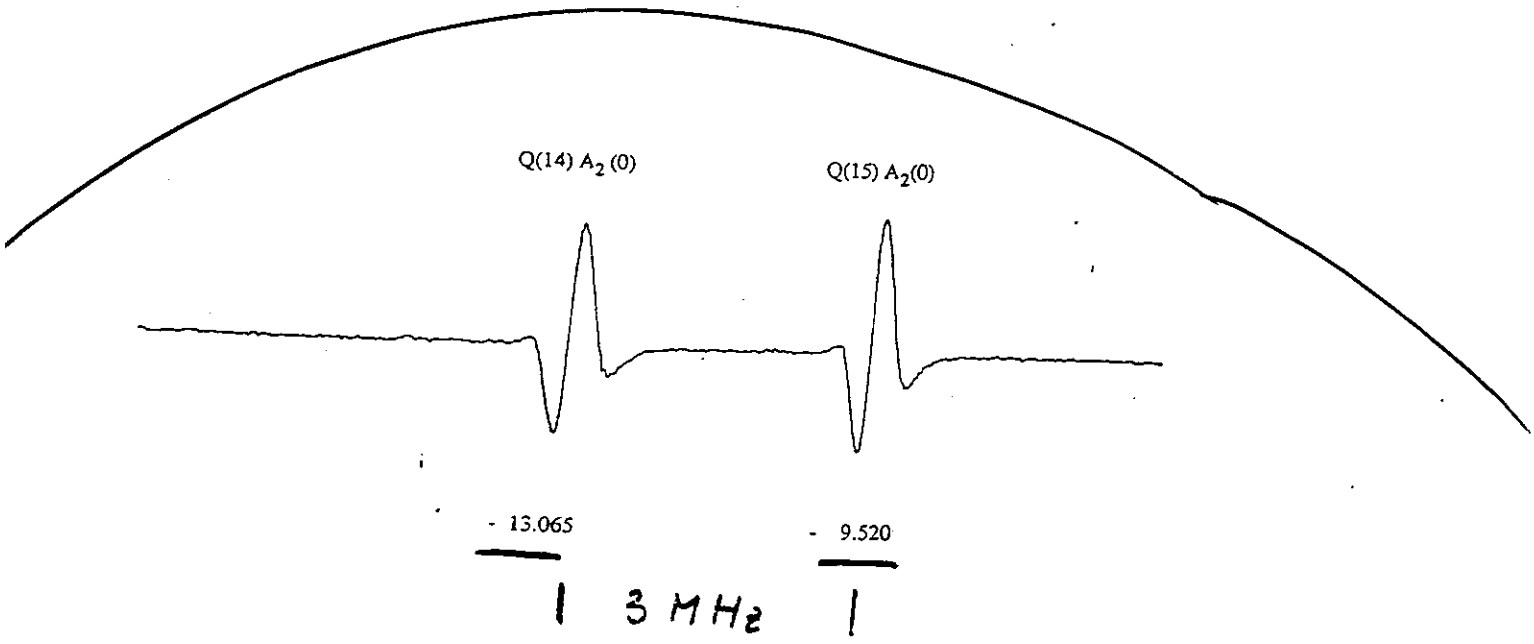

MOLECULES $\nu = 2BJ + \ldots$

ATOMS FINE STRUCTURES

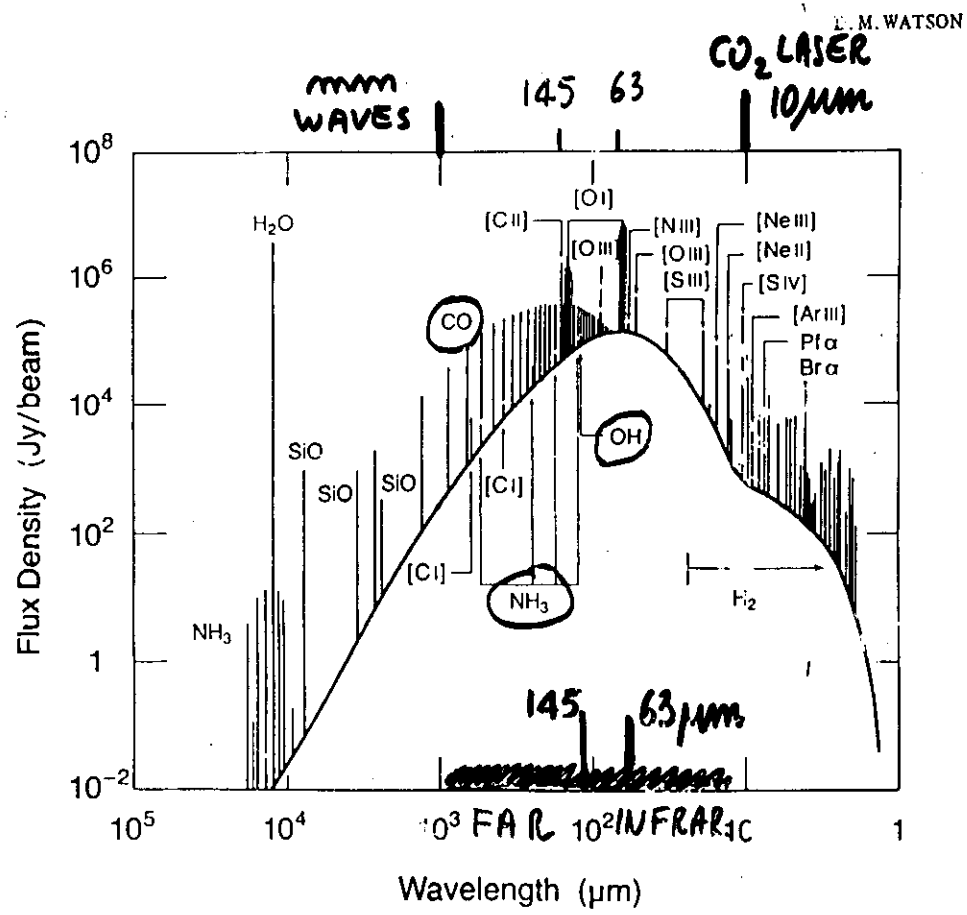

Figure 1: The spectrum of Orion-KL. Omitted for clarity are numerous molecular rotational lines in the millimeter-wavelength region which are present with antenna temperatures as high as about 20 K, the free-free continuum emission of M42, and all of the hydrogen recombination lines but the "alphas."

ASTROPHYSICS

HETERODYNE MEAS. ACCURACY < 1 MHz

RELATIVE SENSITIVITY (Absorption Spectroscopy)

ABSORPTION COEFFICIENT (A.C.)

$$\frac{(N_{LOWER} - N_{UPPER})(\mu)^2 \nu^2}{(LINE\ WIDTH)}$$

$$\simeq \frac{N_{LOWER}\left(1 - e^{-\frac{h\nu}{kT}}\right)(\mu\nu)^2}{\left[\nu_{DOPPL} + \frac{1}{\tau_{coll} + \tau_{rad}}\right]}$$

REGION	TRANS	THz ν	$1 - e^{-\frac{h\nu}{kT}}$	$\frac{1}{\nu_D + 1/\tau_c + \tau_{rad}}$	$(\mu\nu)^2$	A.C.
μWave	ROT	.03	.01	1	10^{-3}	10^{-5}
FIR	ROT	1.0	.2	1	1	.2
FIR	ROT	3.0	.5	1/2	9	2.5
IR	VIB	30.0	1	1/60	9	.15
VIS	EL.	500	1	1/1000	3×10^5	300

BUT, FOR ATOMS...

...magnetic dipole

DENSITY OF FREQUENCY MATCHES

3×10^{13} Hz

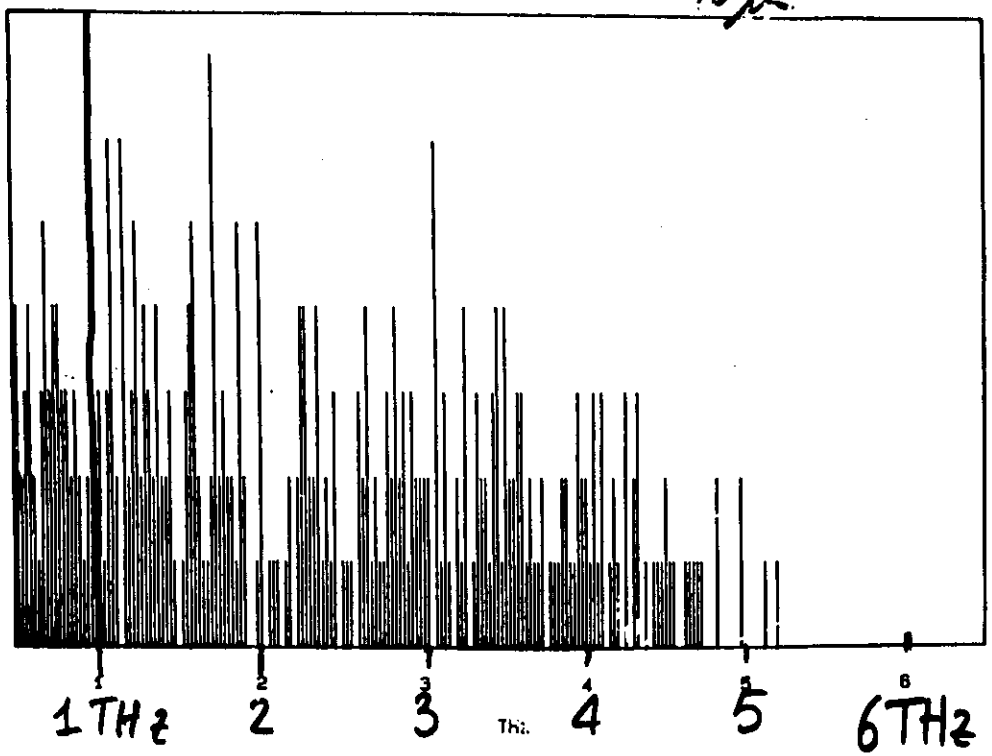

Figure 3. Density of frequency matches.

1 mm

50 μm

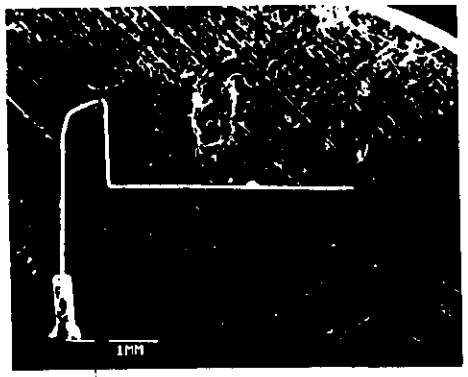

LENGTH
2.7 mm

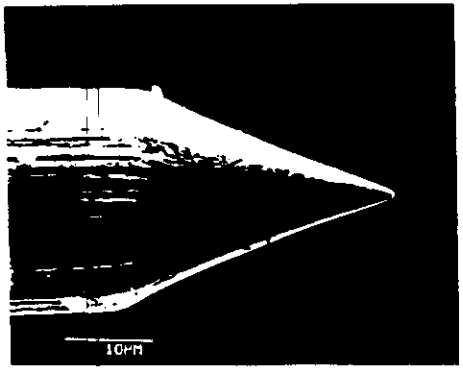

ANGLE
15°

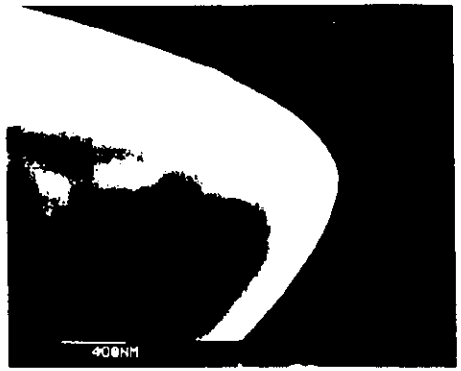

TIP RADIUS
3000 Å

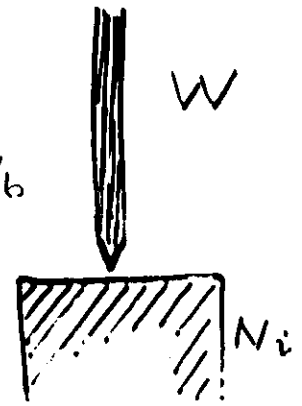

$\nu_x = k \cdot \nu_0 \cdot \ldots \cdot \nu_i \pm \nu_b$

$i = f(v) = \frac{V}{R} + \frac{i''}{2} V^2 + \frac{i'''}{3!} V^3 + \ldots$

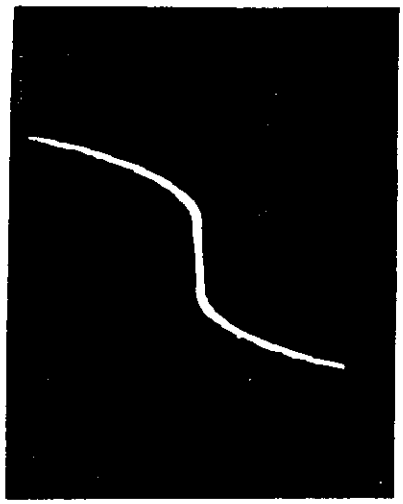

W-Co

3rd ORDER
(2nd negligible)

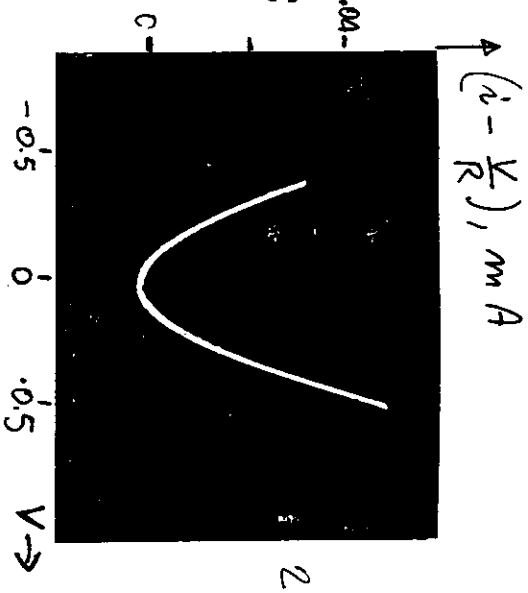

W-Ni

2nd ORDER

(3) "THREE WAVE" MIXING
(ONLY TWO LASERS)

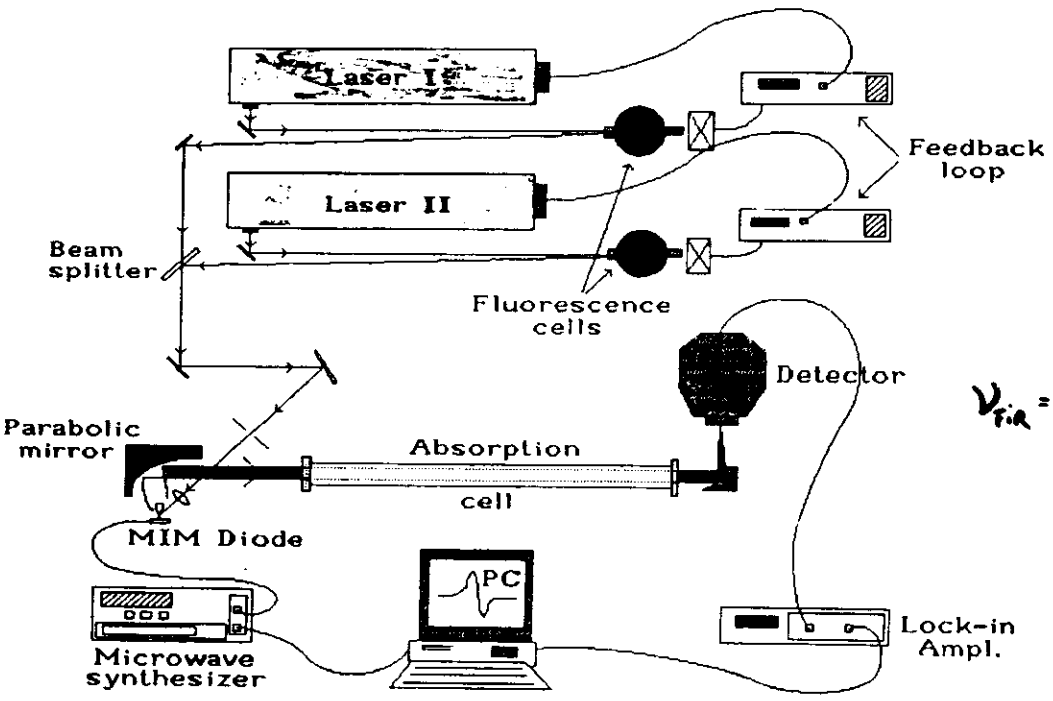

$\nu_{fin} = |\nu_1 - \nu_2| \pm \nu_{\mu w}$

FIRENZE APPARATUS

Last months also:
Toyama Univ, JAPAN
MATSUSHIMA

EVENSON, INGUSCIO, JENNINGS J. Appl. Phys. 57, 956 (85)

"THE MIXER"

- Nickel 2nd order
- Cobalt 3rd order

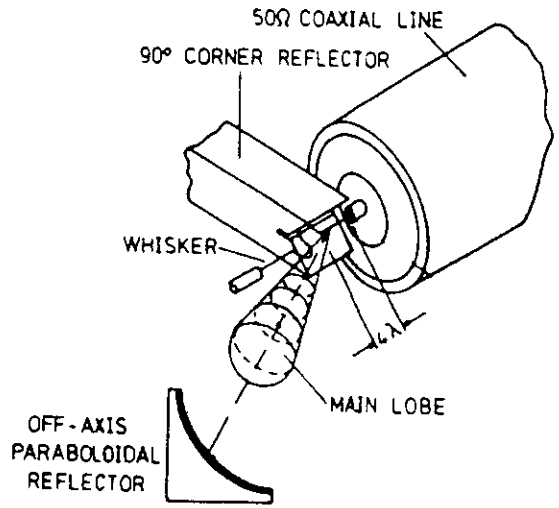

BETTER COLLIMATION
LINEAR POLARIZATION

- Extension of the precision typical of the neighbouring microwave region (Heterodyne techniques)
- Use of frequency stabilized infrared sources (CO_2 lasers)

Tunable Far Infrared spectrometer

- Continuous tunability (0.3 - 6 THz; 1000 - 50 μm)
- Doppler limited resolution (FIR linewidth: a few tens of kHz)
- $1/10^4$ minimum detectable absorption (1 sec time constant)
- $1/10^8$ average accuracy

AN EASY EXPERIMENT (STABLE POLAR MOLECULE) TO TEST THE APPARATUS.
J. Mol. Spectros. 1991

A spectroscopic example: hyperfine structure of HBr ... and more

A SMALL PORTION OF THE FAR INFRARED SPECTRUM OF THE ATMOSPHERE

From
B. Carli
J. Quant. Spectros. Rad. Transf
32, 397 (1984)

BLACK BODY RADIANCE

SPECTRAL RADIANCE

$$S(\sigma, h_F, \theta) = \int_{\tau(\sigma,S_b)}^{\tau(\sigma,o)} B[\sigma, T(s)]\, d\tau(\sigma, s)$$

ATM. TRANSMISSION τ

$$\tau(\sigma, s) = \exp\left[-\int_o^s \sum_i k_i(\sigma, p, T)\, q_i(s)\, \rho(s)\, ds\right]$$

STRENGTH | LINESHAPE | DENSITY

ABSORPTION COEFFICIENT

$$k_i^{lu}(\sigma, P, T) = S \cdot g(\sigma - \sigma_0) \cdot N$$

$$S \propto |u|^2$$

WE NEED A HIGH SENSITIVITY LABORATORY TECHNIQUE TO GET

100 Km ——> 1 m
unstable species

- LINE FREQUENCIES
- COLLISIONAL LINESHAPES
- LINE STRENGTHS

Fourier Transform

vs.

Tu-FIR

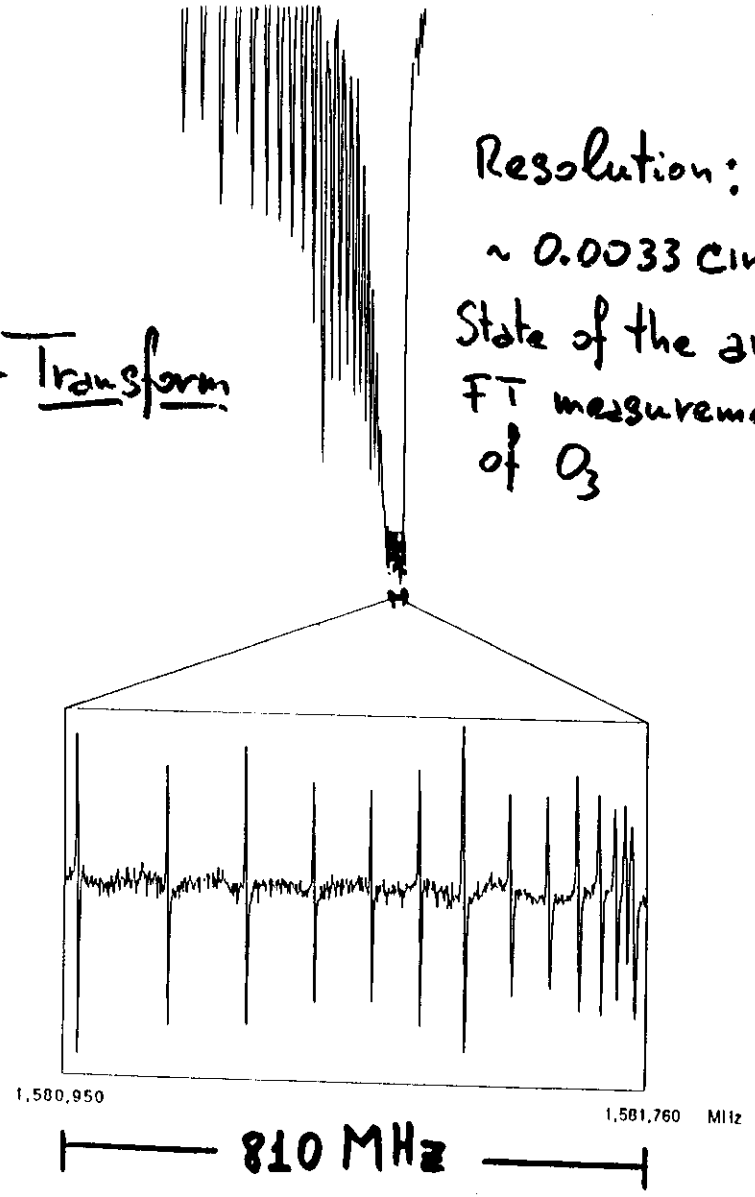

Resolution:

~ 0.0033 cm^{-1}

State of the art FT measurement of O_3

FREQUENCY ACCURACY

CO_2 absolute frequency ± 3 kHz

" Lock uncertainty ± 25 kHz (± 7 kHz best)

$\Delta\nu_{FIR} = 35$ kHz (10 kHz best)

$\Delta\nu_{TRANSITION}$ ~ $\Delta\nu_{FIR}$ for good S/N

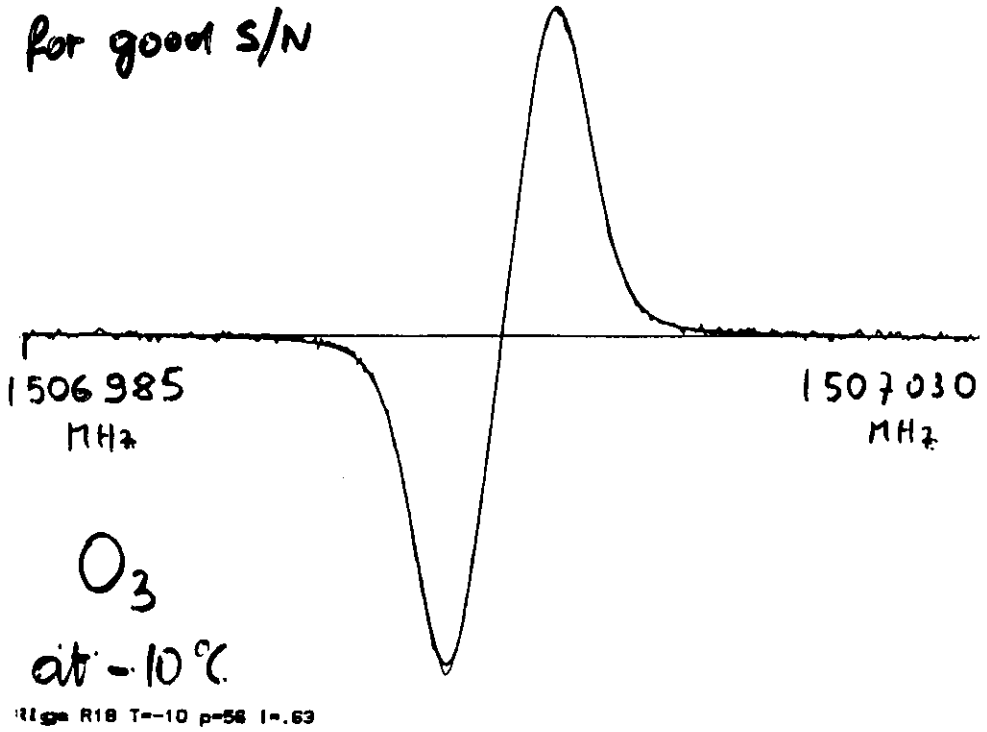

O_3 at -10 °C

Ridge R18 T=-10 p=56 I=.63

UPPER ATMOSPHERE
ATOMIC OXYGEN IN THE G.S.

LMR
K.EVENSON

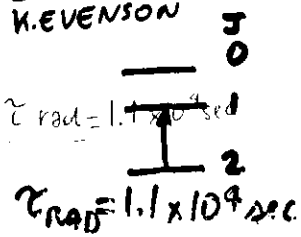

$\tau_{RAD} = 1.1 \times 10^4$ sec.

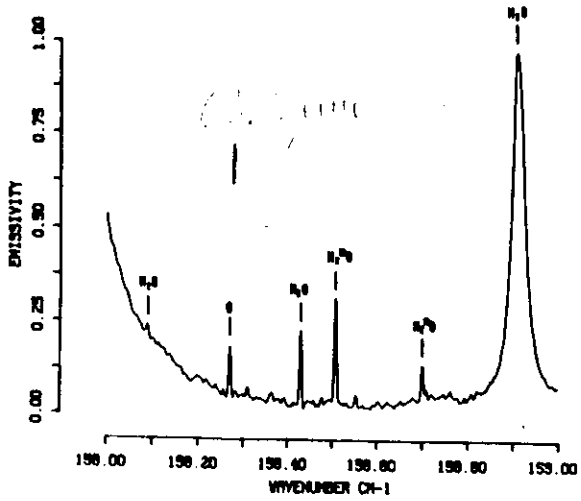

LMR
P.DAVIES

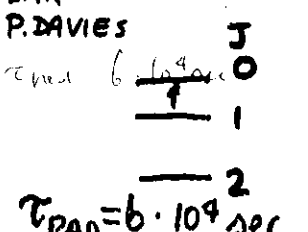

$\tau_{RAD} = 6 \cdot 10^4$ sec.

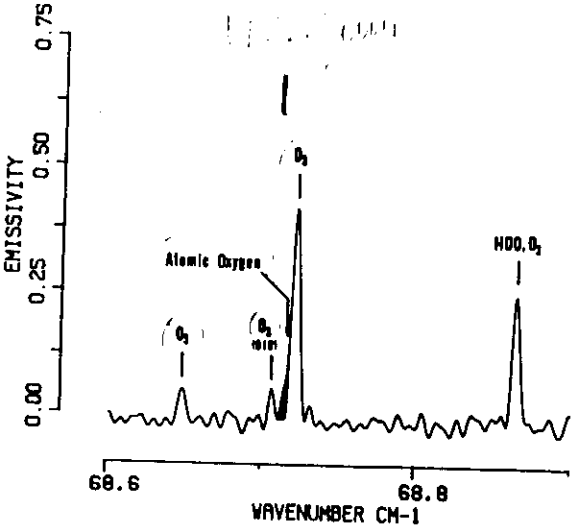

GLOW DISCHARGE

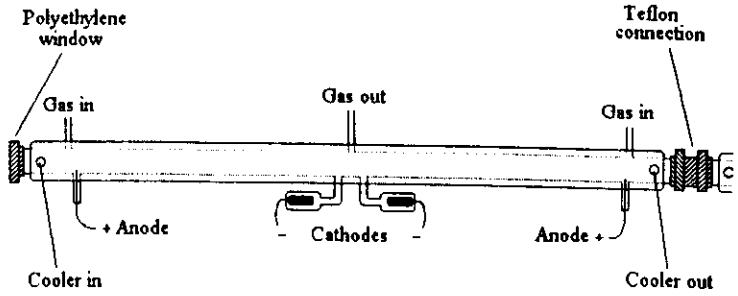

O

HEAT PIPE

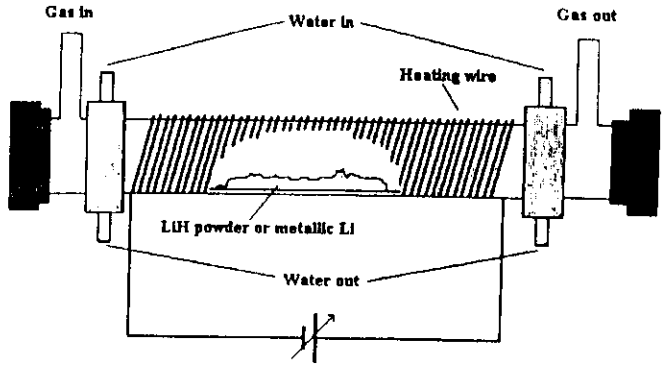

LiH

"SPECIAL" DISCHARGE
+CHEMICAL REAC.

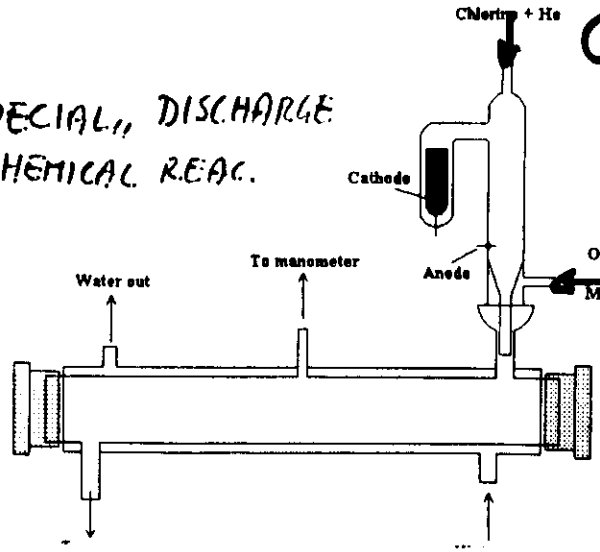

$Cl_2 + He$

$O_2 + CH_3OH$

HO_2

A:\atox2d.4

HO_2 - MOTIVATION

Quantitative measurement in the atmosphere is a high priority
(HO_2 important constituent of HO_x chemical cycle which regulates the earth's stratospheric ozone).

Balloon based measurements of relatively strong far infrared rotational lines in <u>emission</u>.
(Future developments include heterodyne detection).

Need for: line positions (OK), line strengths (OK), <u>pressure broadening which determines the linewidths in the atmosphere</u>

P.B. is essential in the analysis of heterodyne spectra to determine the contributions from HO_2 at various tropospheric altitudes.

Lines recorded in the atmosphere....

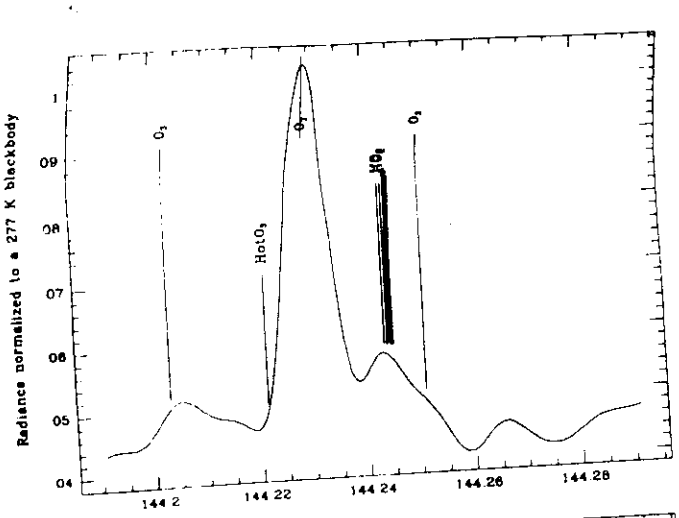

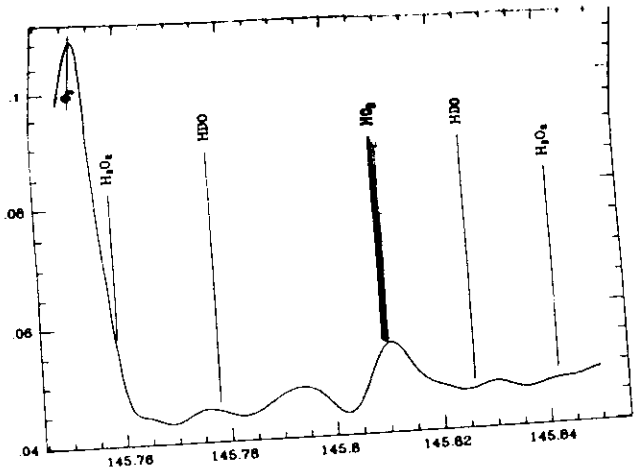

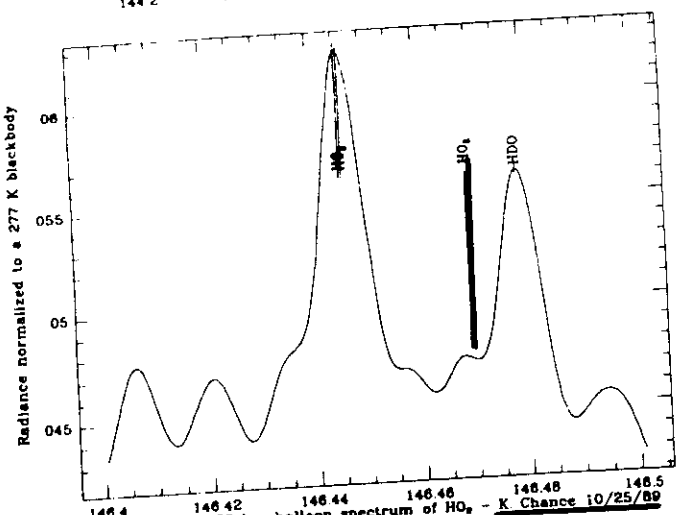

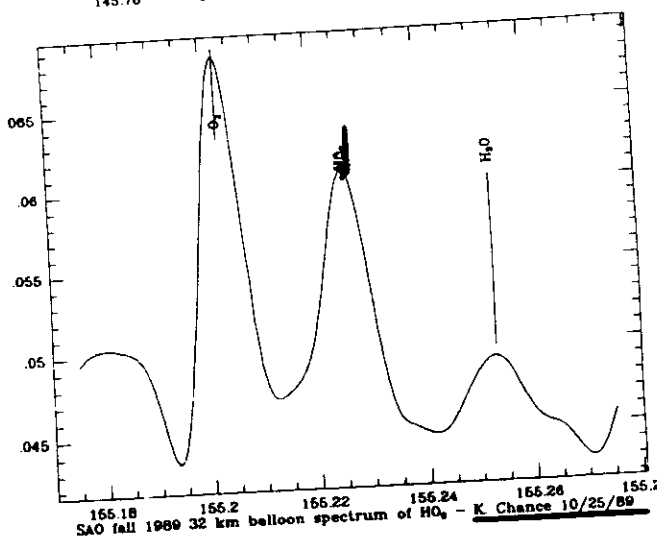

HO_2 cell

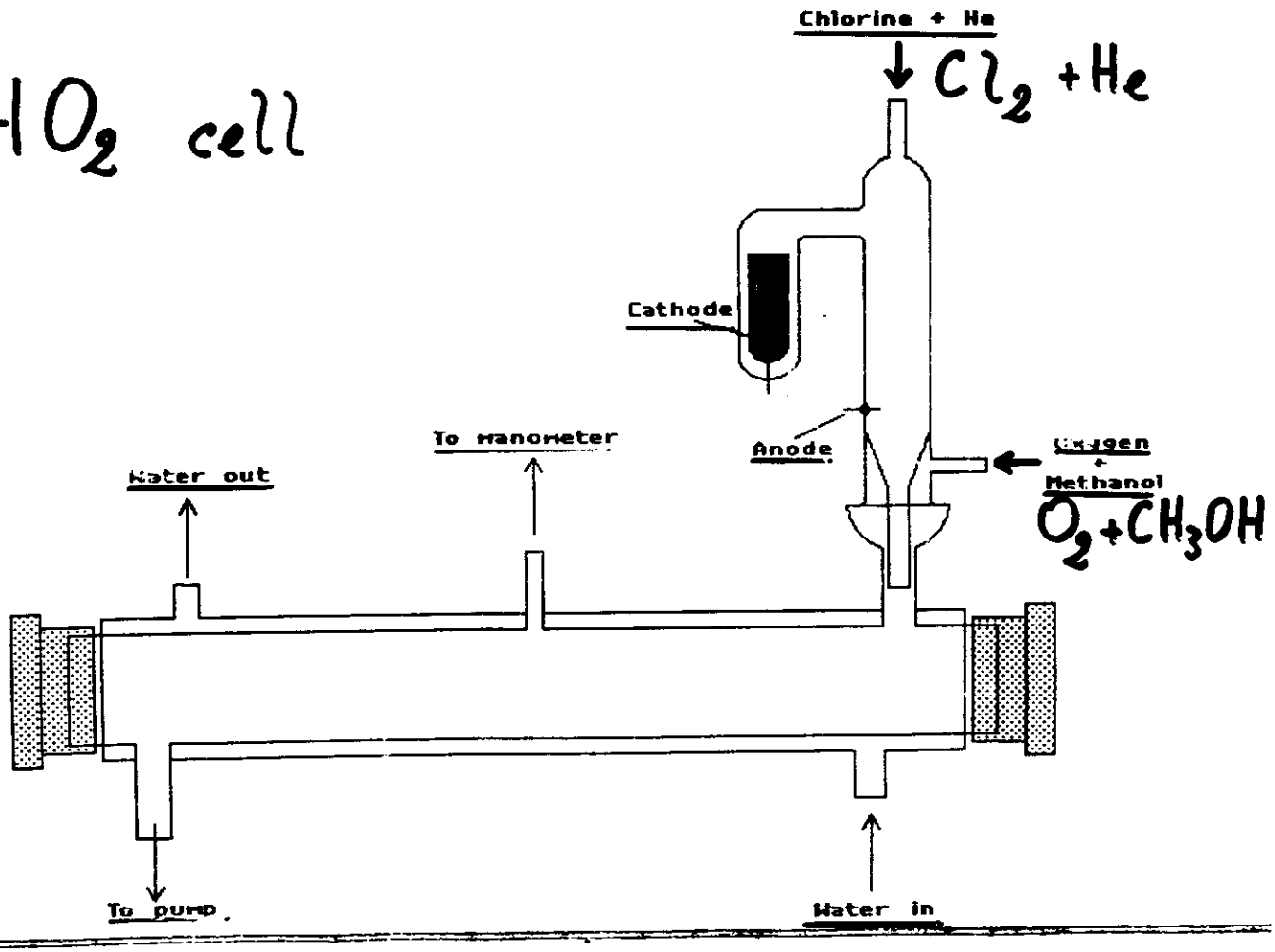

CHEMISTRY FOR HO_2 PRODUCTION IN THE LABORATORY

$$Cl + CH_3OH \longrightarrow CH_2OH + HCl$$

$$CH_2OH + O_2 \longrightarrow \boxed{HO_2} + H_2CO$$

Net $Cl + CH_3OH + O_2 \rightarrow HO_2 + HCl + H_2CO$

(3)

.... and in the lab

HO_2

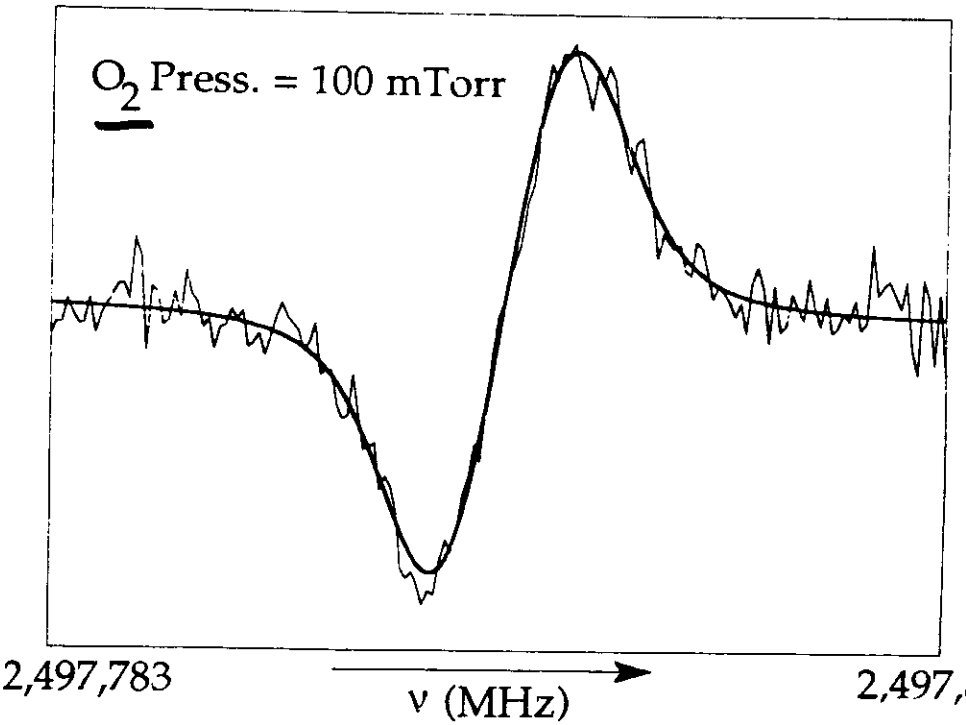

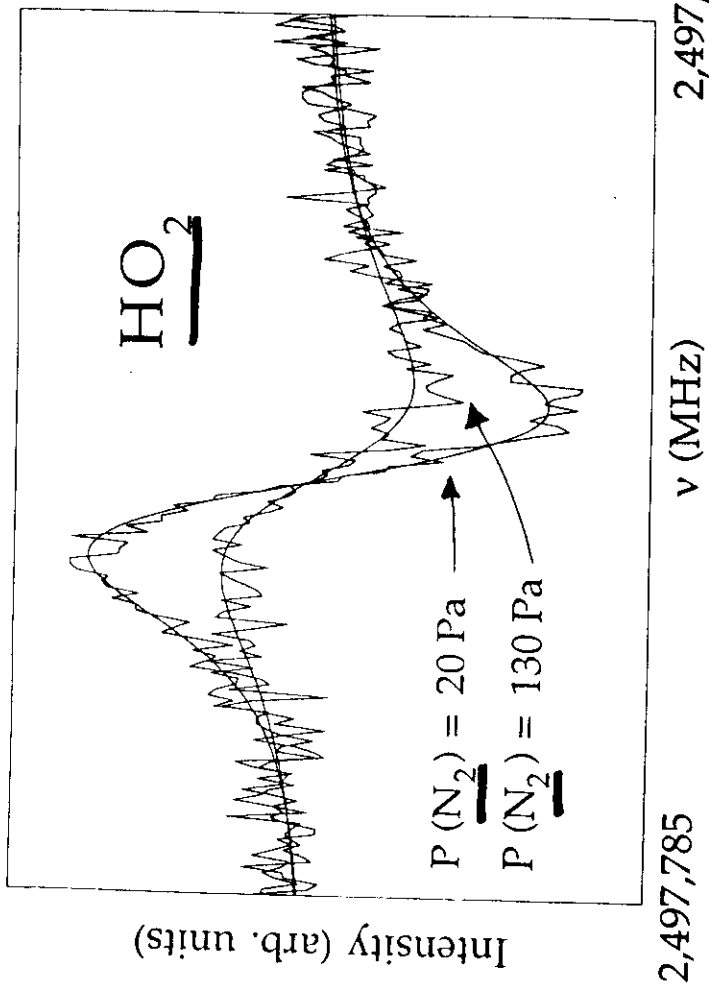

Results

$\gamma(H_2) = 47.4 \pm 4.9$ kHz/Pa
$(6.3 \pm 0.6$ MHz/Torr$)$

$\gamma(O_2) = 19.9 \pm 1.6$ kHz/Pa
$(2.7 \pm 0.2$ MHz/Torr$)$

$\underline{\gamma(air)} = 91.6 \pm 3.8$ kHz/Pa
$(5.6 \pm 0.5$ MHz/Torr$)$

at $T = 300 \pm 1$ K

(1σ uncertainties)

γ uncertainties still better than 10%

STARK CELL

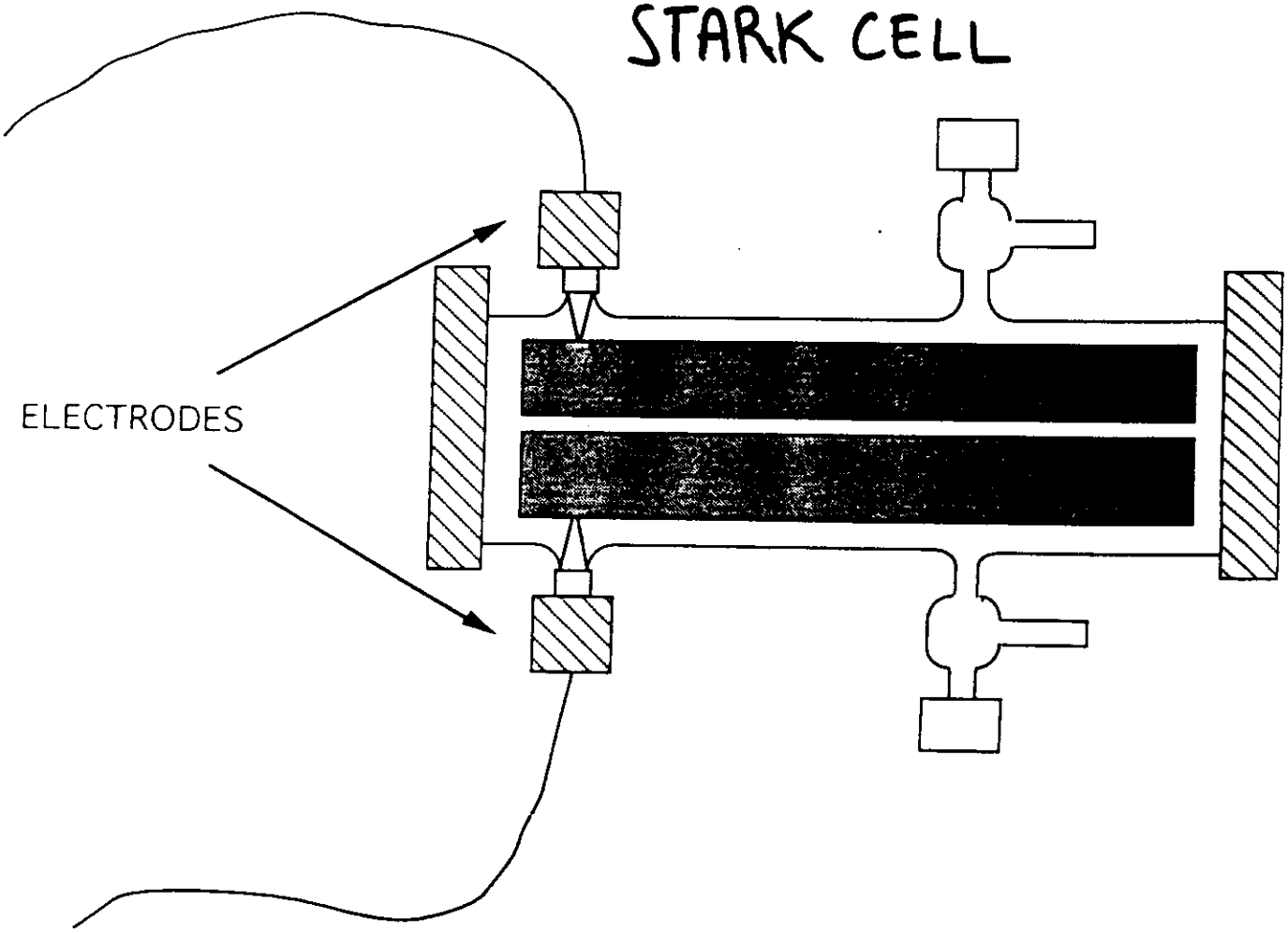

(55) CH_3OH at 328 μm $3_{0,-3} - 2_{0,-2}$ $\Delta\Pi = 0$

$J: 2 \rightarrow 3$

5 components expected.

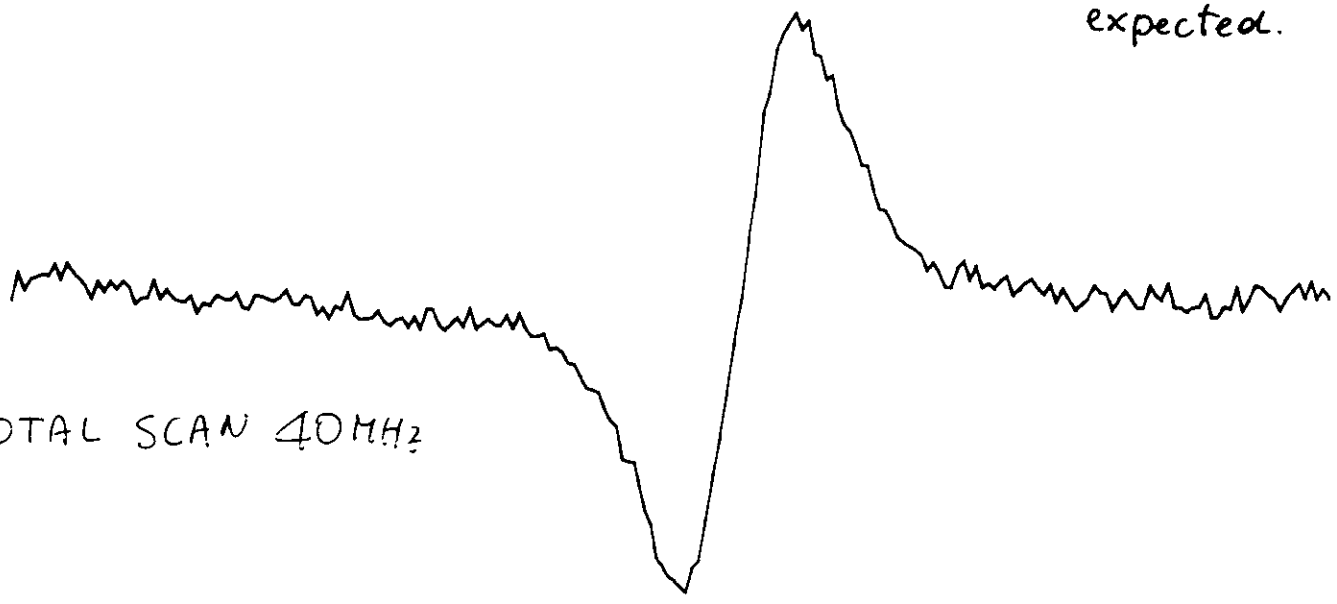

912126.434 MHz

912086.434

$E = 0$ Volt/cm

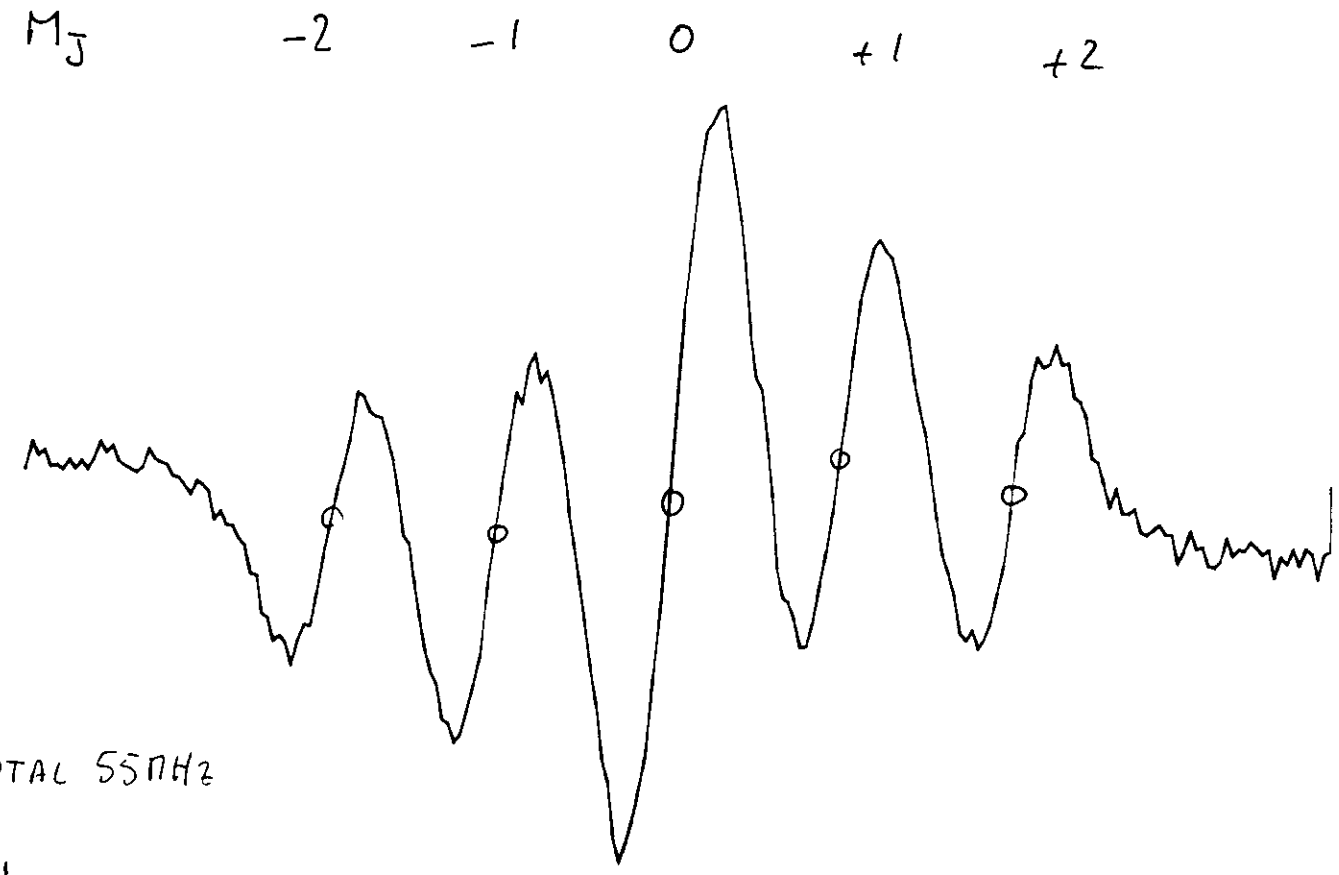

$E = 200$ Volt/cm

(23)

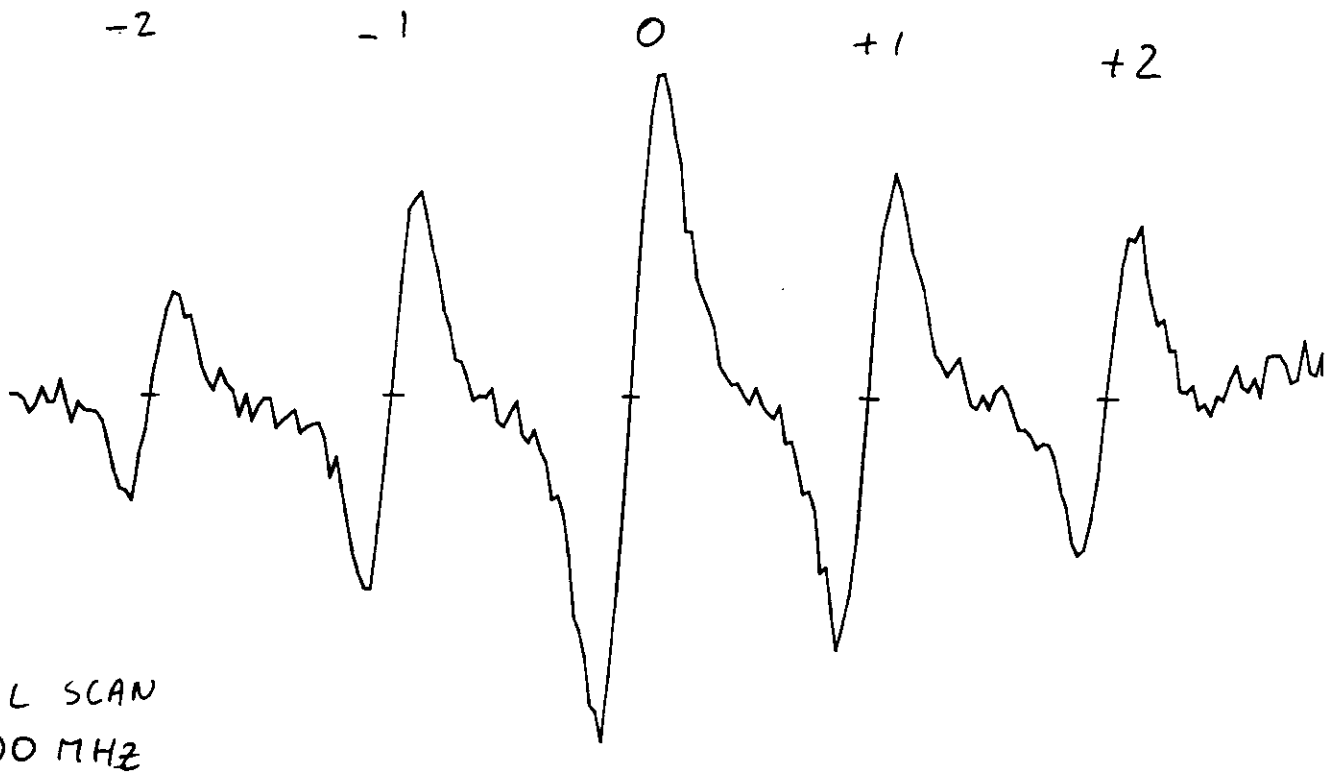

$E = 500$ Volt/cm

LITHIUM HYDRIDE

✓Simplest neutral heteronuclear diatomic molecule
✓Test for theoretical models and breakdown of Born-Oppenheimer approx.
✓Search in astrophysical environments (ISO satellite)

Cosmological implications:

- Search in high redshift regions
- Primordial nucleosynthesis

Need for accurate values of frequencies to detect these lines or to extrapolate to uninvestigated regions.

LiH

MOTIVATIONS

EXTREMELY LIGHT
(ab initio theories, Born-Oppenheimer approximation breakdown ...)
VERY LARGE DIPOLE (5.9 D)
(Collisional: test of dipole-quad...)
COSMOLOGICAL

PROBLEMS

PRODUCTION REQUIRES HIGH TEMPERATURE, HIGH DISSOCIATION RATE

EXPERIMENTAL SETUP

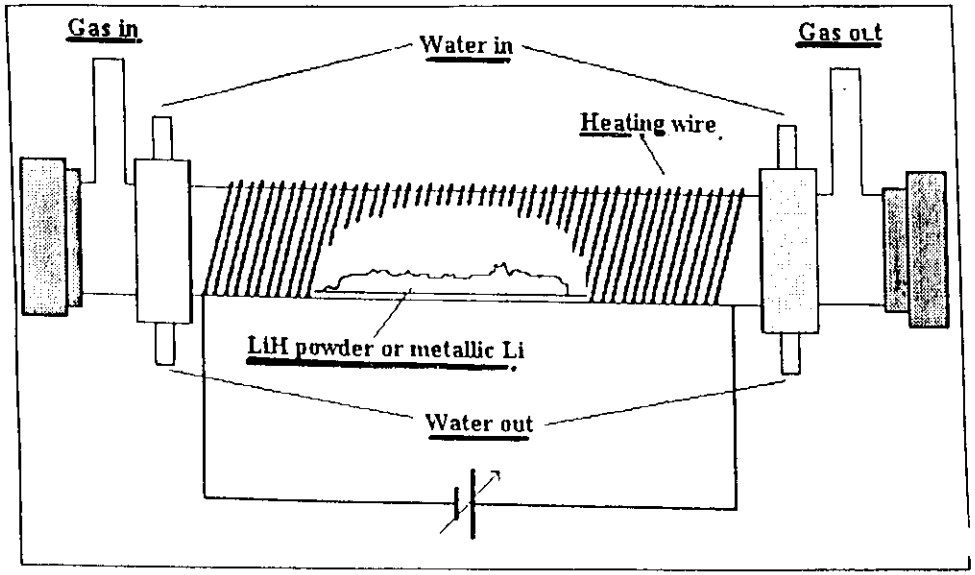

- Cell temperature: ~ 500 ÷ 600 °C
- All possible combinations of ^{7}Li, ^{6}Li, H, D
- Various vibrational states, from ground to v = 2 excited level

$^{6}Li/^{7}Li \simeq 0.08$ natural abundance

Deuterium enriched sample

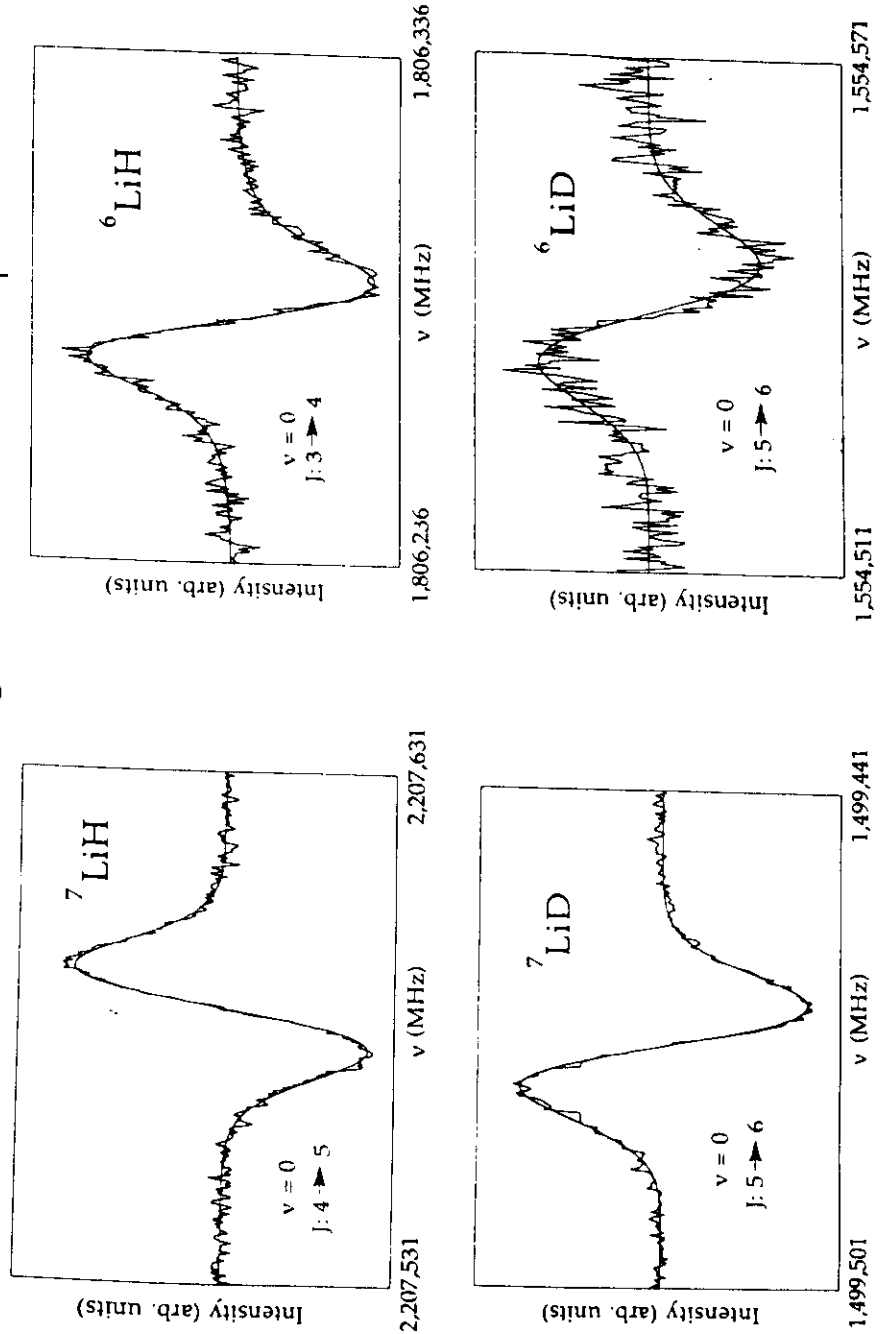

ALL THE POSSIBLE ISOTOPE COMBINATIONS

GROUND VIBRATIONAL STATE; NATURAL ABUNDANCE $^6Li \simeq 7\%$

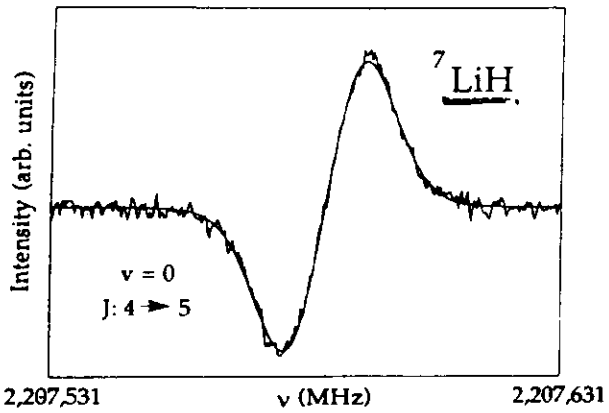

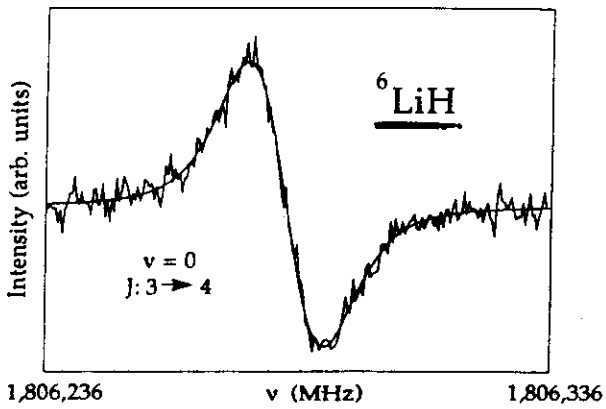

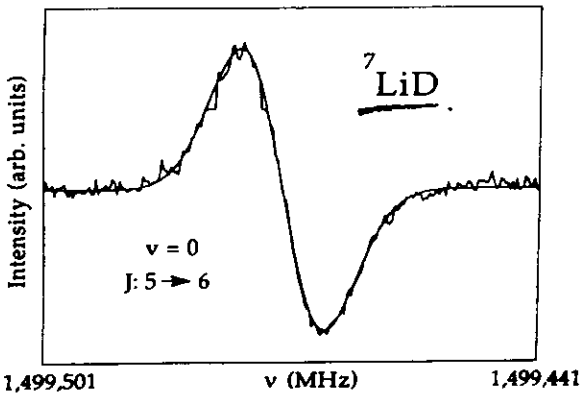

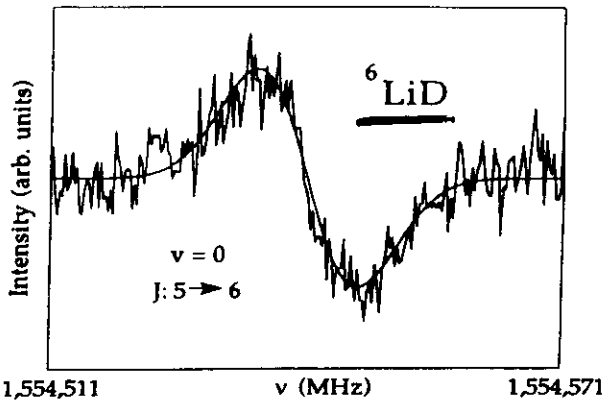

FRIDAY POSTER 039

(53)

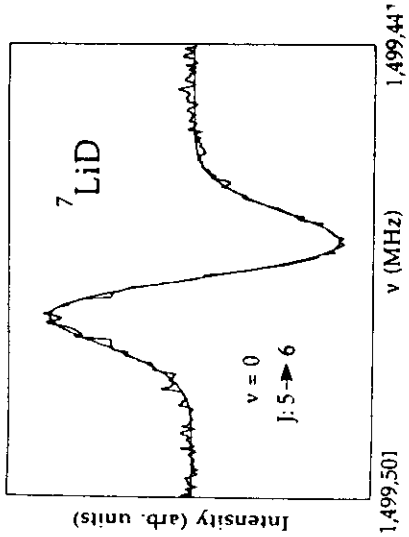

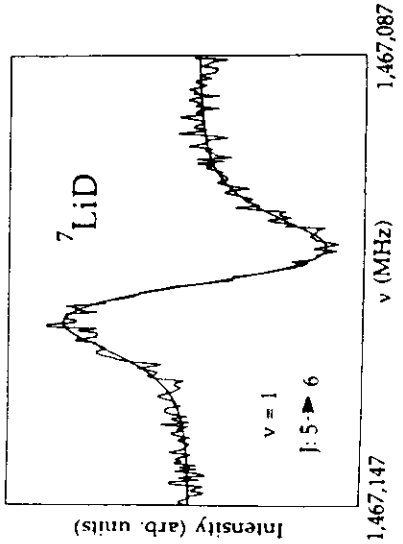

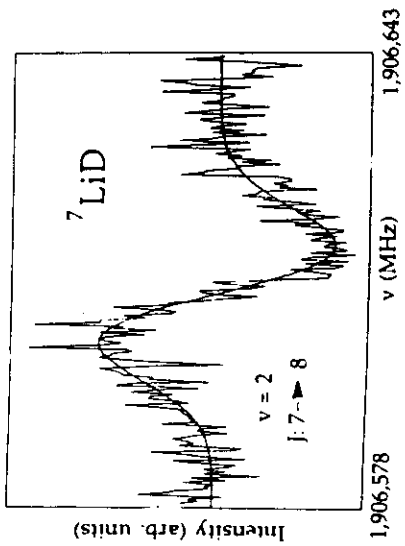

P = 16% (V=0)

P = 27% (V=0)

THE ASTROPHYSICAL JOURNAL, 330:L135-L136, 1988 July 15

HD

FREQUENCY MEASUREMENT OF THE $J = 1 \leftarrow 0$ ROTATIONAL TRANSITION OF HD[1]

K. M. EVENSON, D. A. JENNINGS, J. M. BROWN, L. R. ZINK, K. R. LEOPOLD, M. D. VANEK, AND I. G. NOLT
Time and Frequency Division, National Bureau of Standards, Boulder
Received 1988 April 15; accepted 1988 April 22

ABSTRACT

The frequency of the astronomically important $J = 1 \leftarrow 0$ rotational transition of hydrogen deuteride (HD) at 2.7 THz (90 cm^{-1}) has been measured with tunable far-infrared radiation with an accuracy of 150 kHz. This frequency is now known to sufficient accuracy for use in future astrophysical heterodyne observations of HD in planetary atmospheres reported by Bezard *et al.* in 1986 and the interstellar medium reported by Bussoletti *et al.* in 1975.

Subject headings: interstellar: molecules — laboratory spectra — molecular processes

A spectrometer using the coherent radiation resulting from the nonlinear mixing of two CO_2 lasers in a metal-insulator-metal diode (Evenson, Jennings, and Petersen 1984) was used to generate the far-infrared radiation. The spectrometer, previously described (Evenson *et al.* 1985), has been used to measure rotational spectra in MgH (Leopold *et al.* 1985), NaH (Leopold *et al.* 1987), OH (Brown *et al.* 1986), ArH[+] (Brown *et al.* 1988), HF (Jennings *et al.* 1987), and CO and HCl (Nolt *et al.* 1987).

The HD was observed in a 19 mm inside diameter and 3.94 m long copper tube, in single transit of about 10^{-7} W of far-infrared radiation used to detect the signal shown in the figure. HD was created in a hollow cathode discharge in a mixture of equal parts of H_2 and D_2 by running the discharge for about 3 minutes. A 20% peak absorption was observed at a pressure of 930 Pa (7 torr). See Figure 1. This absorption is somewhat larger than that expected using a value of 8.83×10^{-4} debye for the dipole moment (Drukopoulos and

[1] Contribution of the United States Government, not subject to copyright. Work partially supported by NASA contract W15-047.

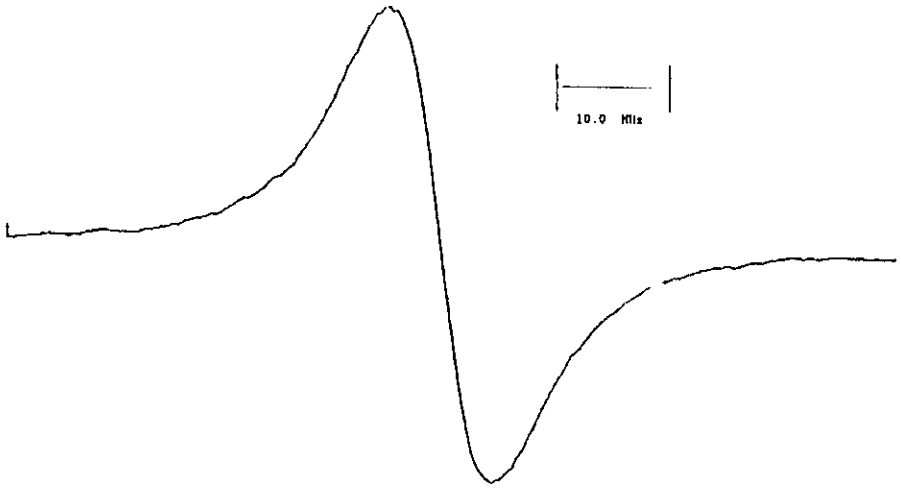

FIG. 1.—Derivative of the *HD* absorption line taken at 930 Pa (7 torr) with a 0.5 s time constant. A 3.5 m path length and a 5 MHz frequency modulation at a 50 Hz rate was used to observe the signal. A gallium-germanium photoconductor detector was used to observe the absorption using approximately 10^{-7} W of tunable far-infrared radiation.

LIGHTEST MOLECULE
HD

$$= -i\hbar\frac{e}{c}\frac{\hbar}{Mc}\varepsilon_{01}\left(x_1\frac{\partial^2 A_0}{\partial x_2 \partial x_1} - x_2\frac{\partial^2 A_0}{\partial x_1^2}\right) = -i\hbar\frac{e}{c}\frac{\hbar}{Mc}\varepsilon_{01}\frac{\partial A_0}{\partial x_2}$$

e da altre analoghe.

Nelle (6') il 2° termine al 2° membro si ottiene con un procedimento analogo

$$-\frac{e}{c}\frac{\hbar}{Mc}\varepsilon_{01}\left(-\frac{\partial A_0}{\partial x_1}\right)\frac{1}{2}\hbar(-i\alpha_1\alpha_2) - \frac{1}{2}\hbar(-i\alpha_1\alpha_2)\frac{e}{c}\frac{\hbar}{Mc}\varepsilon_{01}\frac{\partial A_0}{\partial x_1} =$$

$$= -i\hbar\frac{e}{c}\frac{\hbar}{Mc}\varepsilon_{01}\frac{\partial A_0}{\partial x_1} \quad \text{ecc.}$$

Fisica. — *Sullo spettro di oscillazione e rotazione della molecola* HD. Nota di G. C. WICK, presentata[(1)] dal Socio E. FERMI.

INTRODUZIONE. – Si suole chiamare spettro di oscillazione e rotazione di una molecola quella parte del suo spettro che è dovuta a oscillazioni dei nuclei intorno alle loro posizioni di riposo e rotazioni della molecola in blocco, non accompagnate da oscillazioni elettroniche; in altre parole quella parte dello spettro che corrisponde a transizioni in cui non variano i numeri quantici elettronici.

Tale spettro non viene mai osservato in molecole biatomiche omonucleari come H_2, N_2, O_2, ecc., fatto che, com'è noto, si spiega mediante semplici considerazioni di simmetria[(2)]. Esso è stato invece osservato in molecole fortemente asimmetriche (molecole polari) come HCl, HBr ecc.

La molecola HD non è rigorosamente omonucleare e deve quindi possedere uno spettro di oscillazione e rotazione; tuttavia è presumibile che data l'alta simmetria della struttura elettronica della molecola, lo spettro sia estremamente debole. Vedremo infatti che lo spettro ha un'origine diversa da quella ordinaria, essendo dovuto alla asimmetria dell'oscillazione dei nuclei (la differenza essenziale tra H_2 e HD è questa: nella molecola di HD il punto di mezzo della congiungente dei nuclei oscilla; si ha quindi, per inerzia, uno scuotimento del sistema elettronico, che produce il momento oscillante); la sua intensità teorica risulta non nulla soltanto in una approssimazione più elevata di quella di cui ci si contenta ordinariamente nella teoria delle molecole. Essa non è però così piccola da escludere la possibilità di osservare sperimentalmente lo spettro[(3)].

(1) Nella seduta del 19 maggio 1935.

(2) Vedi per un orientamento generale, il libro di E. FERMI, *Molecole e cristalli*; la dimostrazione rigorosa vedi R. DE L. KRONIG, *Band Spectra and Molecular Structure*.

(3) Il dott. H. Beutler mi ha gentilmente informato che sono in corso esperienze a questo proposito. Devo anche ringraziare il dott. Beutler, avendo io appreso l'esistenza del problema qui trattato da una sua lettera, cortesemente mostratami dal dott. U. Fano.

ATT: R. Accad. Naz. Lincei
Mem. Cl. Sci. Fis. Mat. Nat.
21, 708 (1935)

(30)

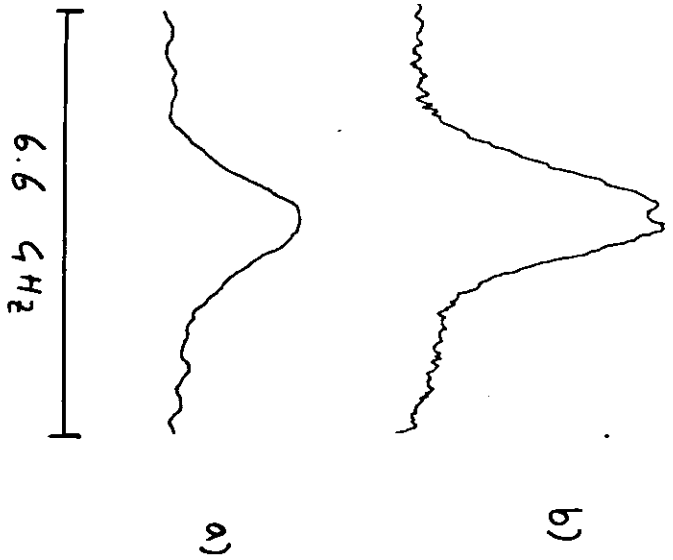
6.6 GHz
a)
b)

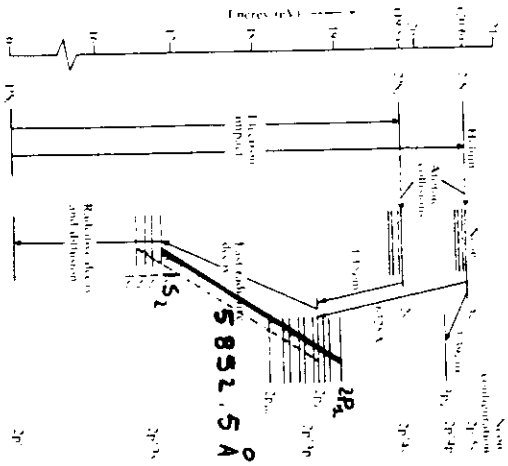
5852.5 Å

(61)

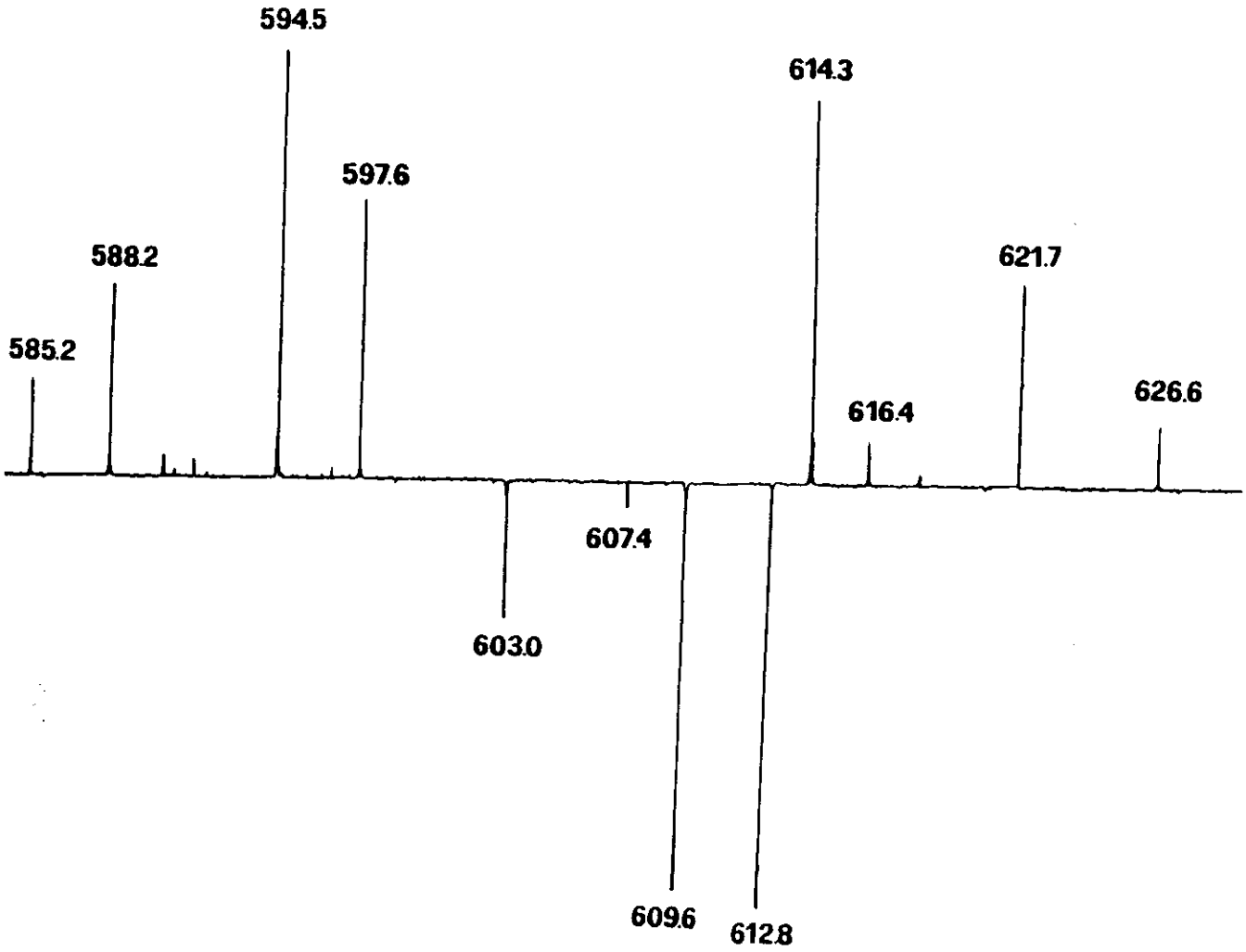
585.2
588.2
594.5
597.6
603.0
607.4
609.6
612.8
614.3
616.4
621.7
626.6

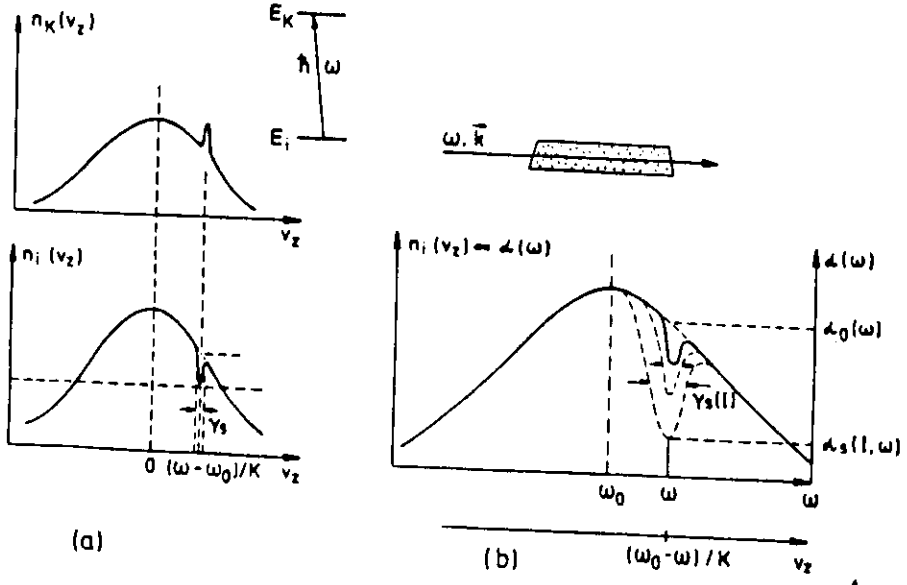

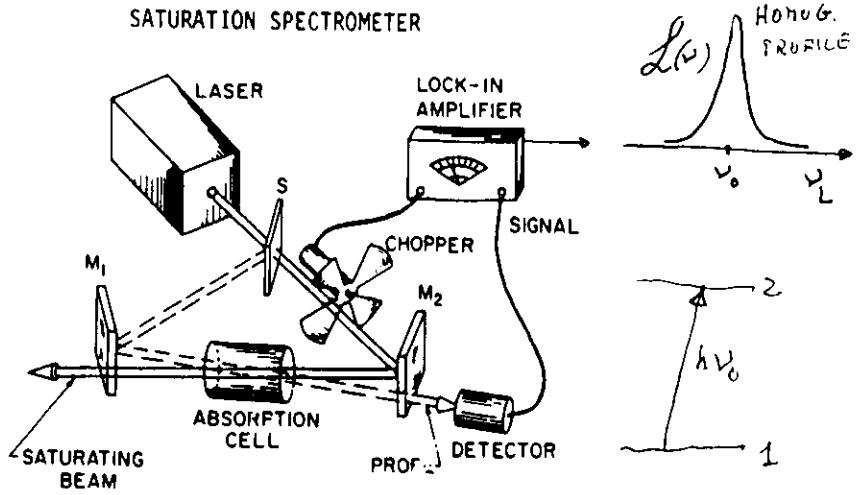

Neon

$1S_4 - 2P_3$

$\lambda = 6074$ Å

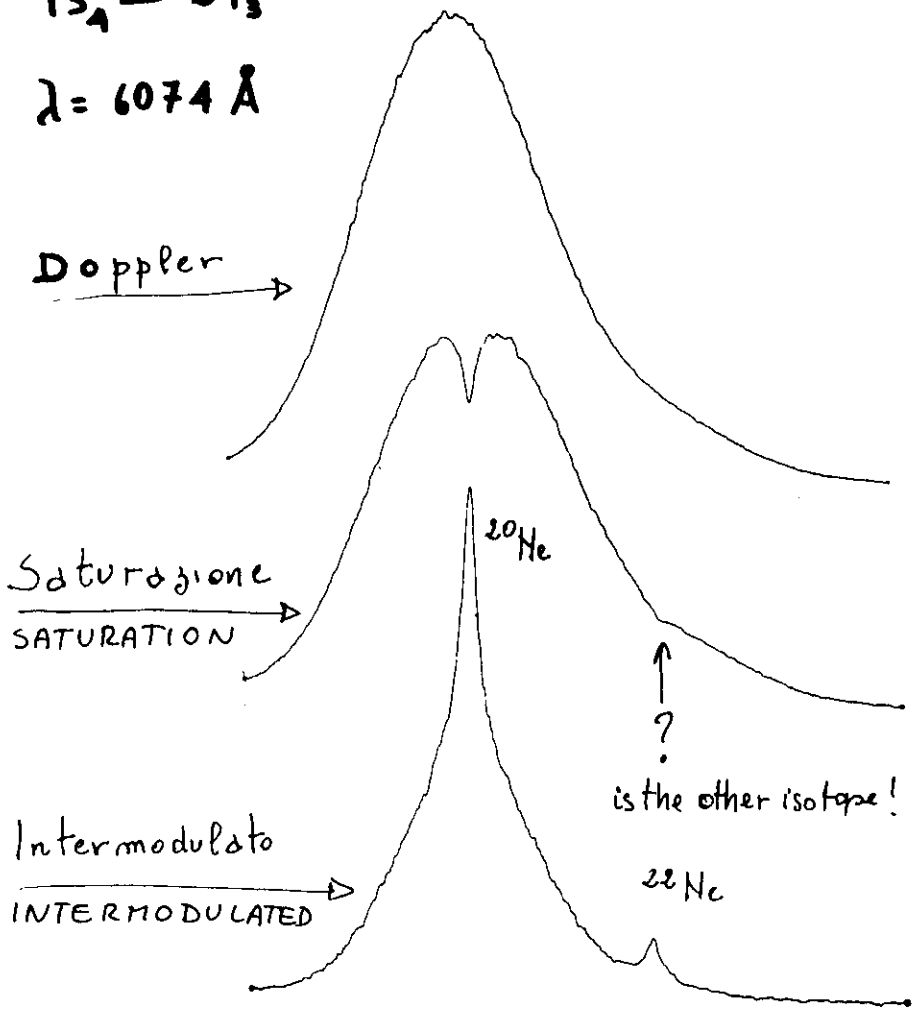

Fig. 25 Neon 6074 Å. Cella a catodo cavo; I = 48 mA, P = 1.6 Torr.
a) profilo Doppler
b) profilo con segnale di saturazione
c) profilo in intermodulazione

RYDBERG

BOHR

$\frac{1}{\lambda} = R\left[\frac{1}{m^2} - \frac{1}{n^2}\right]$

$R = 2\pi^2 m e^4 / h^3 c$

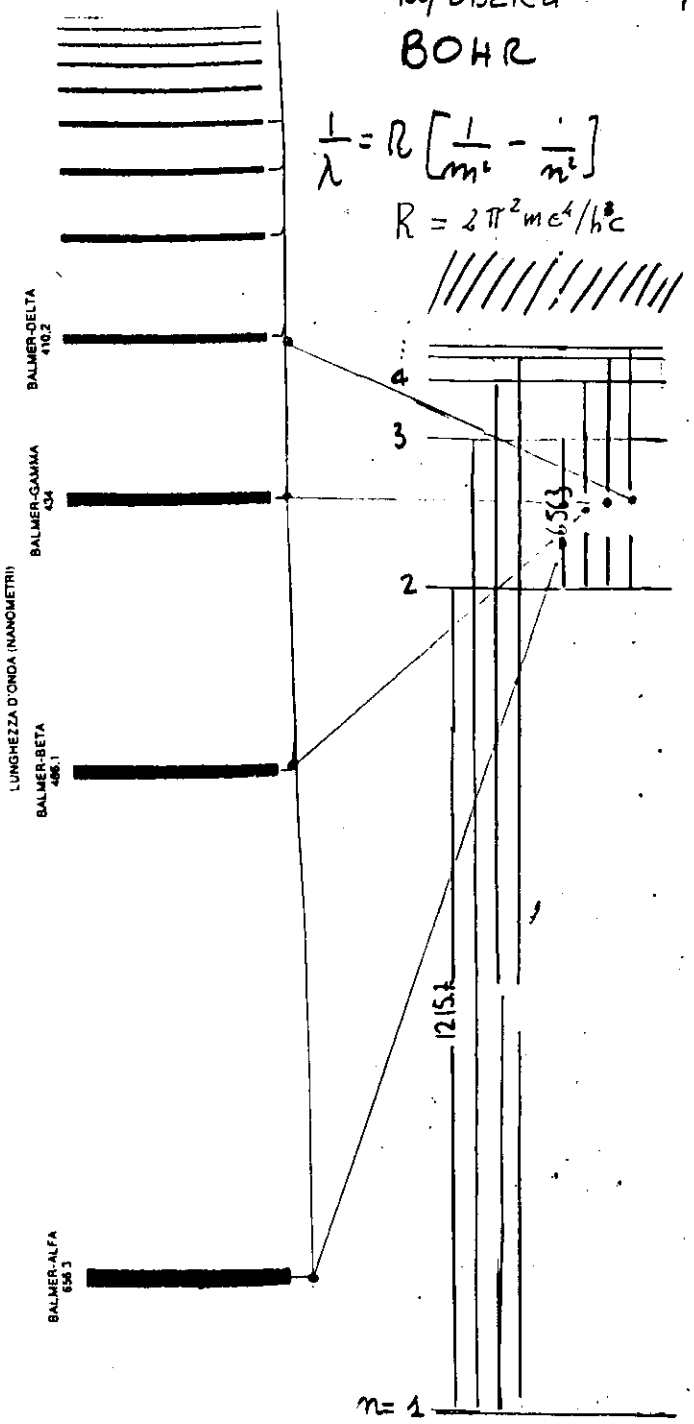

15 B. Scheumann, D. Meschede, T. W. Hänsch, J. L. Hall

. . . 20 years later

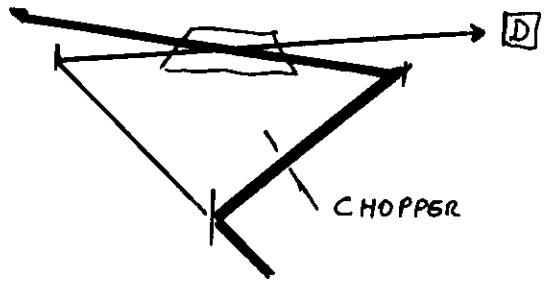

HYDROGEN BALMER-α LINE

Doppler-free saturation spectrum
recorded with free running diode laser

(InGaAlP laser diode
Toshiba TOLD9211,
T=-70°C, 5 mW at 656 nm)
Index guided

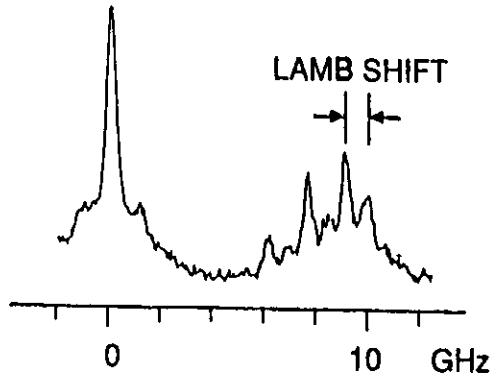

VELOCITY CHANGING COLLISIONS

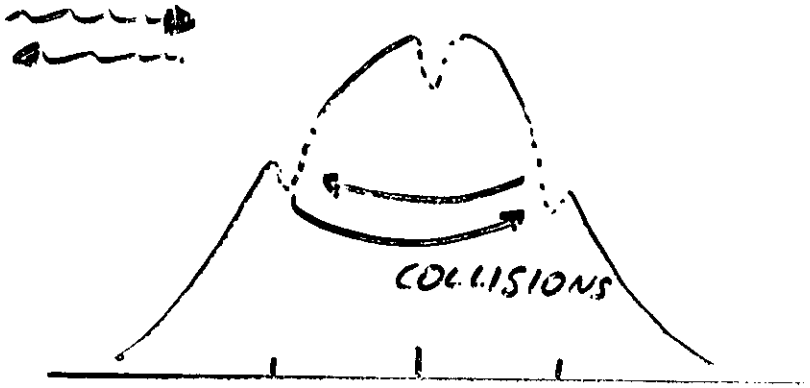

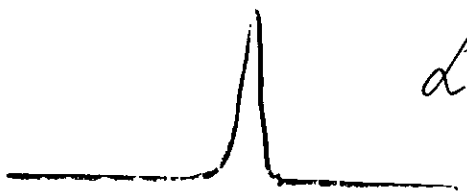

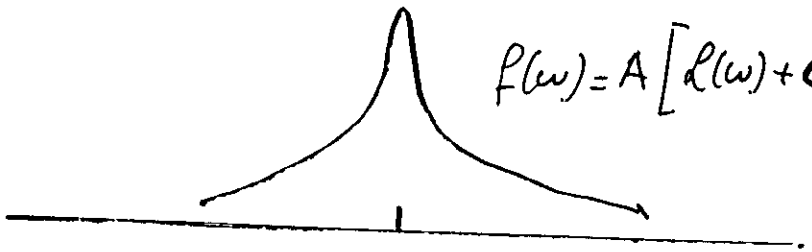

$$C \sim 2\sqrt{\pi}\, \ell_{q2}\, \frac{\Gamma_1 \gamma}{\gamma_1 \Delta\nu_D}$$

$$A\left[\frac{\gamma^2/4}{-\gamma^2/4 + (\nu-\nu_0)^2} + C\exp\left(-\frac{\nu-\nu_0}{\sqrt{5}\nu_D}\right)^2\right] \times \eta$$

$$C = 2\sqrt{\pi}\,\ell_{q2}\,\frac{\Gamma\gamma}{\sqrt{5}\,\Delta_D}$$

O_2/Ar (.1/5 Torr)

$\Delta\nu_D = 2\,GHz$ (520 °K)

$\gamma = \Delta\nu_{hom} = 386\,MHz$ (FWHM)

$C = 0.39$

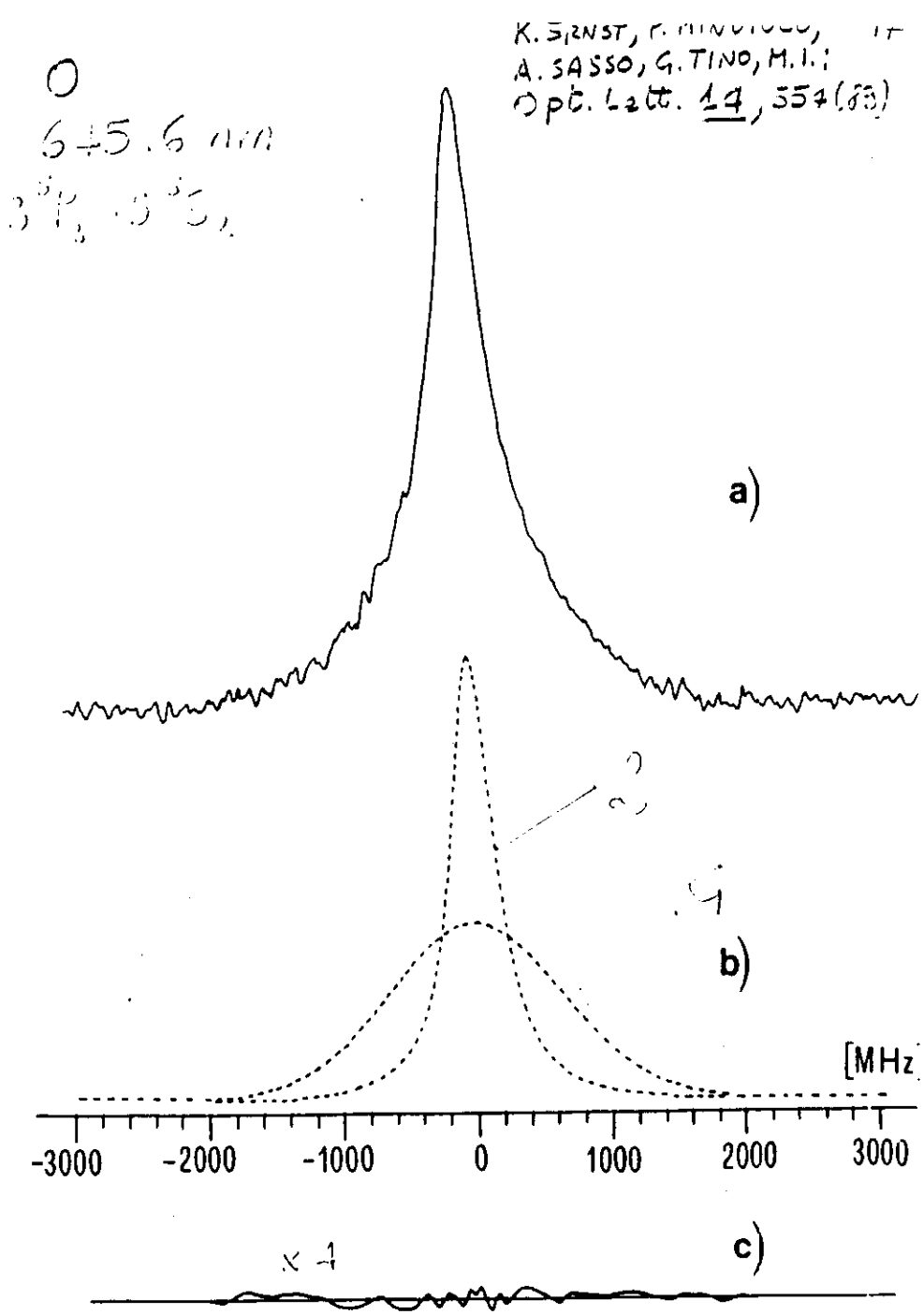

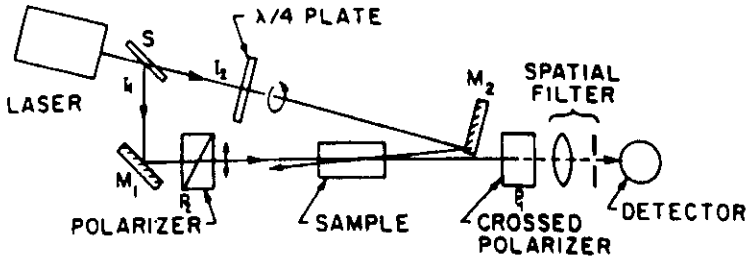

Fig.10.34. Schematic experimental arrangement for polarization spectro

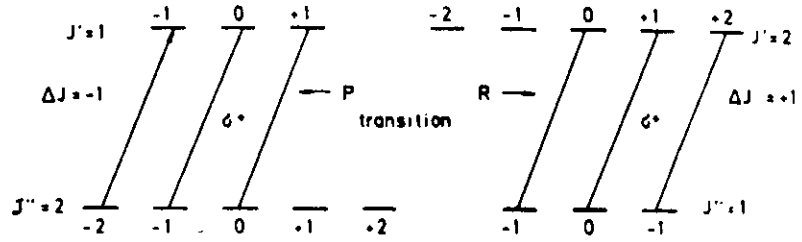

CON LUCE POL. CIRCOLARE
PROVOCO UN'ORIENTAZIONE
(SAT. SELETTIVA IN M)

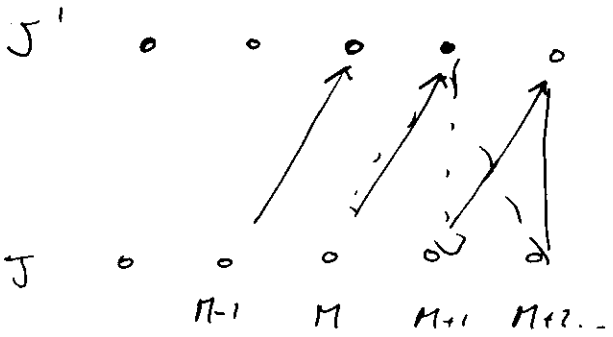

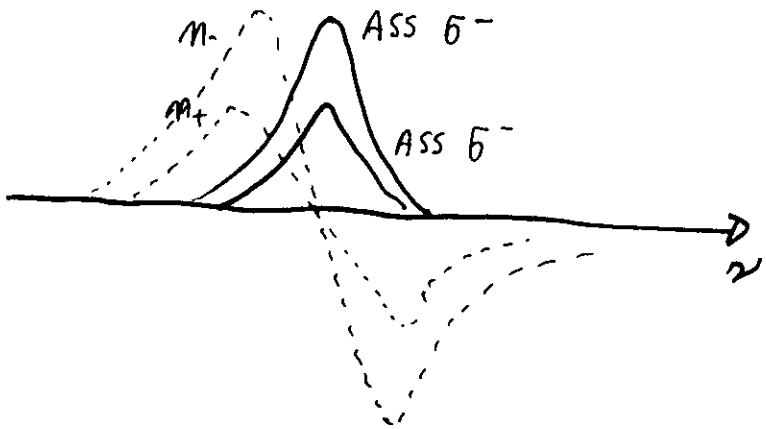

CIRCULARLY POLARIZED LIGHT
CREATES AN ORIENTATION
(SATURATION SELECTIVE IN M)

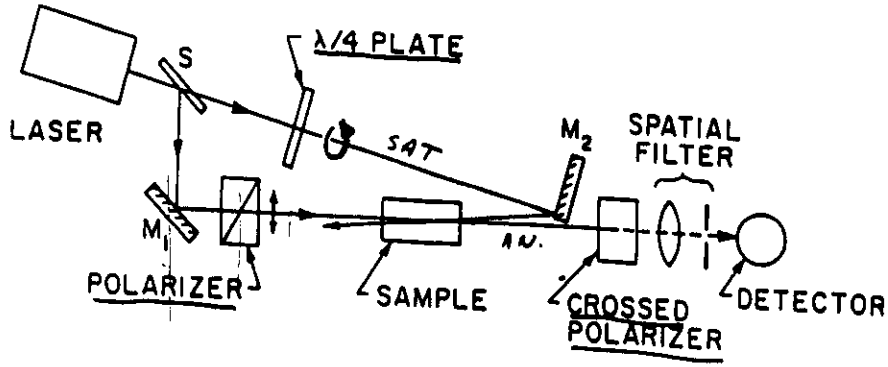

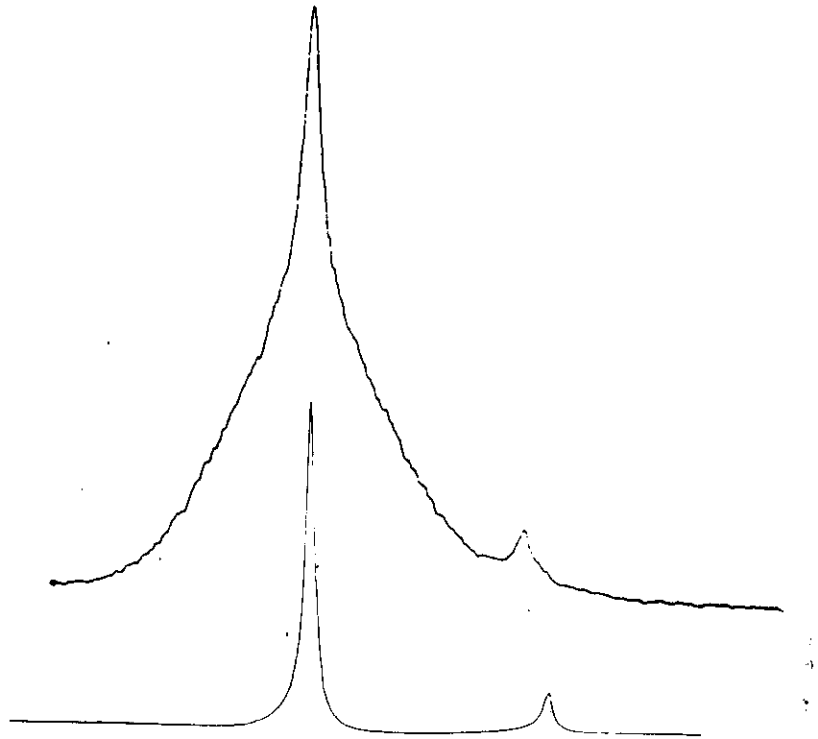

DOPPLER + HYPERFINE

15 comp J even ~EQUAL INTENSITY

21 comp J odd FOR J > 30

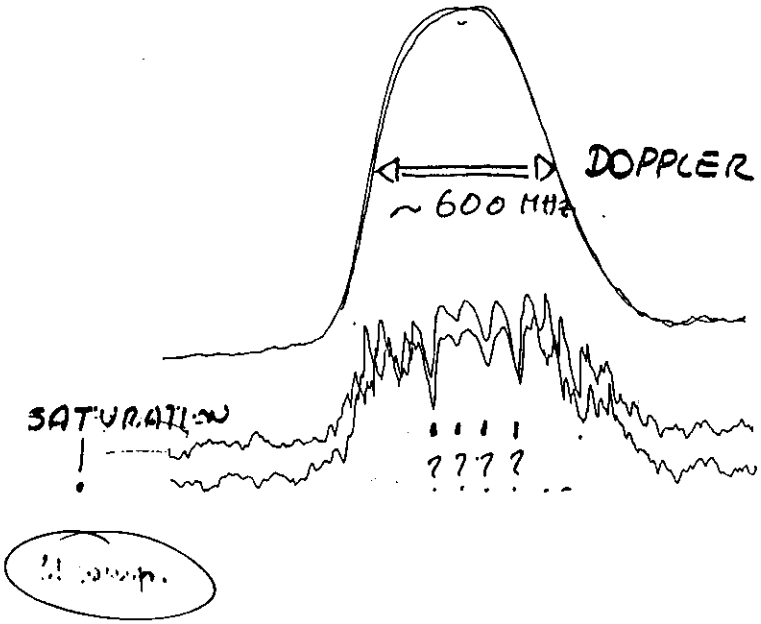

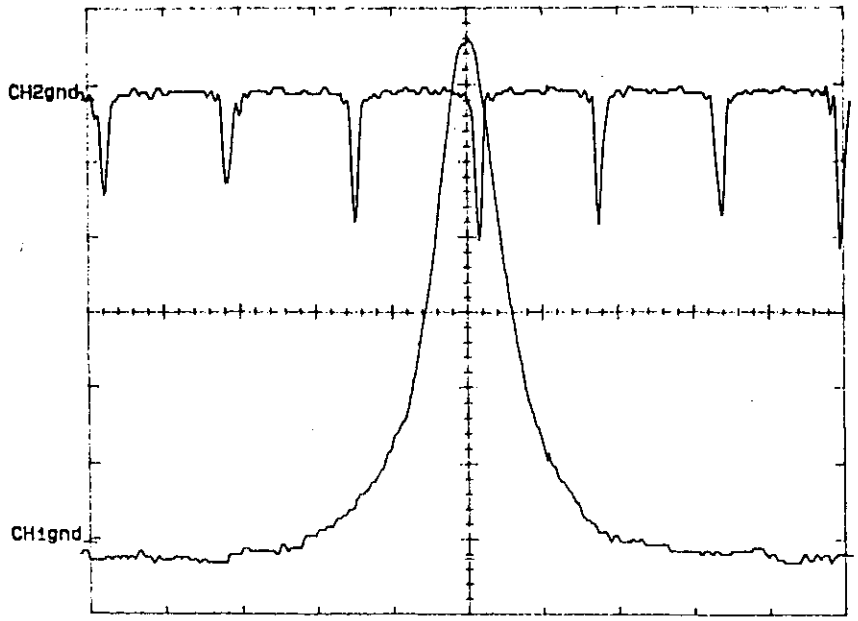

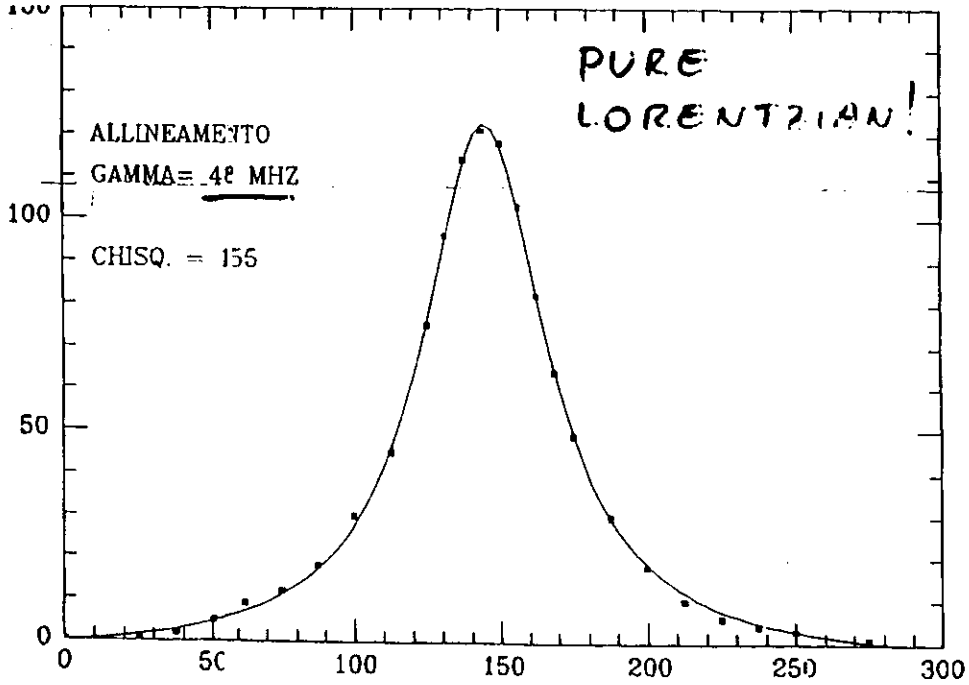

Fig. 22 Struttura iperfina della molecola di Iodio .
Profilo di assorbimento con fascio opposto saturante .

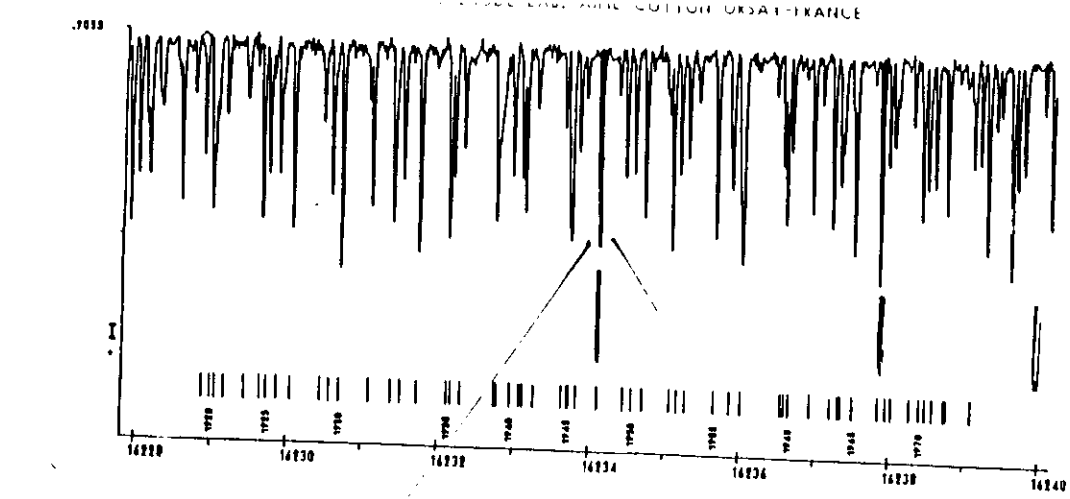

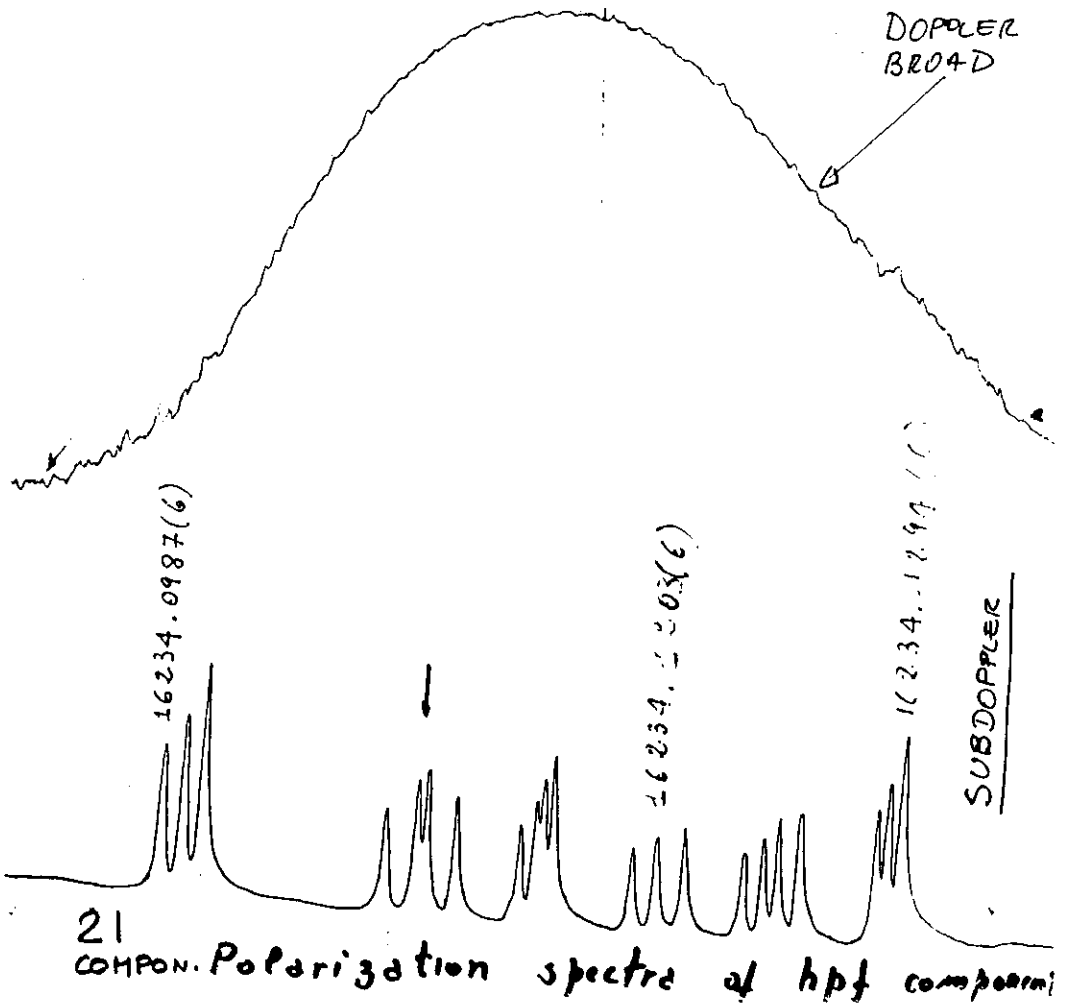

21
COMPON. Polarization spectra of hpf componni

SEMICONDUCTOR DIODE LASER

DIRECT INTERBAND LASER TRANSITION

(GaAl)As

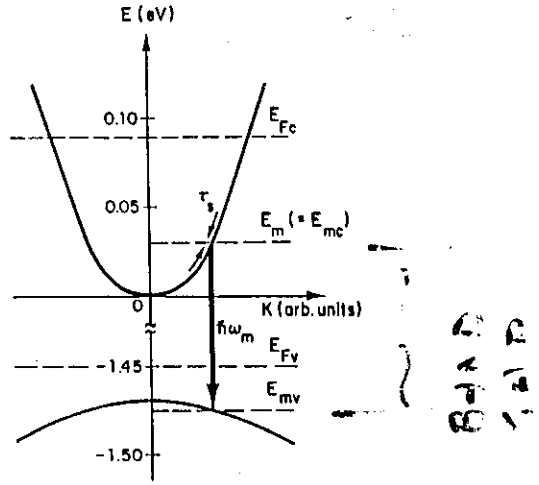

fig. 8 Schematic diagram of the simplified band structure of (GaAl)As showing the direct interband laser transition.

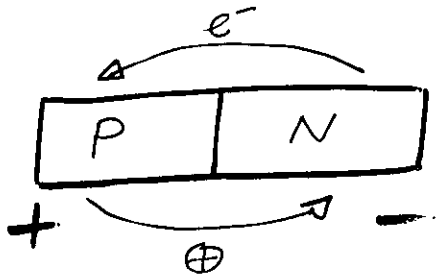

Also InGaP
InGaAsP

TYPICAL STRUCTURE

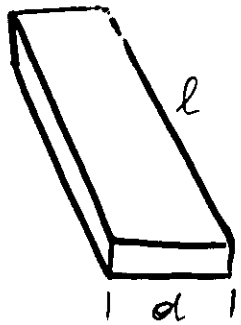

l 100 ~ 500 μm

d 0.1 ~ 2 μm

d 2 ~ 20 μm

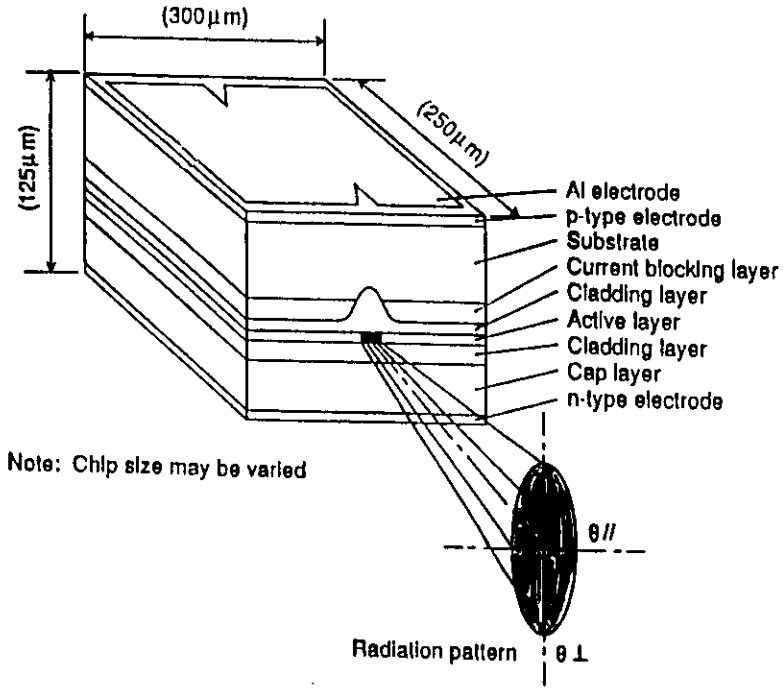

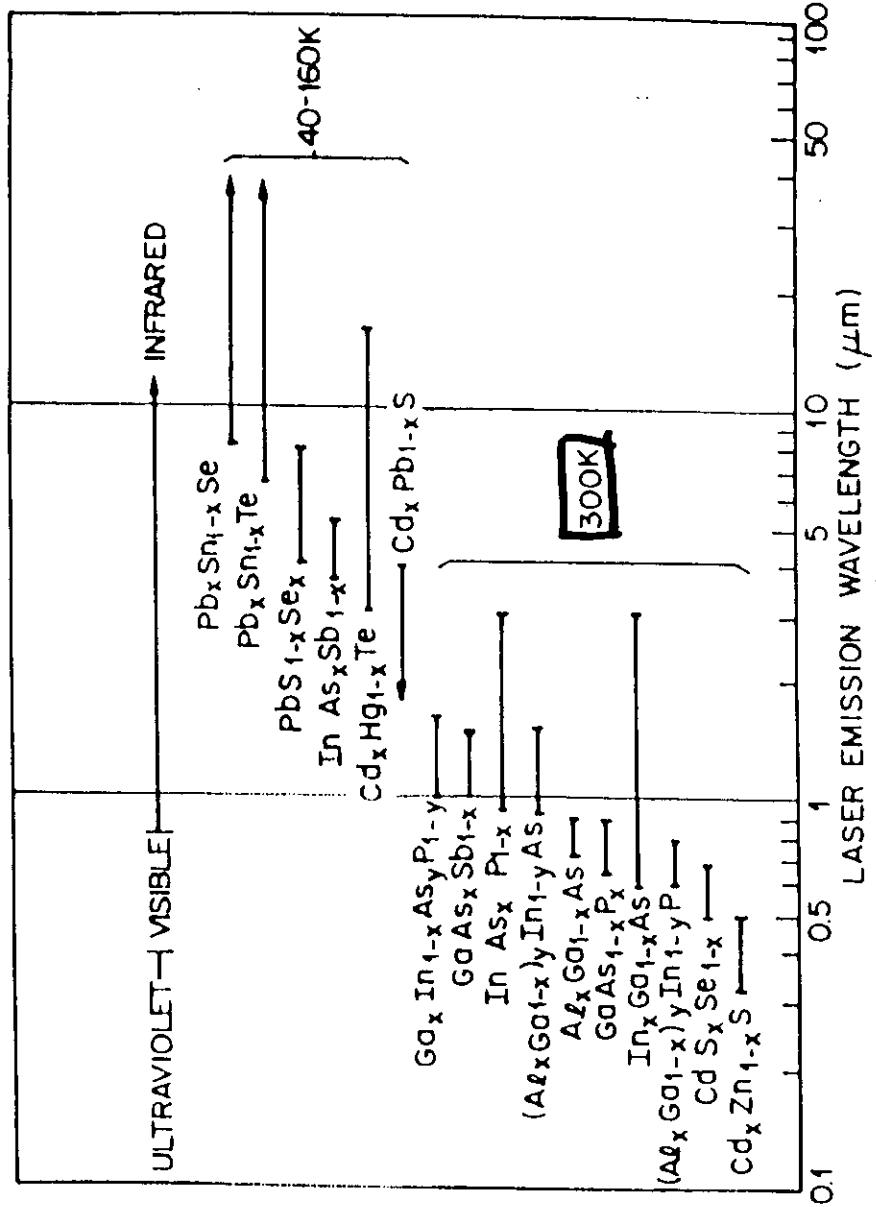

Emission wavelenghts of direct semiconductors

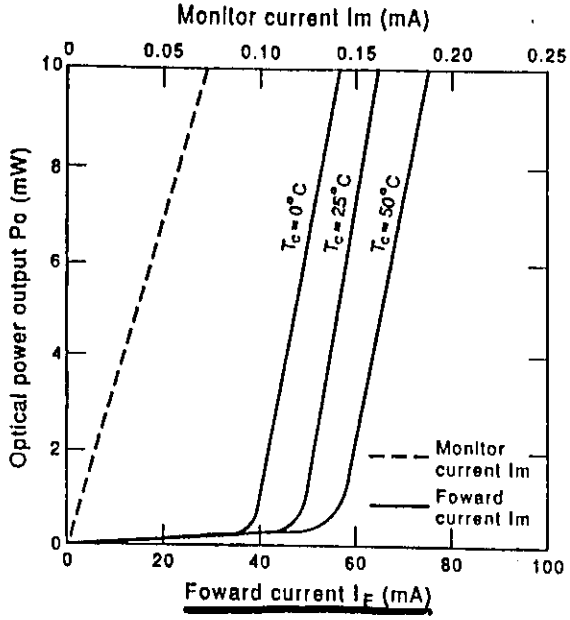

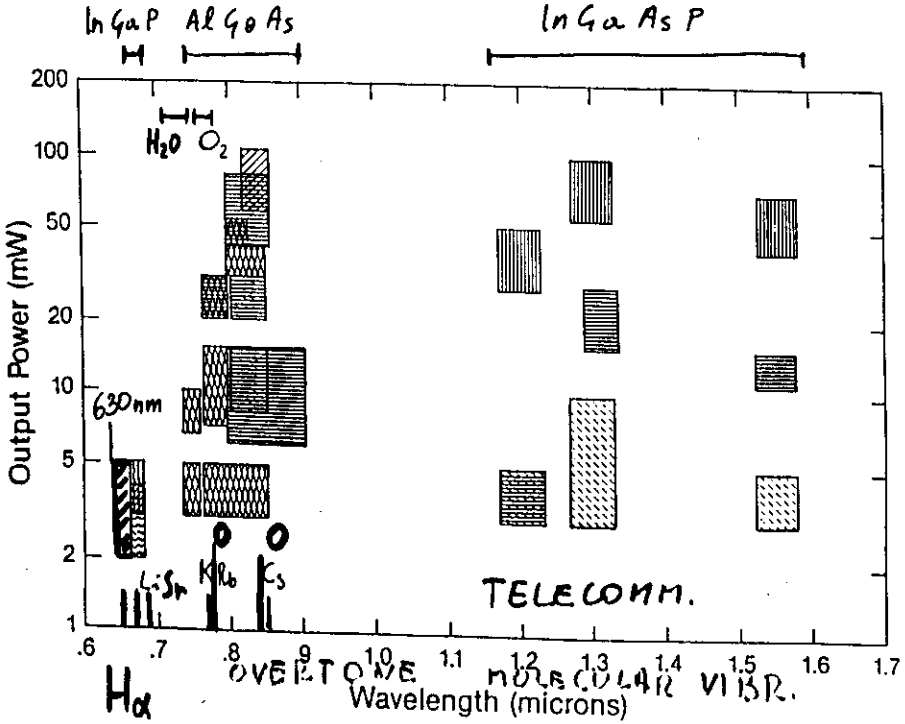

STAIRCASE WITH SLOPING STEPS

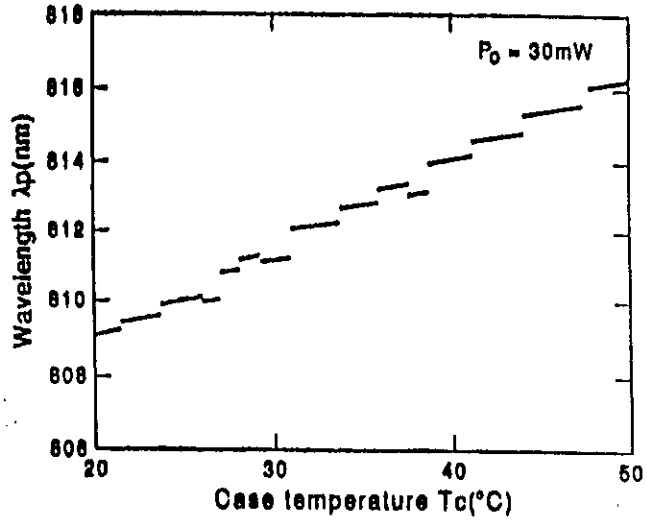

SLOPE OF EACH STEP : .06 nm / K
TUNING OF CAVITY MODE (10GHz)

JUMP BETWEEN STEPS: .25nm/K
LONGITUDINAL MODE HOPPING
BECAUSE OF GAIN CURVE SHIFT.

BANDWIDTH OF THE GAIN ~ 40 nm
LONGITUDINAL MODE SPACING:
0.3 nm ~ 100 GHz

STABILITY REQUIREMENTS

CURRENT mA

JOULE EFFECT

$\sim$ 3 GHz / mA SLOW

REFRACTIVE INDEX FAST

$\sim$ 300 MHz / mA

(frequency chirping)

TEMPERATURE mK

$\sim$ 10 GHz / °C

LINEWIDTH

100~500 μm
0.1~2 "
2~20 "

VERY SHORT CAVITY LENGTH L

SIGNIFICATIVE BROADENING DUE TO THE QUANTUM FLUCTUATIONS OF PHASE (Schawlow-Townes)

$$2\Gamma = (\pi h \nu \Gamma_c^2 / P)\, n_{sp}$$

n_{sp} ← pop. factor

P ← intrac. power

$$\Gamma_c \propto 1/L$$

Γ_c: PASSIVE RES. LINEW.

$$\Delta\nu \sim 10\ \text{MHz}$$

... for high resolution spectroscopy we need a narrower and continuosly tunable source

FEEDBACK

ELECTRONIC (MUST BE VERY FAST)

OPTICAL

LONGER (NARROWER Γ_c) CAVITY
BECAUSE IT IS COUPLED WITH
AN EXTERNAL "REFLECTOR"

REFLECTORS : MIRRORS, FIBERS,
ETALONS, FABRY PEROTS, GRATINGS

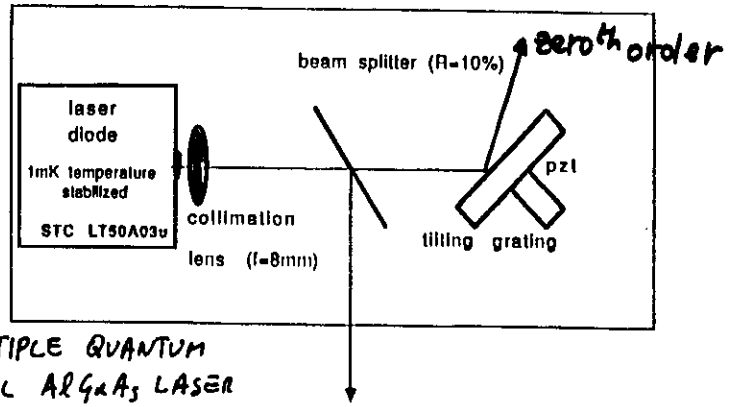

MULTIPLE QUANTUM
WELL $AlGaAs$ LASER
AT 845nm

also "regular" heterostructure lasers

also "red" InGaP lasers

See for instance :
C. Wieman, L. Hollberg
Rev. Sci. Instr. 1991

InGaP laser at 690nm

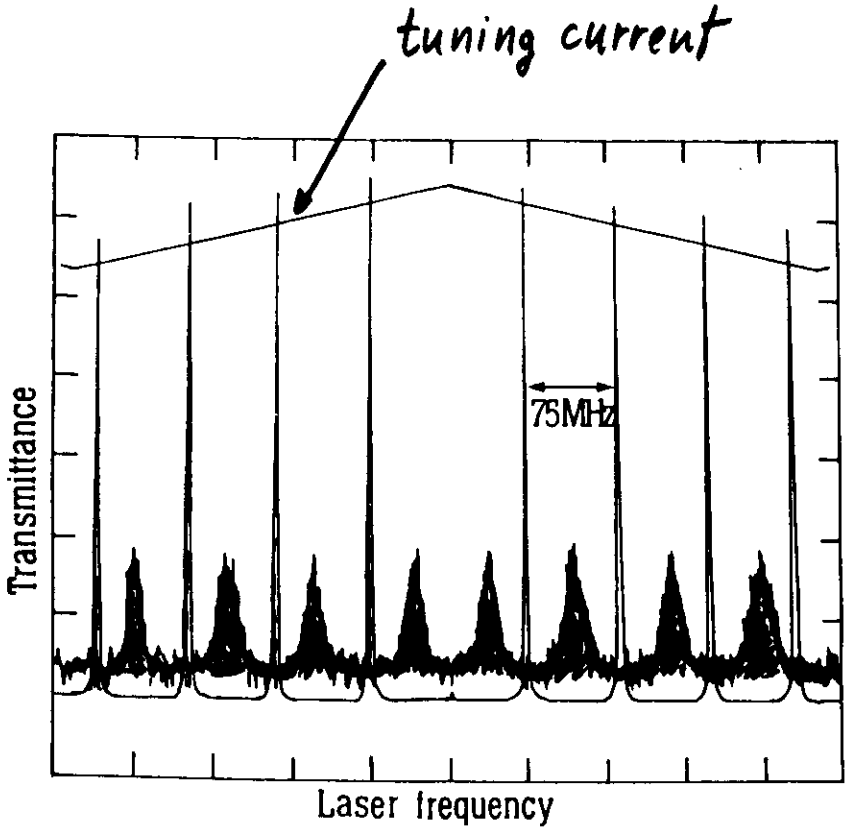

G. Tino, M. de Angelis, L. Gianfrani, M. Barsanti, M. I.
Appl. Phys. B (1992) (NAPOLI + FIRENZE)

AMPLITUDE NOISE

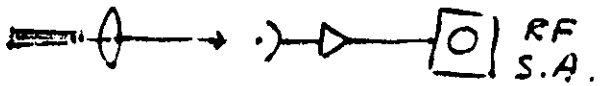

WIEMAN + Hollberg

DIODE

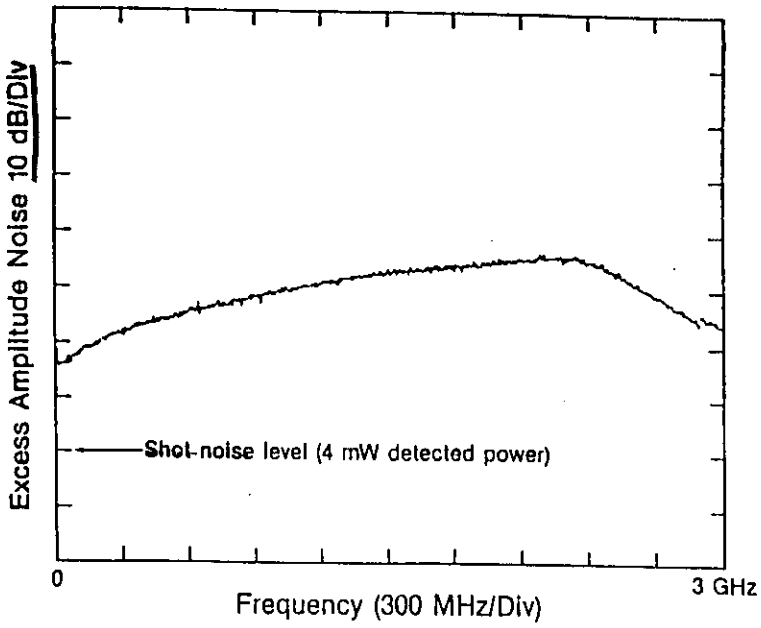

DYE

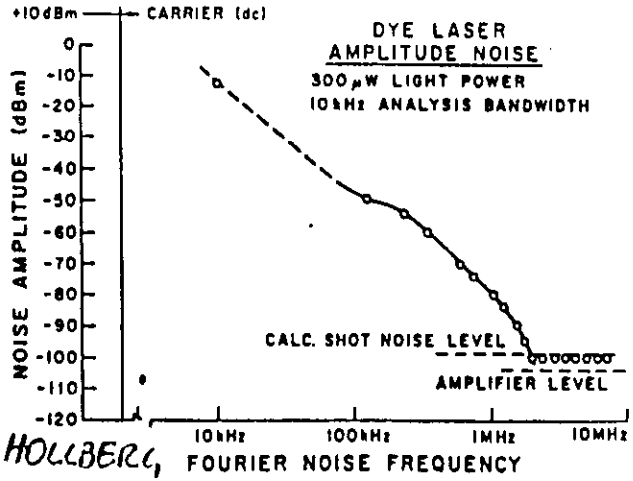

HALL + HOLLBERG,

SHOT NOISE $\propto \sqrt{N_{phot}}$

800 nm, 5mw $\sim 10^{-8}$

here we are a factor
10 ~ 20 db worse, so
we expect $\frac{\Delta I}{I} \sim 10^{-6}$

↓

HIGH SENSITIVITY IN PURE ABSORPTION EVEN FOR VERY WEAK TRANSITIONS

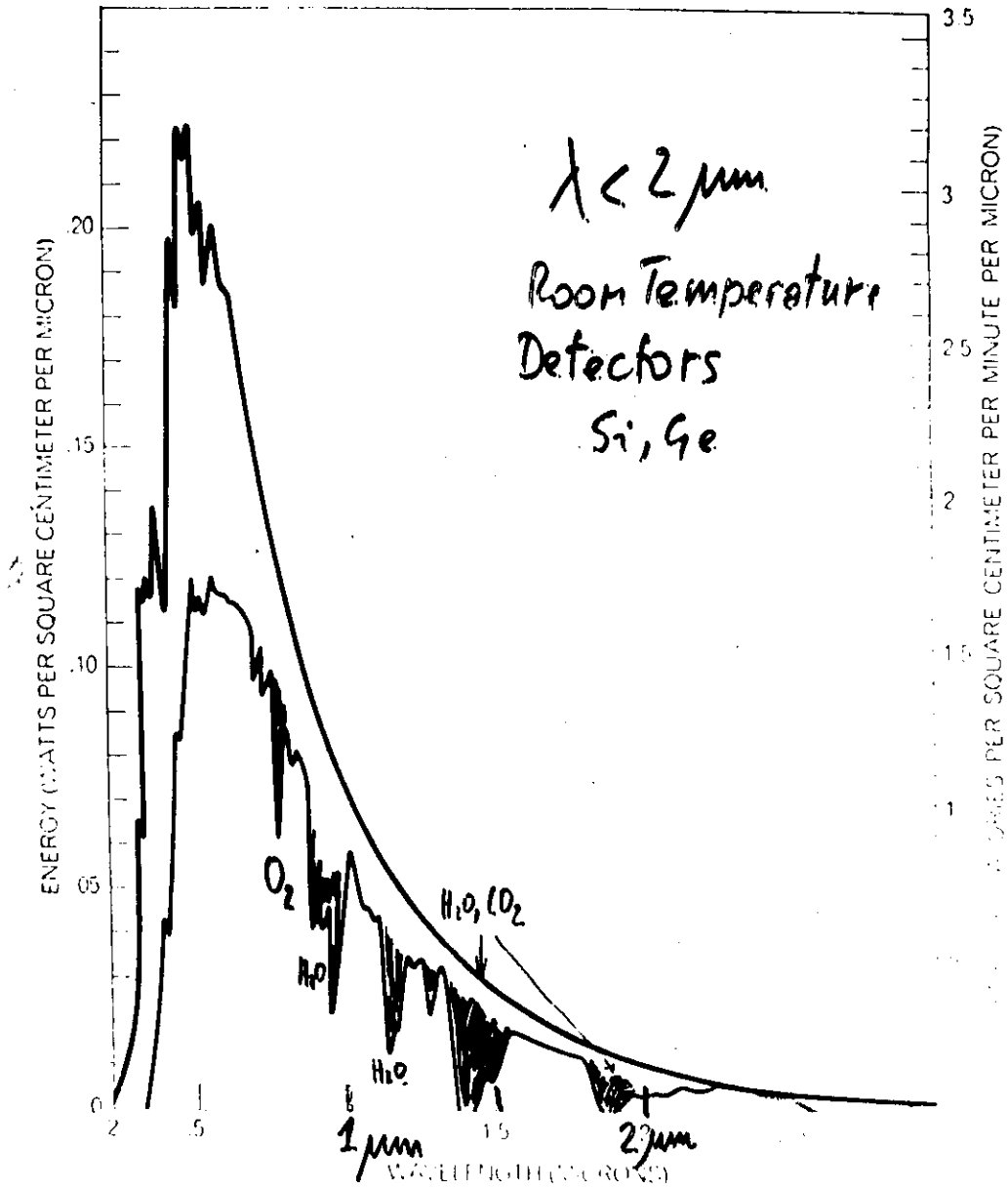

SPECTRAL DISTRIBUTION of solar radiation reaching the earth

INTRACAVITY (BROAD. DYE LASER)

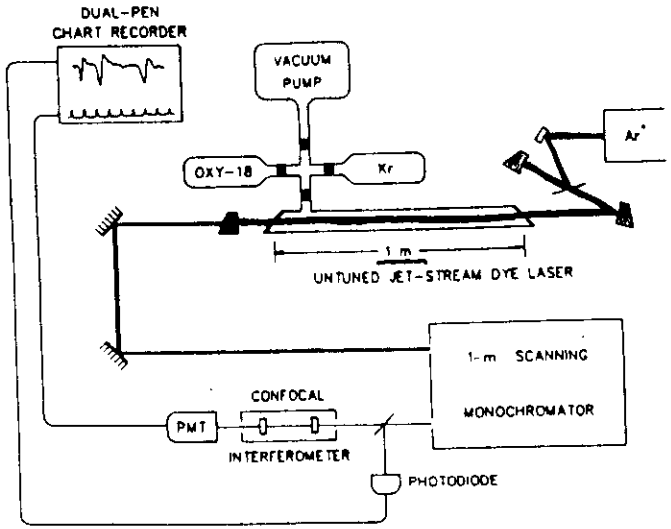

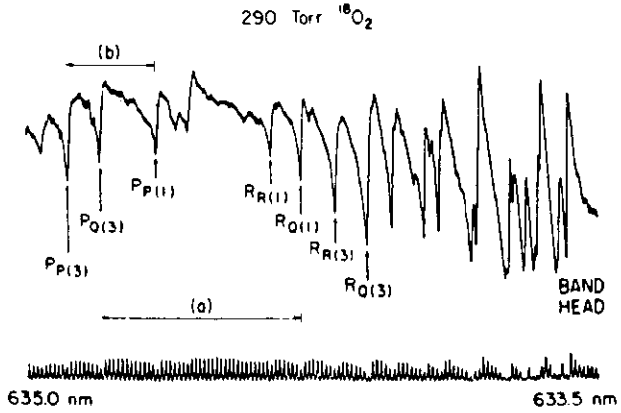

Hänsch, Schawlow

DETECTION OF MOLECULAR OXYGEN ($^{16}O_2$) AT 760 nm

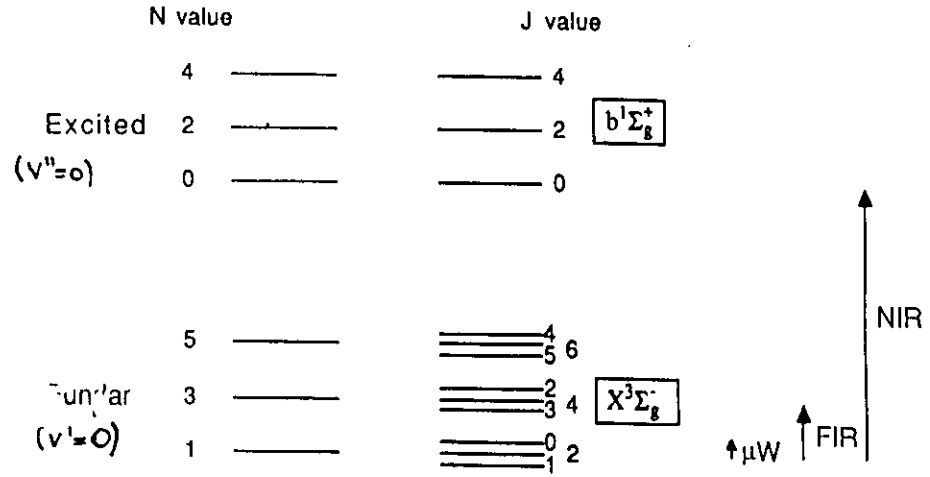

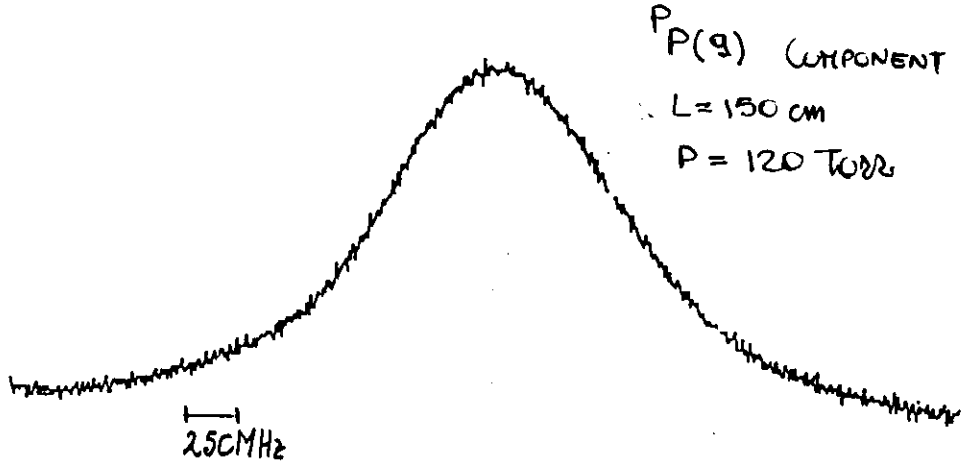

O_2

$b^1\Sigma_g^+$ — Term system

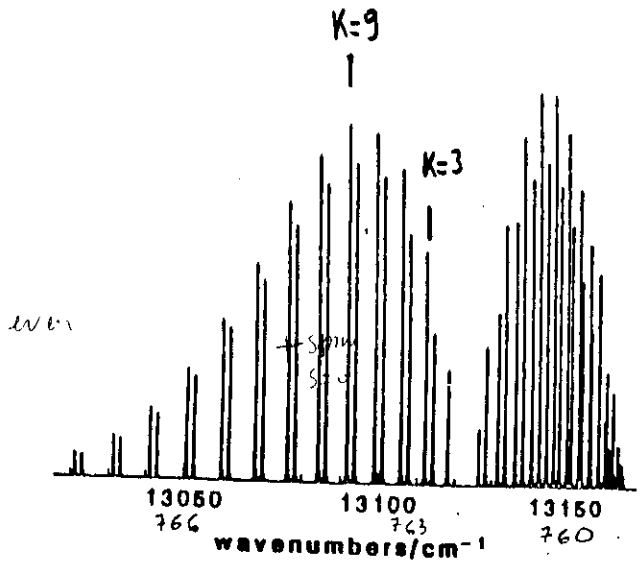

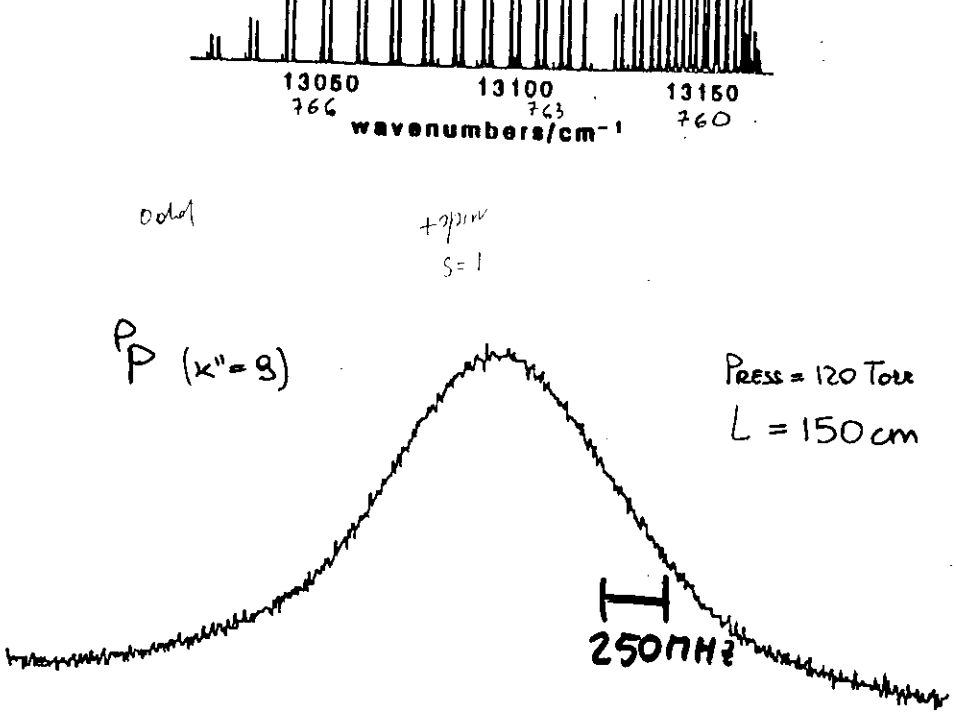

Preparing molecules in the singlet,
Pressure broad...

METHANE

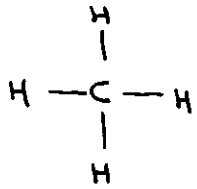

WATER

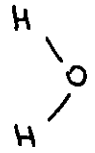

AMMONIA

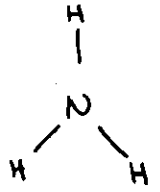

ACETYLENE

CARBON DIOXIDE

ETHYLENE

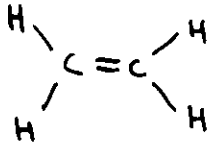

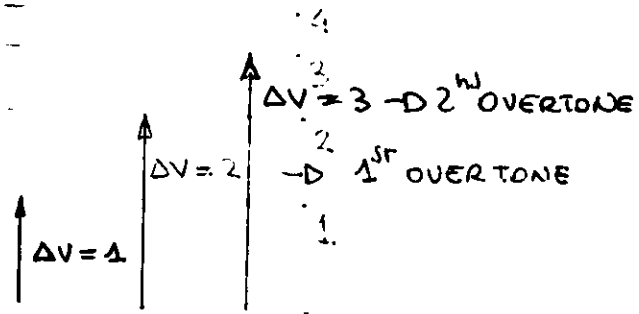

MOLECULE	$\nu_{cm^{-1}}$	λ nm	TRANSITION
CO_2	12672.4	789	$00^0 0 \rightarrow 0^0 5$
	12774.7	782	$00^0 0 \rightarrow 10^0 5$
HCN	11674.4	856	$00^0 0 \rightarrow 10^0 3$
	12635.9	791	$00^0 0 \rightarrow 00^0 4$
H_2O	12151.2	822	$000 \rightarrow 2.1$
	12562.0	796	$000 \rightarrow 013$
C_2H_2	11600.1	862	$000 \rightarrow 013$
	11782.9	848	$000 \rightarrow 211$
	12675.7	788	$000 \rightarrow 103$
C_2HD	12263.0	815	$00000 \rightarrow 30100$
	12735.0	785	$00000 \rightarrow 40010$
NH_3	12609.2	793	$4\nu_1$
CH_4	11885.0	841	$4\nu_3$
	12755.0	782	$2\nu_1 + \nu_2 + 2\nu_3$
$HC \equiv C - C \equiv H$	12706.2	787	$\nu_1 + 3\nu_4$
C_6H_6	11500	869	$\Delta\nu = 4$
HI	11950	836	$\Delta\nu = 6$
HCl	13300	750	$\Delta\nu = 5$
IBr	12576	795	$A^3\Pi_1 \leftarrow X^1\Sigma^+$
HOOH	12600	793	$5\nu_{OH} + \nu_{oo}$
C_2D_2	12111	825	$000 \rightarrow 500$
	12628	791	$000 \rightarrow 302$
	11946	837	$000 \rightarrow 401$
	12347	810	$000 \rightarrow 203$
CH_3D	11602	861	$2\nu_1 + 2\nu_2$
O_2	13100	763	$b^1\Sigma_g^+ \leftarrow X^3\Sigma_g^-$

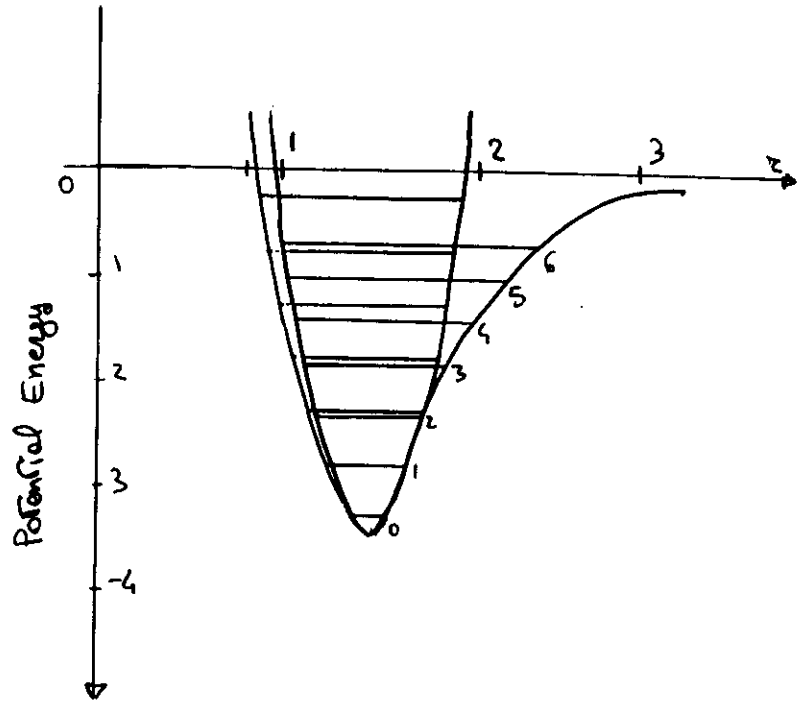

HARMONIC MOTION

$x = r_0 \sin 2\pi\nu_0 t$

$E(\nu) = h\nu_0 \left(v + \frac{1}{2}\right)$

ANHARMONIC MOTION

$E(\nu) = h\nu_0 \left(v + \frac{1}{2}\right) - h\nu_0 x_e \left(v + \frac{1}{2}\right)^2 + h\nu_0 y_{00} \left(v + \frac{1}{2}\right)^3 + \ldots$

TRANSITION STRENGTH

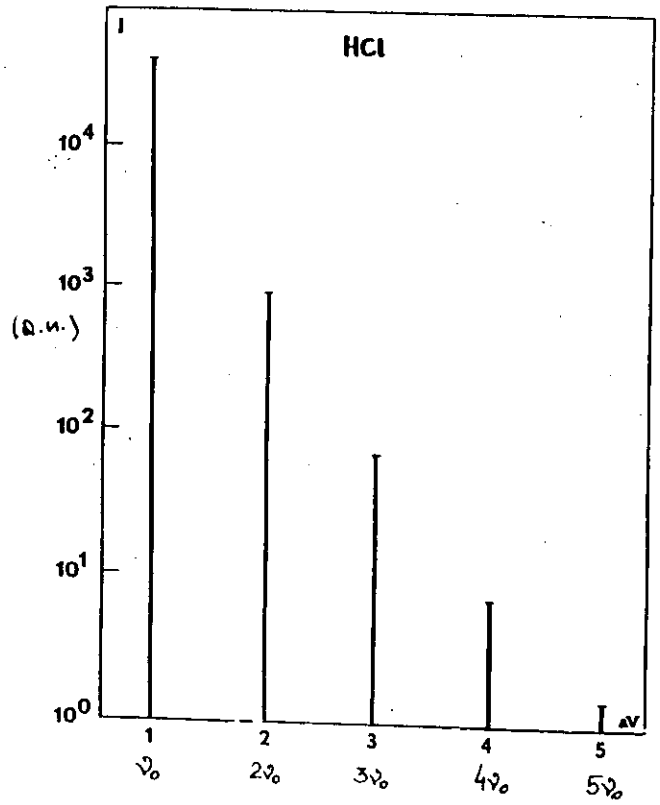

ACETYLENE

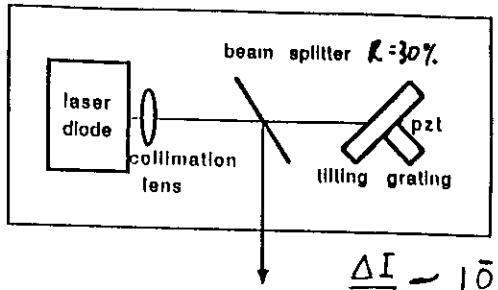

$\frac{\Delta I}{I} \simeq 10^{-6}\ \sqrt{Hz}$ at 1 KHz

F. PAVONE, K. ERNST, F. MARIN
G. D. LONARDO and M. I. APPL. OPT.

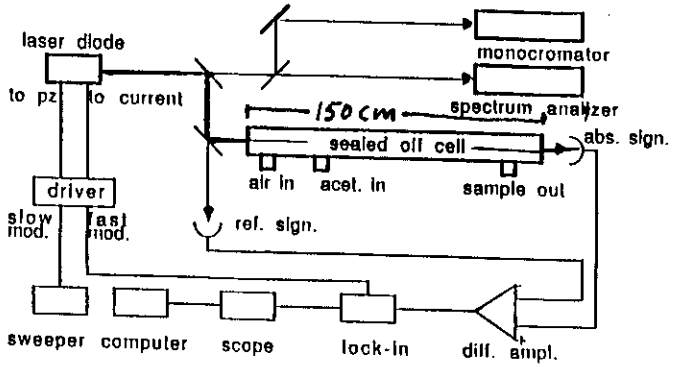

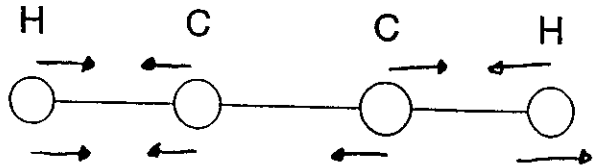

$\nu_{CH} \sim 3300\ cm^{-1}$

$1\nu_1 + 3\nu_3 \sim 4\nu \sim 13000\ cm^{-1} \rightarrow 780\ nm$

(BAND HEAD $12676\ cm^{-1}$)

(OTHER 3 OVERTONE BANDS IN THE DIODE LASERS RANGE)

DERIVATIVE SIGNAL

COMPONENT P(11)

a)

PRESS. C_2H_2 = 10 Torr

b)

PRESS. C_2H_2 = 30 mTorr

3rd OVERTONE METHANE ABSORPTION

λ = 886 nm

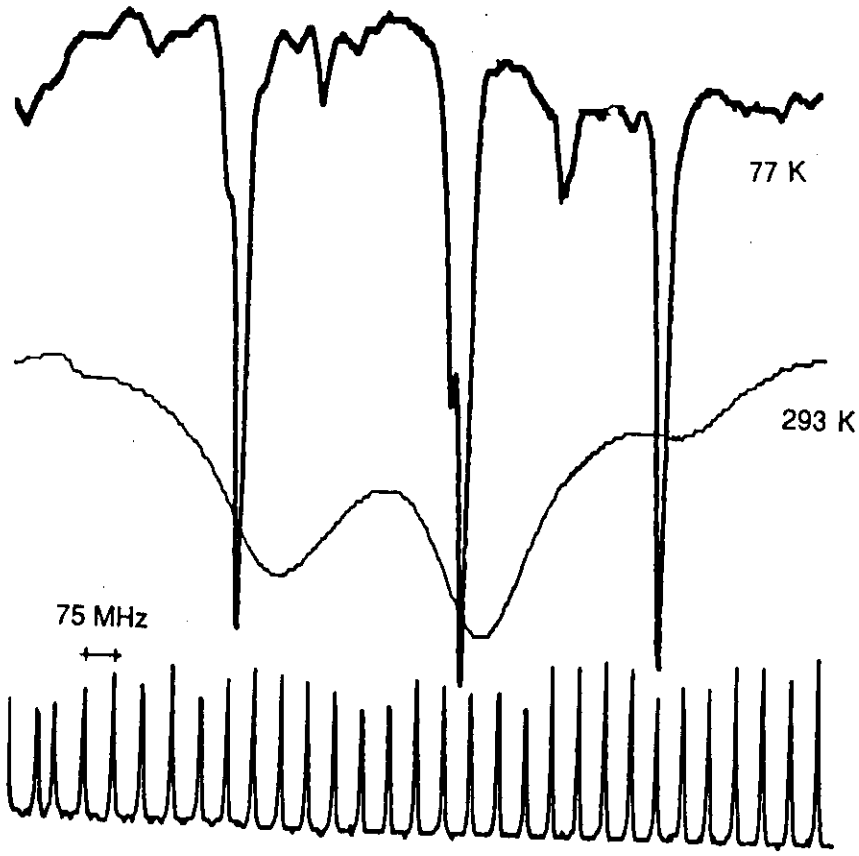

Components of the combination bands $3\nu_1 + \nu_3$

$2\nu_1 + 2\nu_3$

$\nu_1 + 3\nu_3$

$4\nu_3$

STUDY OF THE BEHAVIOUR OF THE ABSORPTION WITH THE PRESSURE

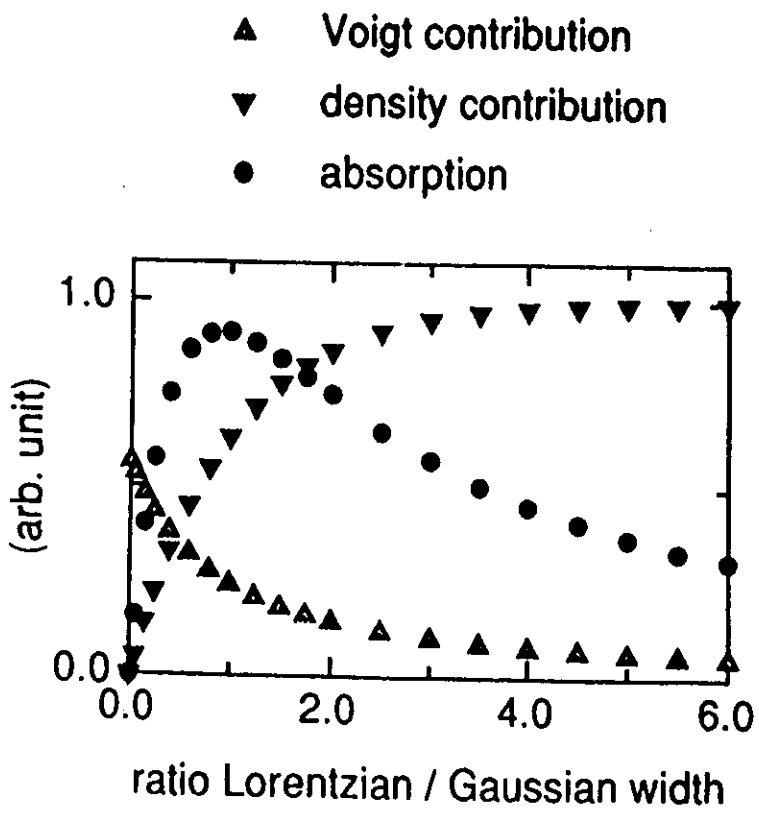

LASER (PEAK ABSORPTION)

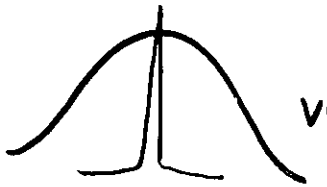

VOIGT : GAUSSIAN + LORENTZIAN

WITH PRESSURE, THE LORENTZIAN CONTRIBUTION INCREASES WITH A BROADENING OF THE LINE AND A DECREASE OF ITS PEAK.

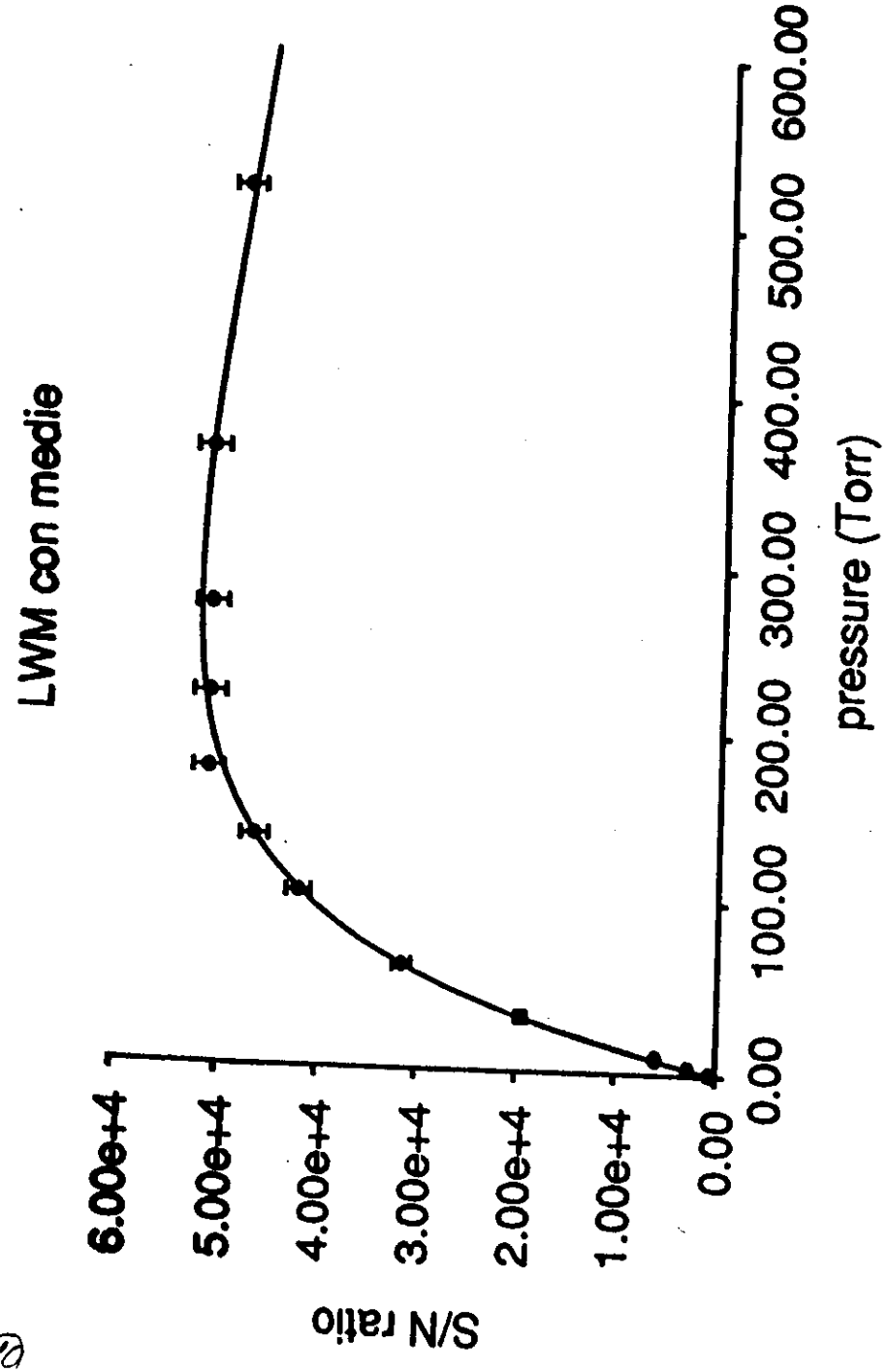

1ST METHOD :

LOW WAVELENGTH MODULATION

MODULATION FREQUENCY 1 KHz

(SMALLER THAN MOLECULAR LINEWIDTH AND THE ABSORPTION IS PROBED BY MANY SIDE BANDS)

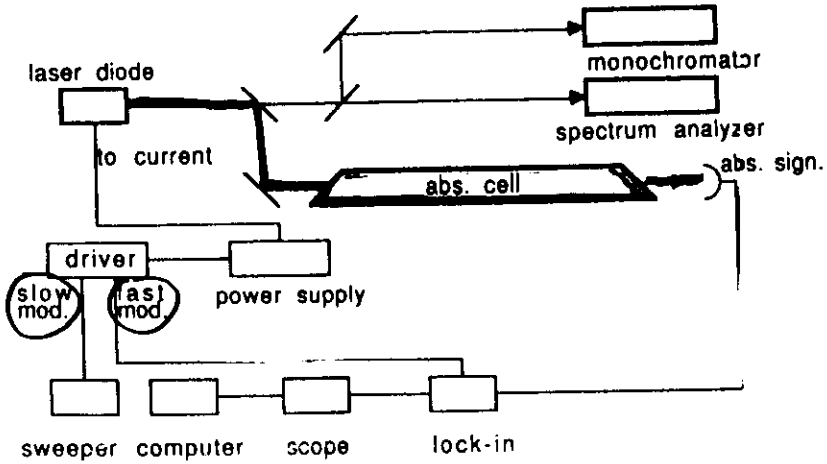

$\alpha_{MIN} = 4.5\ 10^{-7}$

CH_4 150cm 0.886 μm

Direct

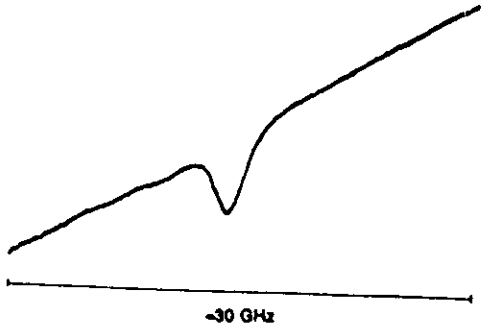

3rd Der

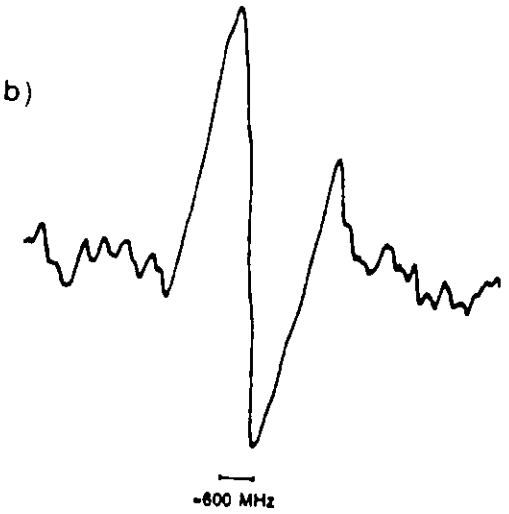

TTFM

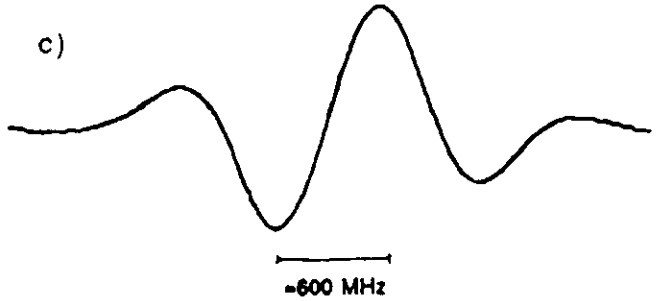

NEAR INFRA-RED SPECTROSCOPY OF MOLECULES USING DIODE LASERS

MINIMUM DETECTABLE ABSORPTION VERSUS THE FREQUENCY MODULATION INDEX (β)

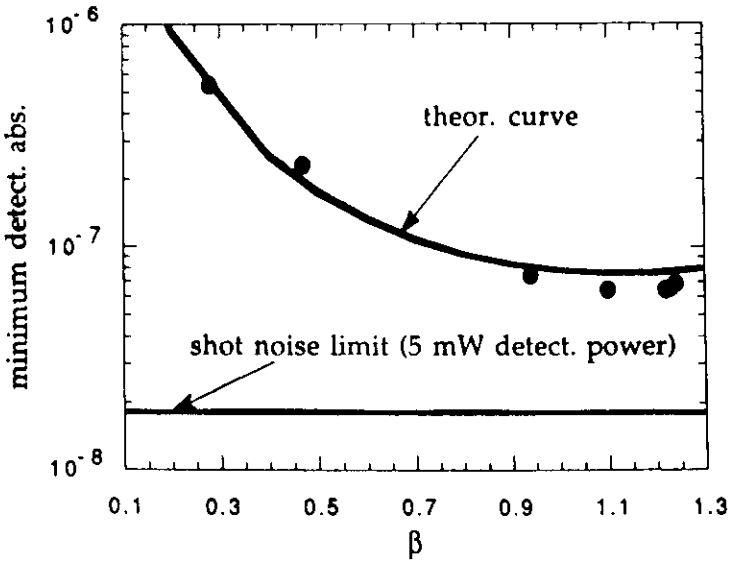

ACTUAL EMISSION RANGE OF DIODE LASERS

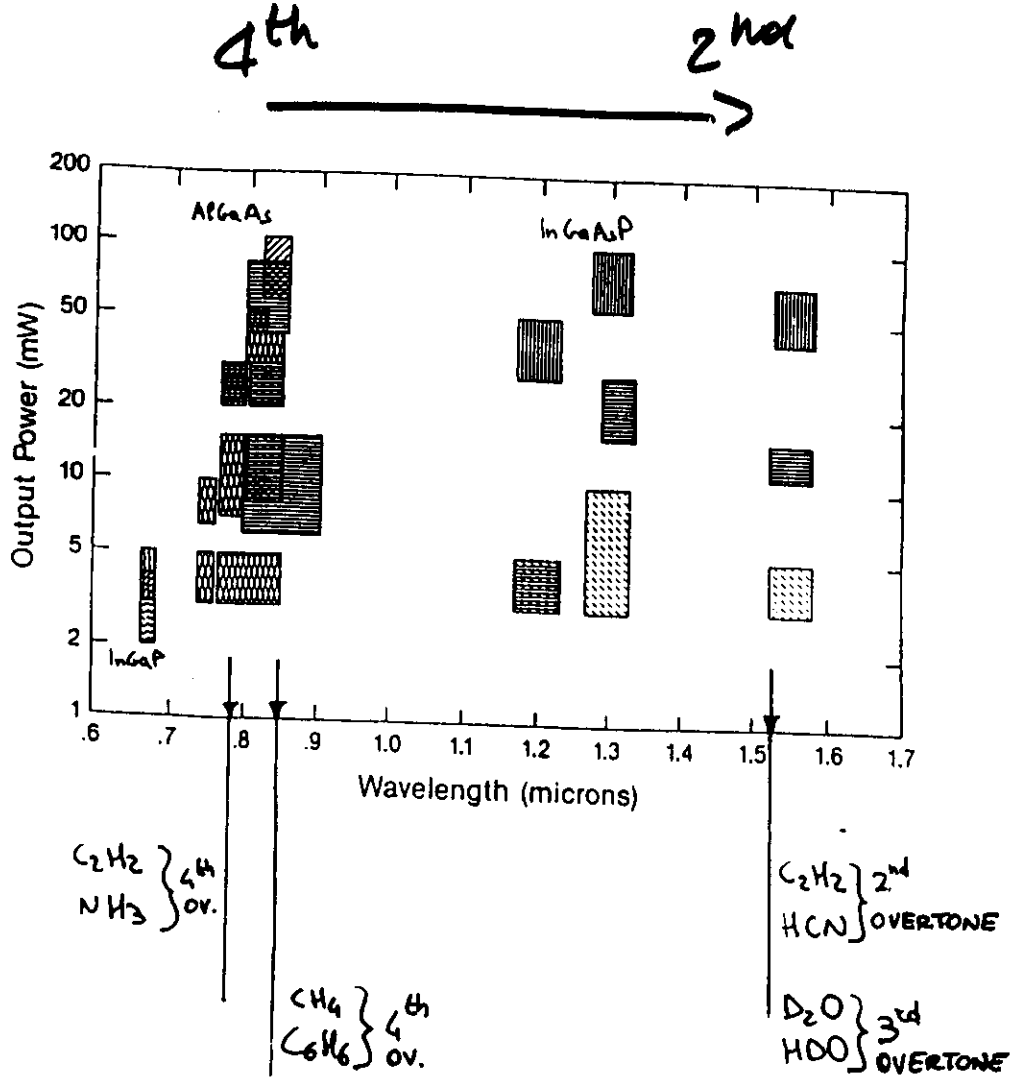

FTS-LENS

HCl

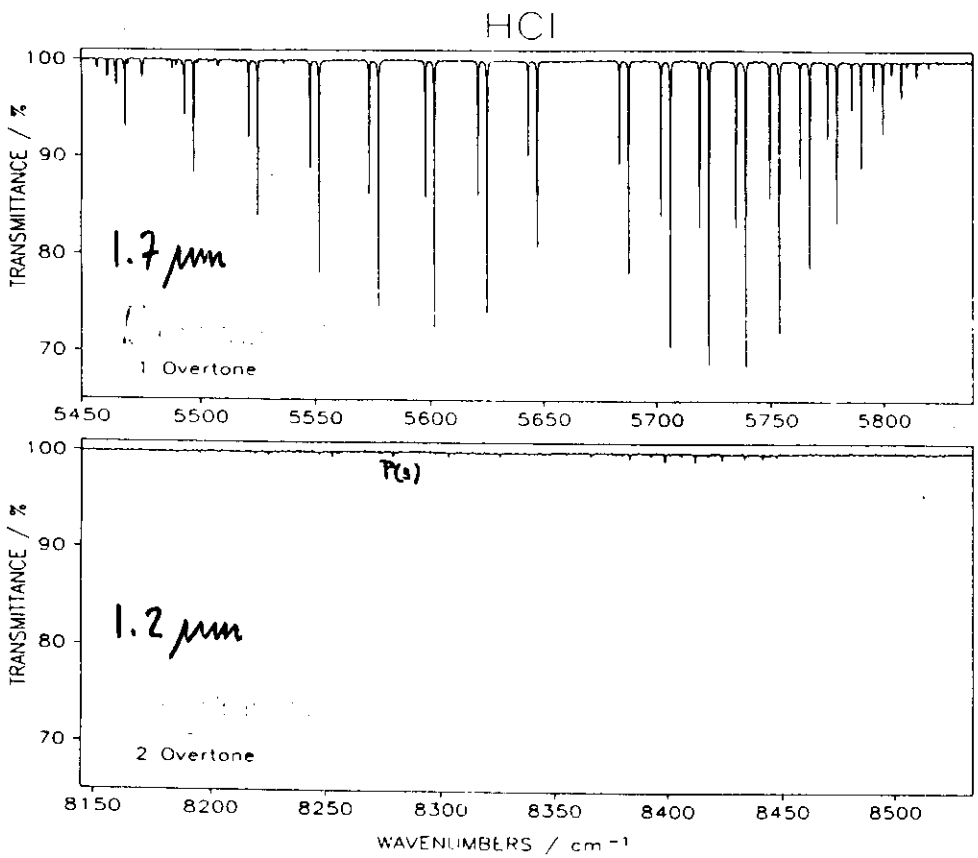
HCl
TRANSMITTANCE / %
100
90
80
70
1.7 μm
1 Overtone
5450
5500
5550
5600
5650
5700
5750
5800
P(3)
1.2 μm
2 Overtone
8150
8200
8250
8300
8350
8400
8450
8500
WAVENUMBERS / cm⁻¹

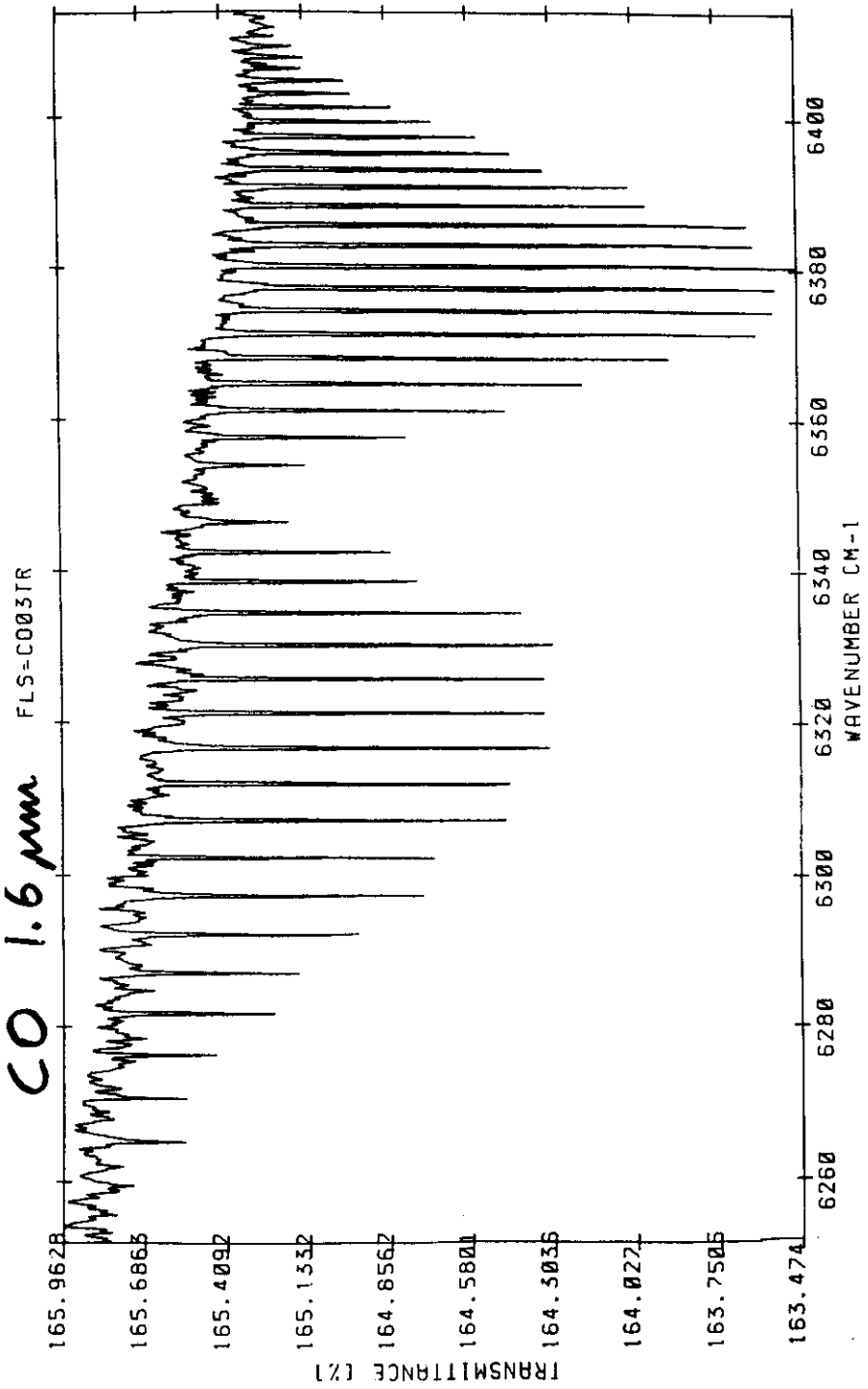
CO 1.6 μm
FLS-C003TR
TRANSMITTANCE (%)
165.9628
165.6862
165.4092
165.1332
164.8562
164.5801
164.3036
164.0272
163.7505
163.474
6400
6380
6360
6340
6320
6300
6280
6260
WAVENUMBER CM-1

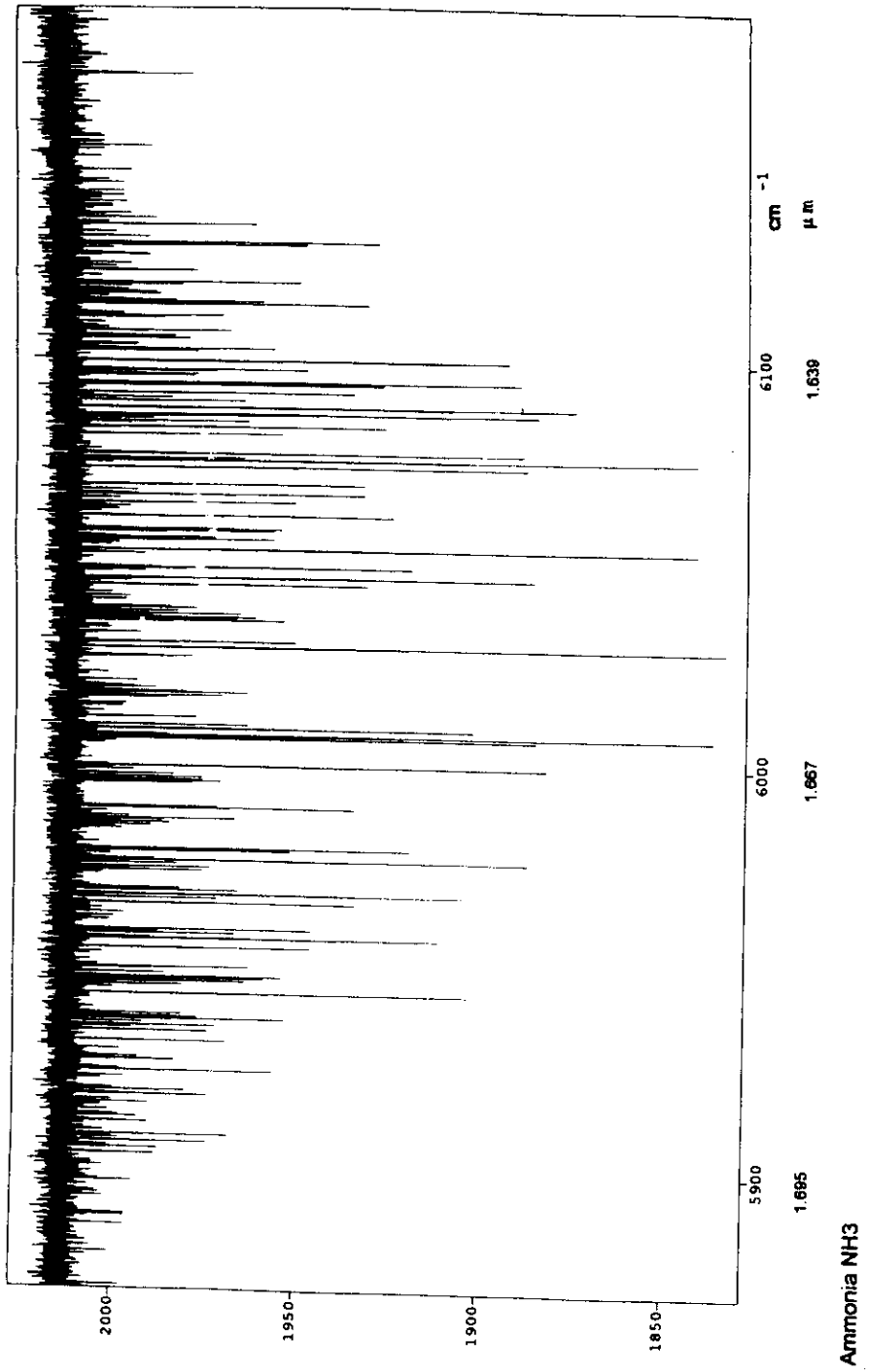

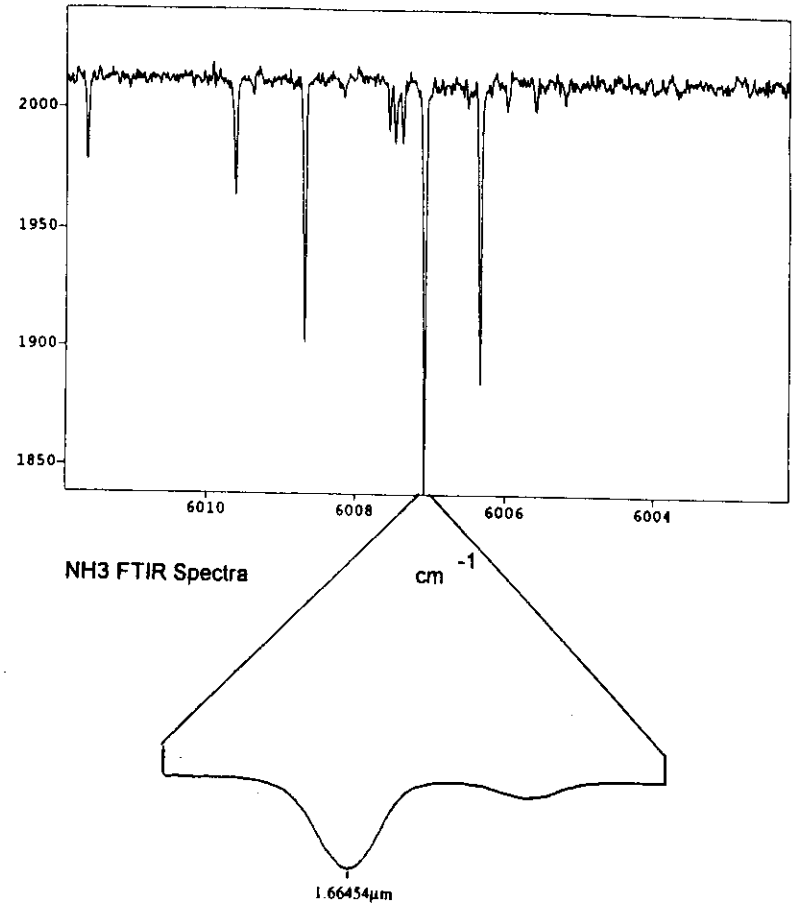

NH3 DFB diode laser Spectra

NH_3 1 Torr 1.64 μm 150cm FIBRES

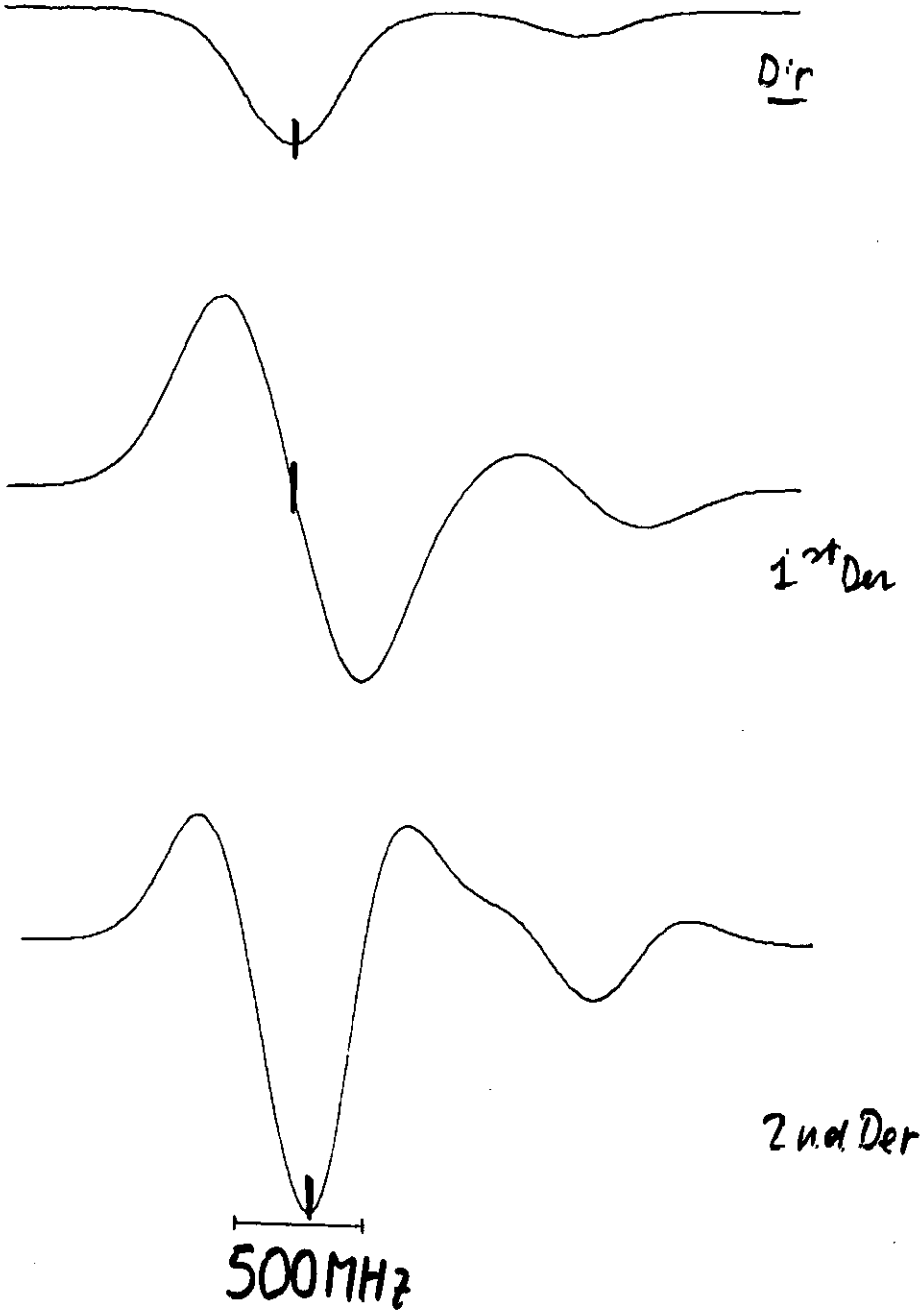

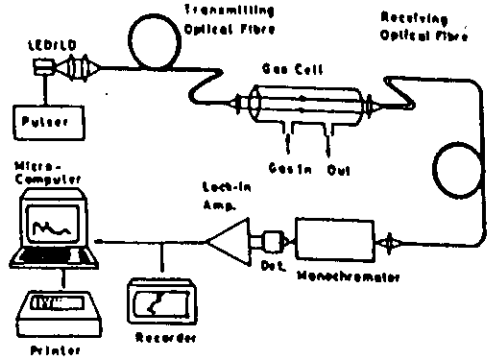

Fig. 7 Block diagram of an all-optical fiber-based remote sensing system for absorption measurement of low-level combustible, explosive, polluting and toxic gases in an absorption cell as the gas sensor head using a LED or LD operated in the near-infrared region.

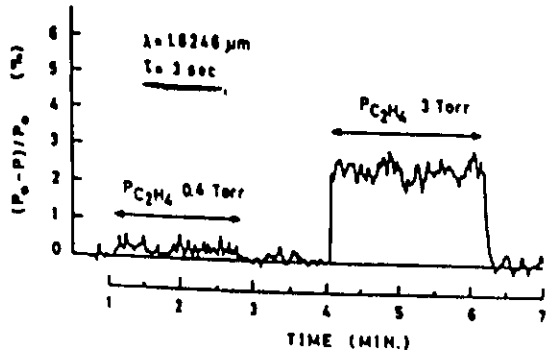

Fig. 8 Real-time detection of C_2H_4 absorption signals in 1 atm. C_2H_4-air mixture contained in a remotely located 50-cm long absorption cell, utilizing a 5-km long, low-loss silica optical fiber link and a 1.64 μm InGaAs LED.

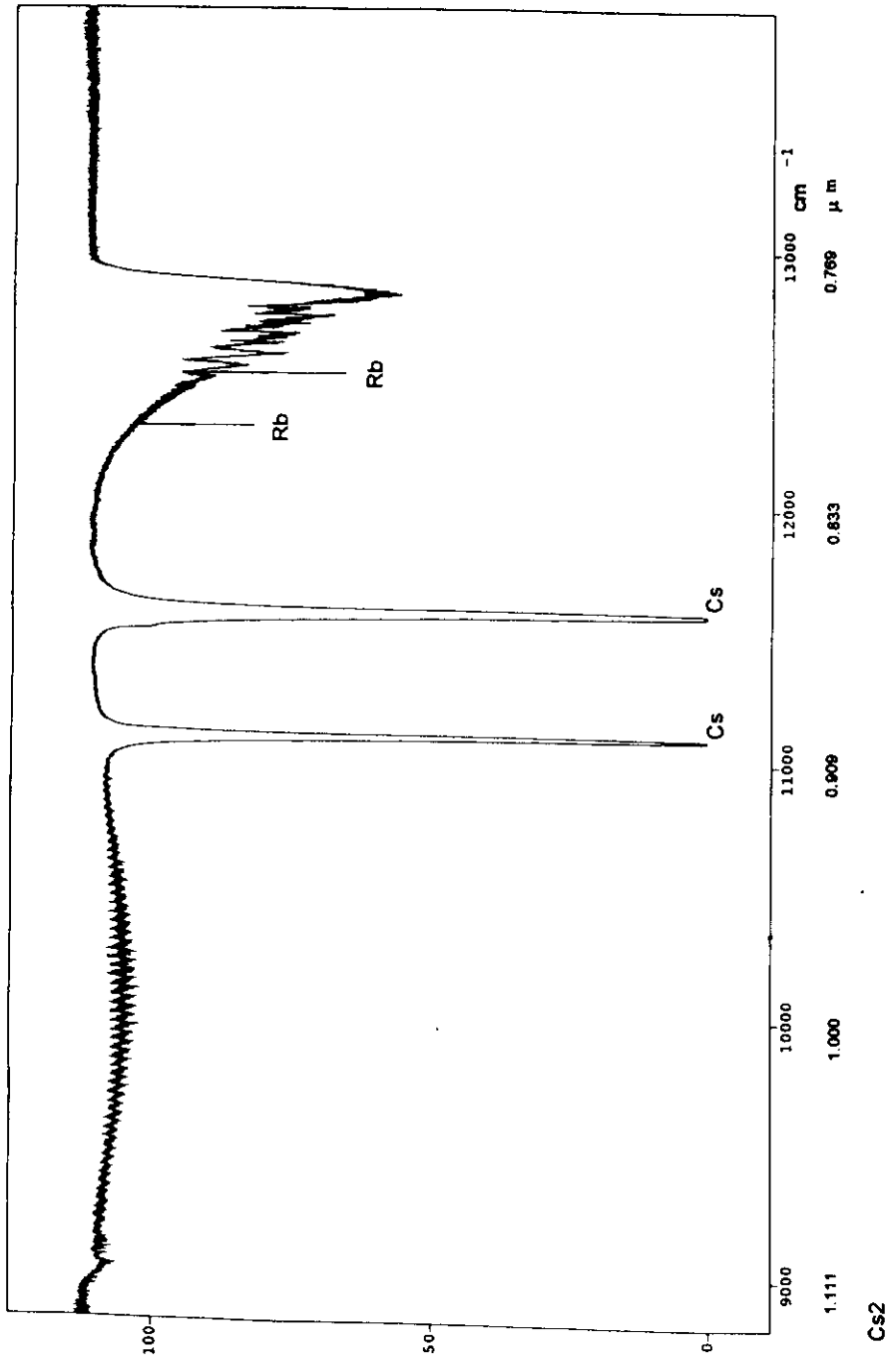

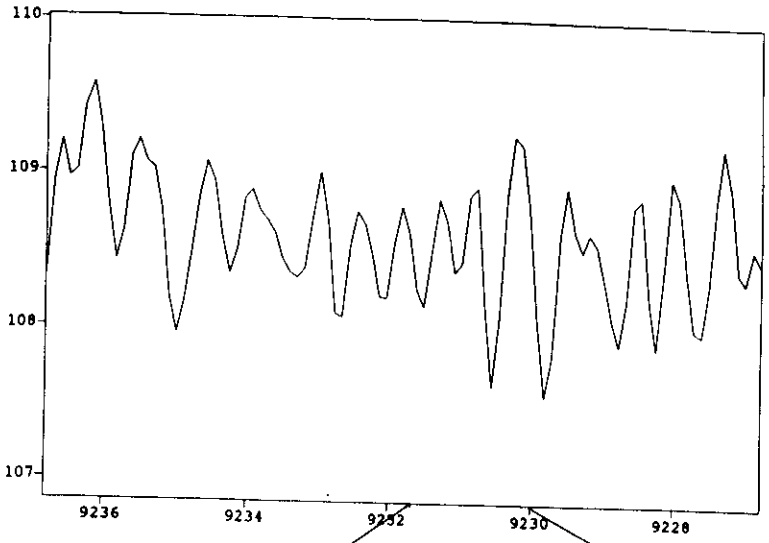

Cs2 FTIR Spectra

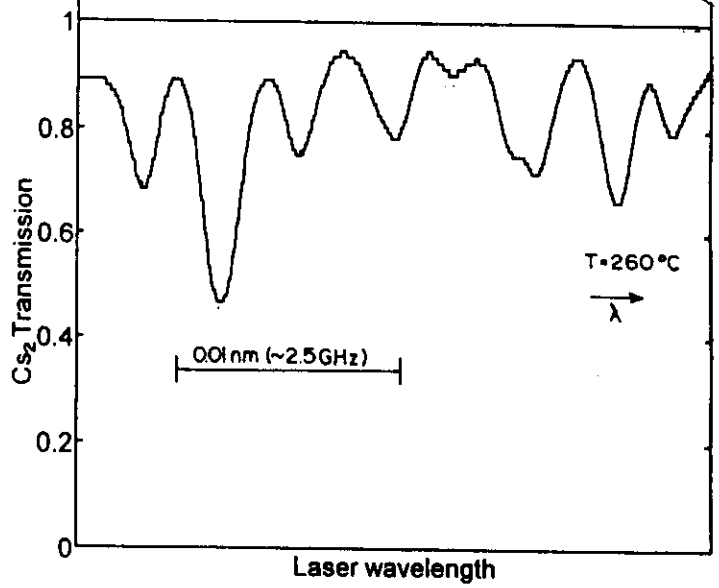

Cs2 DBR diode laser Spectra

Frequency locking to molecular Cesium

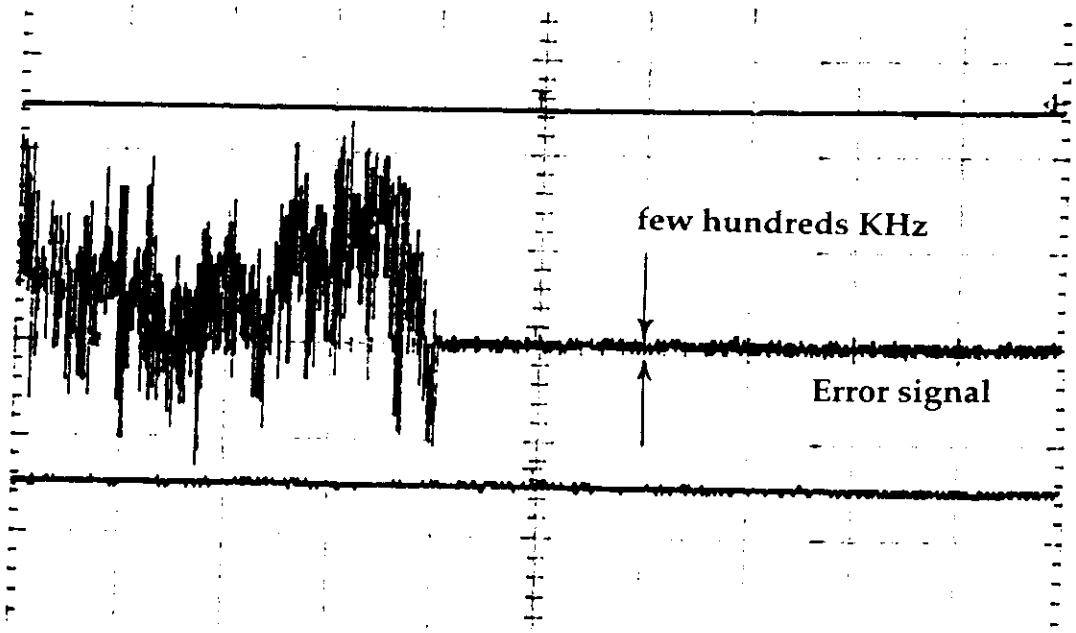

Molecular Cesium versus Helium